



IntechOpen

# Recent Advances in Flood Risk Management

*Edited by John Abbot and Andrew Hammond*





---

# Recent Advances in Flood Risk Management

*Edited by John Abbot  
and Andrew Hammond*

Published in London, United Kingdom

---



## IntechOpen





*Supporting open minds since 2005*



Recent Advances in Flood Risk Management  
<http://dx.doi.org/10.5772/intechopen.78505>  
Edited by John Abbot and Andrew Hammond

#### Contributors

Mohamed Daoudi, Abdoul Jelil Niang, Daniel Maposa, Miho Ohara, Naoko Nagumo, Badri Bhakta Shrestha, Hisaya Sawano, Faustino De Luna, Oscar Fuentes-Mariles, Judith Ramos, Jesús Gracia Sánchez, Yeou-Koung Tung, Yin-Lung Chang, Jinn-Chuang Yang, Chehao Chang, Tung-Lin Tsai, Guangwei Huang, Yusuke Yamazaki, Yoshio Tokunaga

© The Editor(s) and the Author(s) 2019

The rights of the editor(s) and the author(s) have been asserted in accordance with the Copyright, Designs and Patents Act 1988. All rights to the book as a whole are reserved by INTECHOPEN LIMITED. The book as a whole (compilation) cannot be reproduced, distributed or used for commercial or non-commercial purposes without INTECHOPEN LIMITED's written permission. Enquiries concerning the use of the book should be directed to INTECHOPEN LIMITED rights and permissions department ([permissions@intechopen.com](mailto:permissions@intechopen.com)).

Violations are liable to prosecution under the governing Copyright Law.



Individual chapters of this publication are distributed under the terms of the Creative Commons Attribution 3.0 Unported License which permits commercial use, distribution and reproduction of the individual chapters, provided the original author(s) and source publication are appropriately acknowledged. If so indicated, certain images may not be included under the Creative Commons license. In such cases users will need to obtain permission from the license holder to reproduce the material. More details and guidelines concerning content reuse and adaptation can be found at <http://www.intechopen.com/copyright-policy.html>.

#### Notice

Statements and opinions expressed in the chapters are those of the individual contributors and not necessarily those of the editors or publisher. No responsibility is accepted for the accuracy of information contained in the published chapters. The publisher assumes no responsibility for any damage or injury to persons or property arising out of the use of any materials, instructions, methods or ideas contained in the book.

First published in London, United Kingdom, 2019 by IntechOpen

eBook (PDF) Published by IntechOpen, 2019

IntechOpen is the global imprint of INTECHOPEN LIMITED, registered in England and Wales,

registration number: 11086078, The Shard, 25th floor, 32 London Bridge Street

London, SE19SG – United Kingdom

Printed in Croatia

British Library Cataloguing-in-Publication Data

A catalogue record for this book is available from the British Library

Additional hard and PDF copies can be obtained from [orders@intechopen.com](mailto:orders@intechopen.com)

Recent Advances in Flood Risk Management

Edited by John Abbot and Andrew Hammond

p. cm.

Print ISBN 978-1-78923-935-5

Online ISBN 978-1-78923-936-2

eBook (PDF) ISBN 978-1-83962-104-8

# We are IntechOpen, the world's leading publisher of Open Access books Built by scientists, for scientists

**4,100+**

Open access books available

**116,000+**

International authors and editors

**120M+**

Downloads

**151**

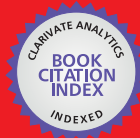
Countries delivered to

Our authors are among the  
**Top 1%**

most cited scientists

**12.2%**

Contributors from top 500 universities



**WEB OF SCIENCE™**

Selection of our books indexed in the Book Citation Index  
in Web of Science™ Core Collection (BKCI)

Interested in publishing with us?  
Contact [book.department@intechopen.com](mailto:book.department@intechopen.com)

Numbers displayed above are based on latest data collected.  
For more information visit [www.intechopen.com](http://www.intechopen.com)







# Meet the editors



Dr. John Abbot is currently a Senior Research Fellow at the Institute of Public Affairs in Australia, and has an adjunct research position at the University of Tasmania. He has worked as a research scientist in the industry and universities including Queensland University, Canada, the University of Tasmania and Central Queensland University. Dr. Abbot holds BSc (Imperial College), MSc (University of British Columbia), MBiotech (University of Queensland) and PhD (McGill University) degrees. He has published over 100 articles, including 12 on the application of neural networks to climatic phenomena, particularly rainfall forecasting. His interest in rainfall forecasting was stimulated by the severe flooding in Queensland during 2010/2011, when the inefficiency of official rainfall forecasts using general circulation models became evident.



Dr. Andrew Hammond is a Senior Lecturer in Geoscience within CQUniversity's (formerly Central Queensland University) School of Engineering and Technology at its Rockhampton North Campus in Central Queensland, Australia, which is located close to the southern portion of the World Heritage-listed Great Barrier Reef. He holds BSc (Hons) degrees in geology and geography from the University of Tasmania, Australia; an M.Appl.Sc. in Soil Science from Lincoln University, New Zealand; and a PhD in Earth Science from Massey University, New Zealand. Dr. Hammond and his research students focus on geohazards (mass movement and floods), pedology, hydrogeology of coastal catchments, geomorphology, sedimentology and mine geology within Central Queensland.



# Contents

<b>Preface</b>	<b>XIII</b>
<b>Section 1</b>	
Flood Risk Prediction and Management	<b>1</b>
<b>Chapter 1</b>	<b>3</b>
New Frontiers in Flood Risk Management <i>by Guangwei Huang</i>	
<b>Chapter 2</b>	<b>19</b>
Flood Damage Reduction in Land Subsidence Areas by Groundwater Management <i>by Yin-Lung Chang, Jinn-Chuang Yang, Yeou-Koung Tung, Che-Hao Chang and Tung-Lin Tsai</i>	
<b>Chapter 3</b>	<b>39</b>
Evidence-Based Contingency Planning to Enhance Local Resilience to Flood Disasters <i>by Miho Ohara, Naoko Nagumo, Badri Bhakta Shrestha and Hisaya Sawano</i>	
<b>Chapter 4</b>	<b>55</b>
Fitting a Generalised Extreme Value Distribution to Four Candidate Annual Maximum Flood Heights Time Series Models in the Lower Limpopo River Basin of Mozambique <i>by Daniel Maposa</i>	
<b>Section 2</b>	
Flood Risk and the Urban Environment	<b>65</b>
<b>Chapter 5</b>	<b>67</b>
Flood Risk and Vulnerability of Jeddah City, Saudi Arabia <i>by Mohamed Daoudi and Abdoul Jelil Niang</i>	
<b>Chapter 6</b>	<b>87</b>
Flood Risk Assessment in Housing under an Urban Development Scheme Simulating Water Flow in Plains <i>by Faustino de Luna Cruz, Oscar A. Fuentes Mariles, Judith Ramos Hernández and Jesús Gracia Sánchez</i>	

<b>Section 3</b>	
Flood Risk and Agriculture	<b>109</b>
<b>Chapter 7</b>	<b>111</b>
Methodology for Agricultural Flood Damage Assessment <i>by Badri Bhakta Shrestha, Hisaya Sawano, Miho Ohara, Yusuke Yamazaki and Yoshio Tokunaga</i>	

# Preface

Flood risk management aims to minimise the human and socio-economic losses caused by floods, while also taking into account potential benefits. Flood risk depends on both the probability of a specific event occurring and the potential impacts. Floodplain management plans can impact on land use planning and thereby reduce flood risk for areas of new development. Flood risk management is more difficult to design and implement for existing developed areas. Modifications such as construction of dams or levees can lessen the impact of floodwaters. Modifications to existing buildings can mitigate flood damage, and appropriate measures can assist community response to floods.

This book is divided into three sections. The first section has chapters dealing with flood risk prediction and management. Topics covered include development of a framework for groundwater management as a component of flood damage management (illustrated for a coastal region in western Taiwan); development of flood assessment frameworks including flood duration, timing and vulnerability (illustrated for Japan); steps for local communities to conduct contingency planning and assist in deciding response strategies (illustrated for the Philippines); possible impacts of climate change on flooding (considered for Thailand) and forecasting of floods (using examples from Mozambique in Africa).

The second section of the book has chapters on flood risk and the urban environment, with specific examples for a coastal urban location illustrated by Jeddah, Saudi Arabia, and an inland urban environment illustrated by Mexico City. The third section deals with assessment of flood risks in the agricultural sector, specifically focusing on flood damage to rice crops in Asian river basins in the Philippines and Pakistan.

Flood risk management is important in many areas of the world. The book illustrates approaches developed for specific locations, but there is reason to believe that many of the approaches presented can be adapted to be generally applicable.

**John Abbot**

University of Tasmania, Australia  
Institute of Public Affairs, Australia

**Andrew Hammond**

CQUniversity, Australia



---

Section 1

Flood Risk Prediction and  
Management

---





# New Frontiers in Flood Risk Management

*Guangwei Huang*

## Abstract

Flood risk management has been studied extensively and intensively in many academic fields from civil engineering, sociology, economics, culture, and even psychology. However, the fact that flooding accounts for a greater number of damaging events than any other type of natural events worldwide on an yearly scale proves that our understanding of flooding is still insufficient, flawed, and fragmented. This chapter intends to shed new light on a number of issues that deserve more comprehensive study in order to advance flood risk management. As a result, a new two-layer framework of vulnerability is proposed, which can lead to a better understanding of, and new approaches to, flood risk management.

**Keywords:** vulnerability, framework, flooding time, flood duration, Ec0-DRR

## 1. Introduction

Flood disaster management includes flood risk assessment, risk mitigation, preparedness, and emergency response and rehabilitation efforts. It can also be classified into before, during, and after event activities. A flood risk assessment is an assessment of the risk of flooding from all flooding mechanisms and consists of three components: (1) hazard identification, (2) vulnerability analysis, and (3) exposure assessment. Mathematically, it can be expressed:

$$\text{Risk} = \text{Hazard} \times \text{Vulnerability} \times \text{Exposure} \quad (1)$$

According to UN-ISDR [1], hazard can be defined as a dangerous phenomenon, substance, human activity, or condition that may cause loss of life, injury or other health impacts, property damage, loss of livelihoods and services, social and economic disruption, or environmental damage. It can be quantified by a probability of occurrence within a specified period of time and within a given area and given intensity. The term exposure is used to indicate elements subject to potential damage due to a hazard. Elements here may be referred to population, houses, facilities, or physical and life infrastructure essential to the functioning of a society or community such as water supply system.

There are many aspects of vulnerability, related to physical, social, economic, and environmental conditions (see, for example, Birkmann [2]). Therefore, vulnerability can be defined in a number of different ways from as simple a notion as the degree of damage to an object exposed to a given hazard, to a more sophisticated one such as the characteristics and circumstances of a community, system, or asset

that make it susceptible to the damaging effects of a hazard. Thus, the choice of definition may depend on its suitability for a particular vulnerability study and its interpretation for policy or action. The fact that it can be approached in manifold ways offers both flexibility and difficulty to use and interpret.

Villagran de Leon proposed a different framework of risk, which consists of hazard, vulnerability, and deficiencies in preparedness [3]. Exposure was treated as a component of the hazard. The term “deficiencies in preparedness” was used to emphasize the lack of coping capacities of a society at risk. The pressure and release model [4] considers disaster as a product of two major forces: natural hazard and vulnerability. It was intended to stress the importance of vulnerability assessment.

No matter what framework one employs to deal with vulnerability and risk, the assessment should go beyond the identification of vulnerability and risk. It should probe into underlying driving forces and root causes in order to reduce or minimize them.

The objective of the present study is to highlight a number of shortcomings in conventional frameworks for flood risk management. A focal point is the framework for vulnerability.

## 2. Shortcomings in conventional frameworks

### 2.1 Hazard component related

Flood hazard is conventionally described by its probability of occurrence and severity (magnitude, duration, and extent of flooding). However, evidence has been mounting that the timing of a flood really matters. On July 7, 2018, Mabi town in Okayama Prefecture, Japan, near the confluence of the Takahashi River and the Odagawa River, was inundated due to levee breaches in the two rivers. As shown in **Figure 1**, the highest water level in the Takahashi River near the river junction occurred at 3:00 AM and exceeded the historical records. In this disaster, more than 50 people perished with 90% of the victims aged from 66 to 91. These elders lived either alone or with a senior spouse. For elders, evacuation during the night is difficult both physically and mentally. Besides, there were media reports and our own interviews heard the same story from people who suffered from inundation in various places in recent years that flood waters entering their homes rose so quickly that they had difficulty to escape. Therefore, inundation is not just a matter of

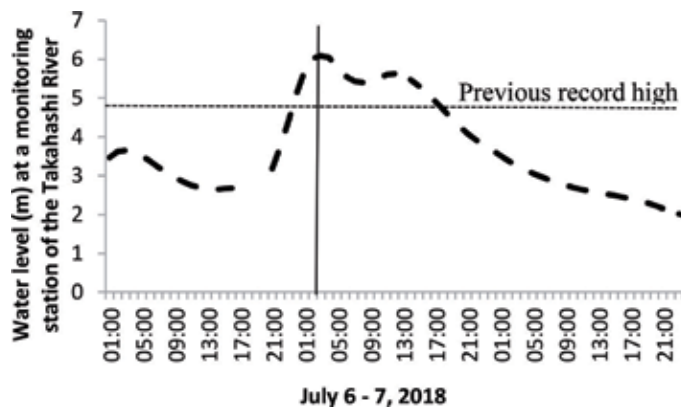


**Figure 1.** Hydrograph of the Takahashi River, Japan, on July 7, 2018, that peaked at 3:00 AM.

depth but also the rate of rising. The rate of inundation depth increase may depend on many factors such as local topography, the presence of structures, and urban drainage systems as well. So far, there is little information on the variation patterns of inundation depth with time during flood disasters. How fast the inundation depth would increase should be given serious consideration in flood risk management plans.

**Figure 2** shows the comparison of rising limb of hydrography at the Sakazu hydrological station between the largest-ever flood of the Takahashi River occurred in 2018, the second largest flood in 2011, and a small flood in 2015. It is clearly seen that the rate of water level increase depended on the intensity of a flood. The larger the intensity, the fast the water level increased. The current flood warning system in Japan is based on four water levels: (1) stand-by level, (2) flood watch level, (3) flood alert level, and (4) flood danger level. Such a warning system is essential for emergency evacuation. However, a problem with this system is that information on how fast the water level may rise from one level to another in an unprecedented flood is not available because it is intensity dependent as shown in **Figure 2**. How to provide real-time forecast on water level rising speed and incorporate it into the warning system is a technical issue to be explored. Besides, a related question is: is there a link between the rate of water level increase in channel and the temporal variation pattern of inundation depth in flooded area? It is also question deserving in-depth study.

On July 30 2011, the Ikarashi River in Niigata Prefecture, Japan, breached around 5:00 AM. In addition to the timing of inundation, other characteristics of this flood can be described as having two consecutive floods or a two-peak hydrological event. For the first peak, a dam in the upstream of the river regulated the peak, but for the even larger second peak, the dam failed to function since it was already at capacity.

These pieces of evidence serve to demonstrate that hazard identification should include flood peak timing and the possibility of multi-peaks in addition to probability and magnitude. However, methodology to consider these factors has not been developed.

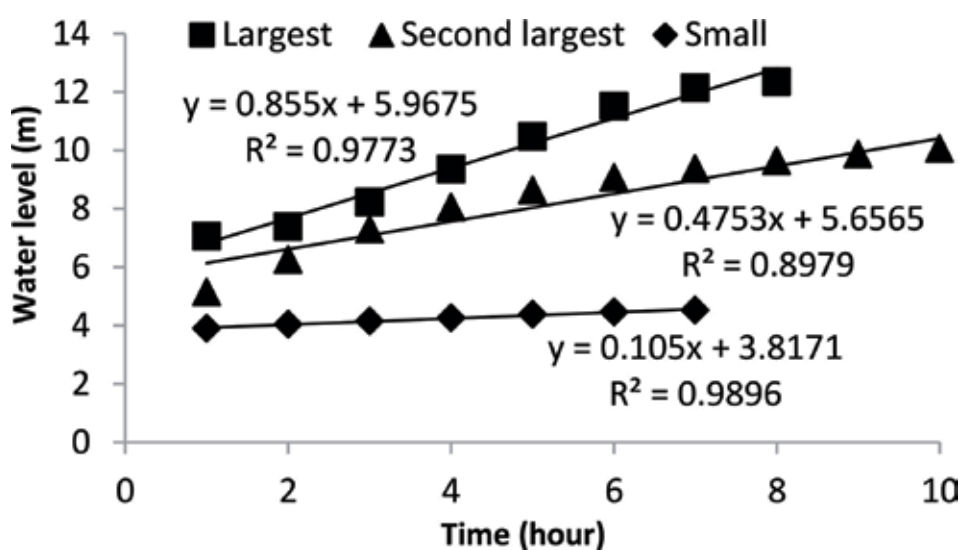


**Figure 2.**  
 Intensity dependency of flood water level rising rate.

## 2.2 Vulnerability component related

Vulnerability can be defined as follows:

$$\text{Vulnerability} = \text{Exposure to risk} + \text{Inability to cope} \quad (2)$$

However, if the framework for risk (1) is used, the definition of vulnerability should simply be inability to cope with hazard since exposure is treated separately. Füssel [5] reviewed the range of definitions of vulnerability and argued that continued plurality would become a hindrance in interdisciplinary research. A common definition of vulnerability is much needed to advance the understanding of vulnerability, yet reaching consensus is challenging. As a matter of fact, some scholars have argued that previous attempts to develop a shared vulnerability framework were superficial [6, 7].

O'Brien et al. [8] presented two dominant interpretations of vulnerability, which they refer to as outcome vulnerability and contextual vulnerability. Outcome vulnerability is considered as the residual exposure to impacts of climatic changes after adaptation responses have been factored in. Studies following this interpretation often take a sectoral view, looking at which/where is likely to be worst affected. Contextual vulnerability deals dynamically with the institutional, biophysical, socioeconomic, and technological conditions that affect the extent of exposure to climate changes and the ways in which those exposed can respond. Studies following this interpretation often take a more multidimensional view in a local setting, looking at how and why groups are affected differently in the context of other changes happening simultaneously. It is, therefore, more suitable to interdisciplinary and transdisciplinary studies. The present study attempts to combine outcome vulnerability and context vulnerability for the purpose of developing a more comprehensive and structured framework.

It is a two-layer structure consisting of system vulnerability (contextual vulnerability) and component vulnerability (outcome vulnerability) as shown in **Figure 3**. Factors affecting system vulnerability can be classified into four categories. (1) The social-economic-demographic category includes factors such as general risk perception, disaster insurance, medical care, GDP, and population distribution. (2) The institutional category includes planning capability, legal system and management capability, such as evacuation operations. (3) The biophysical category includes landform and land use, river basin scale, and river dynamics. Steep river channels often generate flash floods that are difficult to predict. On the other hand, mild waterways may generate much larger floods that could be more destructive if overflow occurred. (4) The engineering category includes flood defense and warning systems.

System vulnerability can be regulated by various structural measures such as levee and retarding basin construction and nonstructural measures such as flood hazard mapping and land use regulation. The interaction of various factors results in residual system vulnerability that is then passed on to component vulnerability (or outcome vulnerability). Component vulnerability is determined by awareness, self-preparedness, community strength, and even local culture. For example, a type of old Japanese house-Mizuka as shown in **Figure 4** is a measure of self-defense. It is a two-house compound, in which one is for everyday living and another is used as shelter in case of emergency. Living in such a house reduced component vulnerability. Nevertheless, the number of such houses in Japan has been largely reduced due to various reasons, especially changes in life style and a lowering of risk awareness.

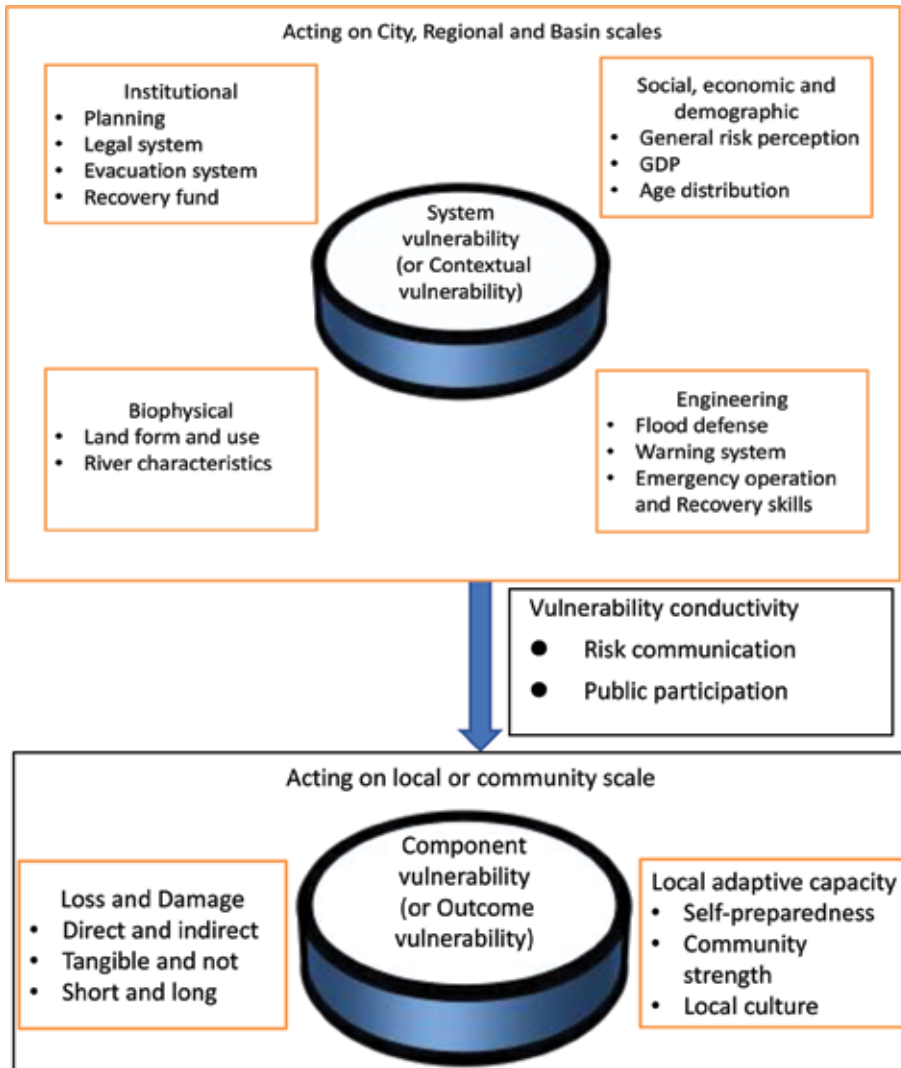


**Figure 3.**  
 A two-layer framework for vulnerability.

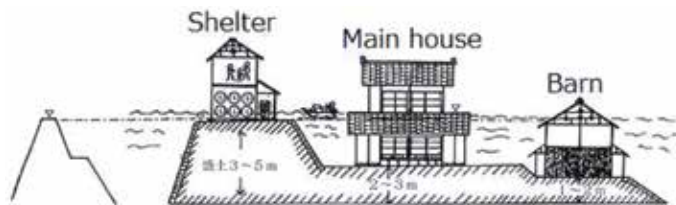


**Figure 4.**  
 A self-prepared traditional house in Japan-Mizuka.

System vulnerability acts at city, regional, or river basin scale, while component vulnerability acts at individual or community scale. The degree of passage from system to component vulnerability is termed as vulnerability conductivity hereafter. It depends upon risk communication and public participation. Risk communication is the exchange of information and opinions, and establishment of an effective dialog,

among those responsible for assessing, minimizing, and regulating risks and those who may be affected by the outcomes of those risks. This is the first attempt to incorporate risk communication into a vulnerability framework and to place one of its roles in the linkage between contextual and outcomes vulnerability.

Flood disasters may cause extensive loss of life and property damage, which is essentially an anthropogenic phenomenon with social roots. However, the dimension of loss and damage has been less focused on vulnerability framing so far. A conventional framework to address loss and damage is the  $C \times L$  framework as below:

$$\text{Risk} = \text{Consequence} \times \text{Likelihood} \quad (3)$$

where (i) likelihood is the probability of occurrence of an impact that affects the environment and (ii) consequence is the social and environmental impact if an event occurs.

This framework combines the scores from the qualitative or semiquantitative ratings of consequence and the likelihood that a specific consequence will occur to generate a risk score and risk rating. Although this risk framework takes into consideration the consequence of an event, it is not suitable for conducting integrated risk and vulnerability analyses. To incorporate loss and damage into the framework (1), vulnerability should be redefined as:

$$\text{Vulnerability} = \text{Inability to cope} \times \text{Potential consequence (loss and damage)} \quad (4)$$

The logic to include loss and damage in vulnerability is justifiable. If the level of impact upon an individual or community is low, then this individual or community is not truly vulnerable although they may not be able to prevent certain consequences from happening. Accordingly, the two-layer framework includes loss and damage as already depicted in **Figure 2**.

Following this vulnerability framework, a policy that is different from the conventional can be proposed as below.

Conventional flood countermeasures have focused on preventing flood waters from reaching populated areas such that blocking may be considered a keyword to describe the concept of conventional flood countermeasures. However, such a zero-risk approach has been shown to be in vain, especially in urban areas. In urban areas, in addition to the problems of asset concentration and surface imperviousness, complex urban structures may affect the behavior of flood waters in the case of inundation. Either intentionally or by chance, roads, railroads, and buildings may function as barriers to keep flood waters from spreading to a wider area [9]. Consequently, urban flooding may be characterized as being confined and deep. It is well documented that the degree of fatality and direct economic cost of flooding is proportional to inundation depth [10]. Therefore, redesigning urban form to transform confined and deep flooding to wide and shallow flooding is a way to reduce vulnerability if the prevention of inundation is not totally avoidable. The concept can be rephrased as “managing flood waters up to your knees”. Policy supporting such a concept can be termed flood sharing. How it can be implemented is a question to be answered.

An important driver of vulnerability reduction is better planning. Poorly planned and managed urbanization leads to growing flood hazard due to unsuitable land use change and increasing flood vulnerability due to development in flood-prone areas and overpopulation of such areas. As shown in **Figure 5**, river flood management planning in Japan starts with setting up a planning scale, which is the level of

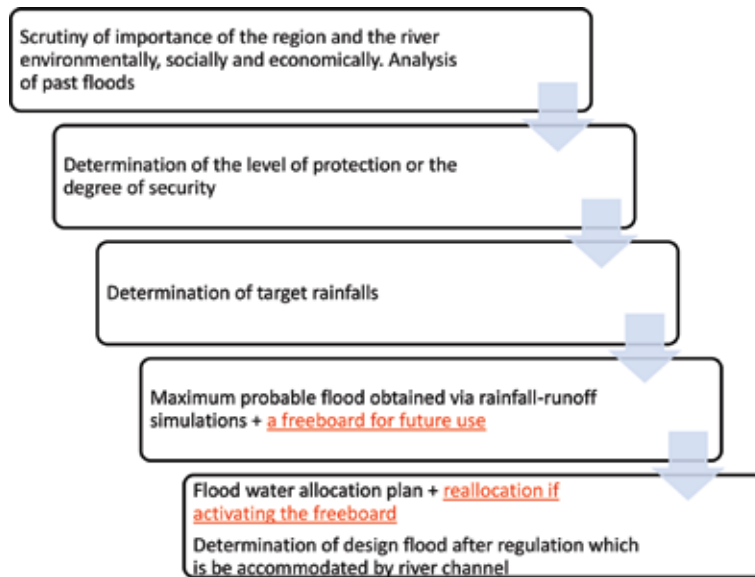


**Figure 5.** Procedure of flood management planning in Japan and a proposed modification (marked with red color and underline).

safety against flood disasters to be provided in the area of concern. The next step is to select a number of target rainfalls for the planning site based on rainfall and historical flood records. Then, by performing rainfall-runoff simulations, a flood hydrograph can be determined as the management target, which is termed as either design flood without regulation or maximum probable flood. Once the maximum probable flood is estimated, allocation of flood water by dam, retarding basin, and river channel will be determined to safely convey flood water to its destination. In this planning procedure, however, the increase of maximum probable flood due to future urbanization is not directly considered. The increase in the total volume of the direct runoff is also not taken into consideration in dam and retarding basin planning. In addition, urban development planners often neglect, or are not aware of, the possibility that development may partially invalidate the river flood management design in operation in the absence of sound development planning. The fact that the maximum probable flood would vary with significant changes in land use, resulting in an increase in peak flow in a river channel, has been given less attention by urban planners in planning development of housing projects along waterways. What is often observed is that countermeasures were being taken to reduce urbanization-induced flood risk years or decades after large-scale urban development, especially after experiencing serious flood disasters. Wording differently, approaches so far have often been reactive, not proactive. Therefore, a key principle of Low Impact Development or of a Sponge City should be that no significant increase in maximum probable flood results from the process of urban development. In Japan, the Act on Countermeasures against Flood Damage of Specified Rivers Running across Cities was put into effect in 2005. According to this law, any urban development with an area larger than 1000 m<sup>2</sup> should not cause any increase in surface runoff. If any increase is likely, permission from the competent authority is required. This law was first applied to the Tsurumi River basin since 2006 and currently implemented in seven river basins across Japan. However, monitoring studies on change of surface runoff in the seven targeted river basins are limited. The overall effectiveness of this regulation has not been validated. **Figure 6** shows where waterlogging occurred



**Figure 6.**

Locations of waterlogging (red dot) occurred in Kawasaki City during the period of 2008–2017 (source: Kawasaki City).

during the period of 2008–2017 in Kawasaki City, which is part of the Tsurumi River basin. **Figure 7** shows where waterlogging occurred during the period of 2006–2010 in Machida City, which is also part of the Tsurumi River basin. Although 3300 storage facilities have been installed in the river basin, inundation is still a frequent visitor to the region. Besides, the waterlogging locations in Kawasaki City are more or less uniformly distributed, while the waterlogging in Machida City mainly occurred along its administrative boundary on the west side. Such a difference in distribution of vulnerable locations may be viewed as one aspect of system vulnerability.

A fundamental issue in implementing this law is that it has not been directly linked to the river flood management planning procedure. To strike a good balance between flood risk reduction and economic development, the present study proposes a new planning scheme as shown in **Figure 5** with red color and underline. For new or redevelopment, the possibility of increasing maximum probable flood should be examined. If it is not possible to deal with the increase in maximum probable flood, the Act on Countermeasures against Flood Damage of Specified Rivers Running across Cities must be strictly implemented. If additional amounts of flood waters can be handled through reallocation such as constructing new or expanding the capacities of existing storage facilities, or by in-channel engineering works such as excavation, then the law can be executed to control the total amount of increase of surface runoff while having a priority setting to give permissions to economically important development projects.

### 2.3 Exposure component related

In cities like Tokyo, flood waters stay on streets for a few hours or a few days at most if inundation occurs. In other places such as Bangkok, however, flood waters



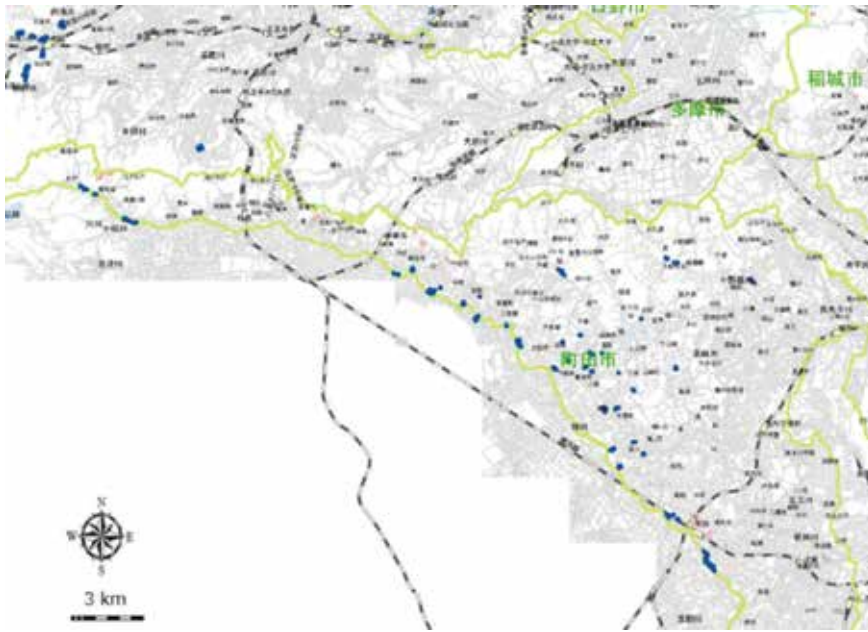


**Figure 7.** Locations of waterlogging (blue dot) occurred in Machida City during the period of 2006–2010 (source: Machida City).

may stay on streets for more than 2 months due to the city's topography and insufficient drainage capacity. In Thailand, the flood damage to Bangkok and five adjoining provinces in 1983 was estimated by the National Statistical Office to be billions of Bath with the bulk of the damage shouldered by the private sector. A study by Tang et al. indicated that flood depth and flood duration were significant factors explaining flood damage in the residential and industrial areas [11].

In view of such a difference in flood water residence time, the duration of inundation should be factored into exposure component, the longer the duration, the higher the level of exposure. Adding such a temporal factor to vulnerability framework will certainly lead to better planning for vulnerability reduction and smooth emergency response. It is also related to disaster insurance. To protect buildings that are constructed in flood-prone hazard areas from damage caused by flood forces, the National Flood Insurance Program (NFIP) in the United States requires that all construction below the base flood elevation must consist of flood damage-resistant building materials [12, 13]. What constitutes flood damage-resistant building materials is indeed duration dependent. The impact of duration is a much less explored research area and is envisioned to gain more attention in the near future.

### 3. Eco-DRR in Japan

Ecosystem-based disaster risk reduction (Eco-DRR) is a relatively new concept to reduce the risk of being exposed to natural hazards by avoiding development in disaster-prone areas or by using natural systems as a way to buffer the worst impacts of natural hazards, maintain the resilience of natural ecosystems and their ecosystem services, and help people and communities adapt to changing conditions [14, 15]. The core thinking of Eco-DRR is based on the realization that disasters cause massive damage to the environment, while degraded environments exacerbate disaster impacts and responding to disasters often leads to additional environmental impacts. Well-managed ecosystems, such as wetlands, forests, and

coastal systems, act as natural infrastructure, reducing physical exposure to many hazards and increasing socioeconomic resilience of people. For example, mangroves and seagrass beds can dissipate the destructive energy of storm surge and Tsunami and prevent coastal erosion while supporting fishing and tourism activities and storing high amounts of carbon. Therefore, Eco-DRR is also aimed at reducing the vulnerability of society and establishing disaster-resilient communities.

Japan has a tradition of using ecosystems for disaster mitigation such as maintaining forests to prevent soil erosion, planting trees along its coast to reduce wind-related disasters, and utilizing paddy fields to store flood waters temporarily. Since 2012, Eco-DRR has been incorporated into national policies and planning of the Japanese government. The Basic Act for National Resilience, enacted in 2013, is aimed at taking advantage of regional ecosystem-based functions to prevent and reduce disasters. Following this Act, Fundamental Plan for National Resilience was established to promote the use of ecosystem-based disaster reduction approaches and assessment of functions of Eco-DRR initiatives provided during nondisaster times. The National Spatial Strategy and the National Land Use Plan, approved in 2015, also called for the promotion of disaster management using natural ecosystems. Furthermore, Japan's Forest Law requires that Disaster Risk Management (DRM) forests should be planted along the coast to prevent damages from blown sand and salt, high tides, and tsunamis. Under such strong policy drivers, a question is "does it work?"

On March 11, 2011, the Great East Japan Earthquake occurred and triggered a major Tsunami. Consequently, the Tohoku area of Japan was so badly hit Tsunami. In total, this disaster caused more than 15,000 deaths, 2800 missing, and approximately 300,000 people being evacuated [16]. Among the disaster-stricken areas, Miyagi Prefecture suffered the most in terms of fatalities and infrastructure damage. Before the disaster, there were 200- to 400-m-wide pine forests along the Sendai Plains of Miyagi Prefecture having protected the area for the past four centuries. Nevertheless, the forest failed to stop the intrusion of the Tsunami. The coastline of Rikuzentakata City, Iwate Prefecture, was also very famous for its 2-km-long and 200-m-wide pine trees as shown in **Figure 8**. Again, the forest was completely destroyed except for one tree after the 3/11 Tsunami. There is no doubt that the forest along the coast of Tohoku region did reduce the energy of Tsunami. Although the forest was destroyed during the disaster, without it, fatalities and property damage would undoubtedly have been much greater. The question is how to quantify its effectiveness in relation to Tsunami height. It is not difficult to imagine that a coastal forest is effective to a Tsunami with low wave height. The information needed is the threshold of wave height above which a coast forest may fail to dissipate the energy of Tsunamis significantly. Koshimizu [17] pointed out that coastal forests could be rendered useless by liquefaction, but no countermeasures had been discussed. Besides, it should not be forgotten that a fallen tree being moved by a Tsunami can kill people and damage houses.

An interesting phenomenon was observed in Ishinomaki City, Iwate Prefecture. Along a portion of the Watanoha coast, the levee was lightly damaged, but the residential area behind was devastated as can be clearly seen in **Figure 9**. The levee height before the disaster was 4 m, and the Tsunami height in Ishinomaki was more than 8.6 m according to Japan Meteorology Agency. This implies that the Tsunami overtopped the levee without much energy dissipation. Otherwise, the levee would have been badly damaged. The same phenomenon may also apply to coastal forests if the height of a Tsunami is much higher than the height of the forest. After the disaster, the Japanese Government decided to invest ¥59 billion to restore 3660 hectares of trees in Tohoku, which were destroyed by the Tsunami [18]. However, as can be seen from Google Earth, the restoration of coastal forests has not produced



**Figure 8.**  
*Coast forest before and after the Tsunami disaster on March 11, 2011.*



**Figure 9.**  
*Devastated residential area behind a coastal levee.*

any visible progress. Instead of coastal forest, concrete levee is expanding along the coast as shown in **Figure 10**. This was also confirmed by author's field survey conducted in July 2018. Despite legislative development with regard to Eco-DRR in Japan, the implementation appears not straightforward. A multilayered defense system combining Eco-DRR measures with conventional concrete-based measures may deserve serious discussion or even debate.

Another case, which has been advocated as an example of Eco-DRR, is the Kabukuri-numa wetland in Osaki City, Miyagi Prefecture, Japan. In the 1970s, it was merely used as a flood-retarding basin. Large-scale dredging of the wetland was planned to increase its flood regulation capacity in 1996. However, in response to environmental concerns, the dredging plan was withdrawn. Instead, the area of the Kabukuri-numa wetland was expanded by transforming surrounding fallow farmland to wetland to meet the flood regulation demand. Furthermore, water was retained in surrounding paddies during the winter so as to function as semi-natural, but still important, habitat for wetland-dependent wildlife. In 2005, the Kabukuri-numa wetland and surrounding paddy fields were registered together as a Ramsar wetland site [19, 20]. As a result of this wetland expansion, a large number of waterfowls overwinter in Kabukuri-numa, eating fallen grain and weeds in the



**Figure 10.**  
*Current situation of defense construction along the Tsunami-hit coast.*

flooded paddy fields. The bird droppings, which are rich in phosphate, function as high-quality natural fertilizers for rice and enrich the soil. Rice cultivated under such an environment is branded as such and can be sold at a higher-than-average price. In addition, the large number of overwintering birds attracts a large number of tourists every winter. Although the ecosystem services of the Kabukuri-numa wetland during nondisaster times have been well demonstrated, its flood regulation capability has not been tested since there have been no large-scale floods in recent decades. In addition, there are concerns over the water quality of the wetland due to the large number and high concentration of birds. Bird droppings entering paddy fields may contribute to rice production but may also impact the water quality of adjacent wetlands if entering into its water body. As a matter of fact, water quality testing in the Kabukuri-numa wetland by the author of this chapter indicated that the water body is already eutrophic. How to make this Eco-DRR initiative sustainable is a question to be answered.

#### 4. Conclusion

The present work highlights a number of subjects in the arena of flood risk management that deserve further in-depth research, as summarized below.

In terms of flood hazard identification, flood peak timing and multi-peak hydrographs should be given more attention.

Due to the existence of various definitions and interpretations of vulnerability, there is a need to combine or group some of the notions, if the integration of all is impossible, for the sake of a better and deeper understanding of what really constitutes vulnerability. Following this line of thinking, a new two-layer framework of vulnerability is proposed, integrating existing concepts to a certain extent. This new framework may help develop new approaches to vulnerability reduction, with new concepts such as flood sharing.

This new framework also suggests that inundation duration should be included in the analysis of exposure.

Eco-DRR is an emerging approach to achieving both flood risk management and environmental conservation and may contribute to local economies as well. However, more cases of Eco-DRR across the world should be collected and analyzed from various angles in order to quantify its effectiveness and promote best practice. In Japan, Eco-DRR is advanced in terms of the legal framework supporting it, but there is great uncertainty in terms of its performance. Innovation is indispensable in reaching a new stage of flood risk management.

## **Acknowledgements**

This work was supported by Sophia Research Branding Project 2016.

## **Conflict of interest**

The authors declare no conflict of interest.

## **Author details**

Guangwei Huang  
Graduate School of Global Environmental Studies, Sophia University, Tokyo, Japan

\*Address all correspondence to: [huang@genv.sophia.ac.jp](mailto:huang@genv.sophia.ac.jp)

## **IntechOpen**

---

© 2018 The Author(s). Licensee IntechOpen. This chapter is distributed under the terms of the Creative Commons Attribution License (<http://creativecommons.org/licenses/by/3.0>), which permits unrestricted use, distribution, and reproduction in any medium, provided the original work is properly cited. 

## References

- [1] UN-ISDR. 2009 UNISDR Terminology on Disaster Risk Reduction. Geneva, Switzerland: The United Nations International Strategy for Disaster Reduction (UNISDR); 2009
- [2] Birkman J, editor. *Measuring Vulnerability to Natural Hazards: Towards Disaster Resilient Societies*. Tokyo: United Nations University Press; 2006
- [3] Villagran de Leon. *Manual para la estimacion cuantitativa de riesgos asociados a diversas*. Guatemala: Accion Contra el Hambre, ACH; 2004
- [4] Blaikie P, Cannon I, Davis B, Wisner B. *At Risk: Natural Hazards, People's Vulnerability, and Disasters*. 1st edn. London: Routledge; 1994
- [5] Füssel H-M. Vulnerability: A generally applicable conceptual framework for climate change research. *Global Environmental Change*. 2007;17(2):155-167
- [6] Pickett S, Burch W, Grove M. Interdisciplinary research: Maintaining the constructive impulse in a culture of criticism. *Ecosystems*. 1999;2(4):302-307
- [7] Newell B, Crumley C, Hassan N, et al. A conceptual template for integrative human-environment research. *Global Environmental Change Part A*. 2005;15(4):299-307
- [8] O'Brien K, Eriksen S, Nygaard L, Schjolden A. Why different interpretations of vulnerability matter in climate change discourses. *Climate Policy*. 2007;7:73-88
- [9] Huang G. From confining to sharing for sustainable flood management. *Sustainability*. 2012;4(7):1397-1411
- [10] Pistrika A, Tsakiris G, Nalbantis I. Flood depth-damage functions for built environment. *Environmental Processes*. 2014;1(4):553-572
- [11] Tang J, Vongvisessomjai S, Sahasakmontri K. Estimation of flood damage cost for Bangkok. *Water Resources Management*. 1992;6:47-56
- [12] FEMA. *Flood-Resistant Materials Requirements for Buildings Located in Special Flood Hazard Areas in Accordance with the National Flood Insurance*. Technical Bulletin 2-93; 1993
- [13] FEMA. *Flood-Resistant Materials Requirements for Buildings Located in Special Flood Hazard Areas in Accordance with the National Flood Insurance Program*. Technical Bulletin 2-08; 2008
- [14] Adger WN, Terry P, Folke HC, et al. Social-ecological resilience to coastal disasters. *Science*. 2005;309(5737):1036-1039
- [15] Estrella M, Saalismaa N. Ecosystem-based disaster risk reduction (Eco-DRR): An overview. In: Renaud F, Sudmeier-Rieux K, Estrella M, editors. *The Role of Ecosystem Management in Disaster Risk Reduction*. Tokyo: UNU Press; 2017
- [16] Ushiyama M. The death toll and characteristics of missing based on information available at the end of 2014. *Research Report of Tsunami Engineering*. 2015;32:61-69 (in Japanese)
- [17] Koshimizu H. *Harnessing the Power of Nature to Protect People and Cities. The World After 3.11* Top Page. Meiji University. Available from: [http://www.meiji.ac.jp/cip/english/after311/interview/interview\\_06.html](http://www.meiji.ac.jp/cip/english/after311/interview/interview_06.html) [Accessed: August 10, 2018]

- [18] Cyranoski D. Rebuilding Japan: After the deluge: Japan is rebuilding its coastal cities to protect people from the biggest tsunamis. *Nature*. 2012;**483**:141-143
- [19] Asano T, Mitsutake S, Hayashi K, et al. Conservation and utilization of a Ramsar site “Kabukuri-numa and the surrounding rice paddies”. *Bulletin of the Hiroshima University Museum*. 2012;**4**:1-11 (in Japanese)
- [20] Kurechi M. Restoring rice paddy wetland environments and the local sustainable society—Project for achieving co-existence of rice paddy agriculture with waterbirds at Kabukuri-numa, Miyagi Prefecture, Japan. *Global Environmental Research*. 2007;**12**:141-152 (in Japanese)





# Flood Damage Reduction in Land Subsidence Areas by Groundwater Management

*Yin-Lung Chang, Jinn-Chuang Yang, Yeou-Koung Tung,  
Che-Hao Chang and Tung-Lin Tsai*

## Abstract

Continuing land subsidence can diminish the effectiveness of an existing flood mitigation system and aggravate the flood hazard. This chapter demonstrates that, through groundwater management with an effective pumping scheme, flood hazard and related flood damage in land subsidence area can be reduced. The chosen study area is in the southwest coast of Taiwan, which has long been suffering from frequent and wide-spread flooding primarily due to land subsidence induced by groundwater overpumping. Numerical investigation in the study area clearly shows that effective management of groundwater pumping can play an important role in long-term sustainable solution for controlling the spatial-temporal variability of future land subsidence, preventing the flood hazard from worsening, reducing the flood damage, and satisfying the groundwater demand.

**Keywords:** flood hazard, flood damage reduction, risk analysis, groundwater management, land subsidence

## 1. Introduction

In the region with scarce or highly variable surface water resource, groundwater is a vitally important source of water for sustainable development of the region. Groundwater pumping without proper control and management could result in a rapid depletion of valuable groundwater resource, which cannot be replenished in a short period of time. Furthermore, the seriousness of land subsidence can be exacerbated, which is concomitant with increased flood hazard and damage. Phien-wej et al. [1] reported that the estimated flood damage attributed to land subsidence in the 1990s amounted to \$12 million annually in Bangkok, Thailand. Nicholls et al. [2], in their assessment of the exposure of population and assets to a 1-in-100 year surge-induced flood event at 136 port cities with more than one million inhabitants, indicated that the climate change and land subsidence contribute about one-third of increased flood exposure for people and assets. The impact of land subsidence induced by excessive groundwater extraction should be carefully examined in deltaic cities, especially in those coastal areas that are under rapid development.

By using inundation models, many studies have shown that flood hazard, after a long period of land subsidence, becomes worsened in cities like Semarang [3] and Jakarta [4] of Indonesia, Shanghai of China [5], and coastal cities around Northern

Adriatic Sea [6]. All the above studies showed that land subsidence results in increased flood inundation depth and areal extent, as well as diminishing effectiveness of existing flood protection systems. Even the flood defense system is upgraded to uphold the protection level, and the flood risk will be worsening with continuing land subsidence. Therefore, an engineered flood defense infrastructure system, jointly with a proper groundwater pumping practice with an aim to reduce land subsidence, could offer a sustainable solution to flood management problems in subsidence prone areas.

The goal for land subsidence mitigation can be achieved through effective management of groundwater pumping by constraining the drawdown. A comprehensive review of groundwater management (GWM) can be found elsewhere [7–9]. The common approach for handling subsidence control in GWM is to set a preconsolidation head as the lower bound of the groundwater level to prevent inelastic soil compaction from happening [10]. However, such an approach considers only the drawdown constraint that does not explicitly relate to the magnitude of land subsidence. To circumvent such deficiency, Chang et al. [11, 12] developed a mixed integer programming model for maximizing total pumpage, subject to drawdown and land subsidence constraints. 1D consolidation equation, which simultaneously considers inelastic and elastic soil compaction, is incorporated explicitly in the subsidence constraints.

As many studies have pointed out that the flood risk in land subsidence prone areas can be reduced through proper GWM (e.g., [1, 5]), and it is rarely found that flooding is explicitly incorporated into the model formulation. Chang et al. [13] developed a groundwater pumping optimization model, in conjunction with land subsidence and inundation models, to mitigate the land subsidence effect on flood hazard in land subsidence areas and satisfy the water demand. The GWM model determines the optimal pumping scheme for (1) minimizing land subsidence, (2) preventing flood hazard from worsening in the future, and (3) satisfying groundwater demand. This chapter, on the basis of the developed optimal groundwater pumping model [13], evaluates flood damage reduction and assesses economic benefit attainable by GWM in land subsidence prone coastal areas.

## 2. Methodology

### 2.1 Analysis framework

**Figure 1** shows the framework of analysis that was applied to a study area in the coastal zone of Taiwan (see Section 3.1 for more detailed descriptions) that is experiencing severe land subsidence problem largely due to groundwater overpumping. It can be seen that the analysis framework contains two major parts in which the first part is on the left branch for predicting the cumulative land subsidence in the study area over a 10-year period (2012–2021) based on the existing groundwater usage without management. Under this scenario, the groundwater pumpage in 2012–2014 in the study area was set to the historical average value as shown in **Table 1**. In 2015, a newly built Hushan reservoir began its service, and the groundwater pumpage during 2015–2021 was adjusted downward according to the planned water supply amount from the reservoir. The left branch of the analysis estimates the ground surface topography in the study area caused by land subsidence after 10 years of using the existing pumping pattern without optimal GWM. Flood hazard and inundation damage in the study area at the end of 2021 are assessed accordingly.

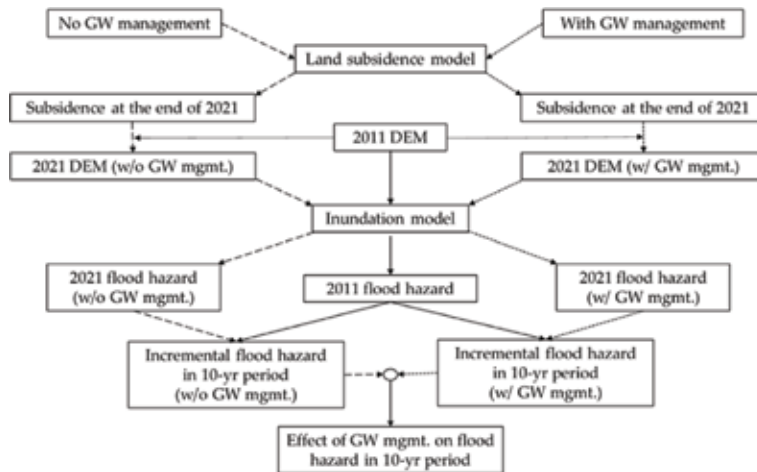


**Figure 1.**  
 Flow chart showing the methodological framework in the study.

Township	Area (km <sup>2</sup> )	Extraction		Recharge	
		Annual (10 <sup>6</sup> m <sup>3</sup> )	Intensity (mm/day)	Annual (10 <sup>6</sup> m <sup>3</sup> )	Intensity (mm/day)
Mailiao	80.17	107.55	3.68	27.25	0.93
Lunbei	58.48	115.89	5.43	7.46	0.35
Taisi	54.10	34.4	1.74	17.13	0.87
Dongshih	48.36	57.33	3.25	7.54	0.43
Baojhong	37.06	54.05	4.00	8.22	0.61
Tuku	49.02	56.6	3.16	6.39	0.36
Huwei	68.74	85.18	3.39	15.25	0.61
Sihhu	77.12	58.26	2.07	25.42	0.90
Yuanchang	71.59	89.01	3.41	9.93	0.38
Total	464.47	658.27	30.13	124.59	5.44

**Table 1.**  
 Groundwater extraction and natural recharge for the nine townships in the study area.

It should be pointed out here that, because of a relatively short management period of 10 years considered in the study, the rainfall condition was assumed to be stationary in assessing flood hazard and inundation damage. The indicators of flood hazard considered include the levee freeboard along the drainage channel systems and the maximum inundation depth in the study area. The freeboard is a measure of margin of safety, which is the vertical elevation difference from the levee crown to the water surface in the drainage channel. A reduction in the freeboard is an indication of increased overtopping potential of the levee system. The maximum inundation depth can be indicative of flooding severity. From the flood inundation simulation, the effect of subsidence on the flood hazard under the existing groundwater pumping practice can be assessed. With flood damage-inundation depth relationships available, the flood inundation risk cost can be assessed.

The second part of the analysis is shown on the right-hand branch of **Figure 1** in which the GWM model is applied to find the optimal pumping scheme by

minimizing the land subsidence effect on flood hazard while, at the same time, satisfying the water demand. After obtaining the optimal pumping strategy, the corresponding land subsidence amounts are obtained to define the land topography in Year 2021. Under a different topography, the corresponding flood hazard indicators and inundation damage are obtained for assessing the effect of GWM.

## 2.2 Inundation and land subsidence models

### 2.2.1 Inundation model

The well-known SOBEK Suite [14], developed by the Deltares Research Institute in the Netherlands, was used in the study to model flood inundation and the associated hazard. Specifically, the hydrodynamic module, which contains 1D-flow and 2D-overland flow submodules, was used to simulate surface water flow in the study area for determining the levee freeboard and inundation depth under the selected design rainfall events.

The major inputs to the SOBEK 1D/2D simulation for this study are as follows:

1. *Rainfall hyetograph*: 24-hour design rainfall with six design frequencies (i.e., 2-, 5-, 10-, 25-, 50-, and 100-year) was used. Their corresponding rainfall amounts were 158, 227, 275, 337, 384, and 432 mm, respectively. All six design storm events follow the same dimensionless rainfall pattern as shown in **Figure 2** [15]. For simplicity, no spatial variation of rainfall in the study area was considered.
2. *Downstream boundary*: since major drainage lines in the study area are connected to the Taiwan Strait, the boundary condition at the downstream end sections was assigned with a wave form shown as the dash line in **Figure 2**.
3. *Channel profile and DEM*: the cross-sectional profile along the drainage lines and DEM within the study area were surveyed in 2012. By considering the trade-off between the accuracy and computational efficiency of hydrodynamic simulation, the grid for the 2D overland flow simulation was set to 120 m. To simulate flood hazard with the projected land subsidence in 2021, the ground

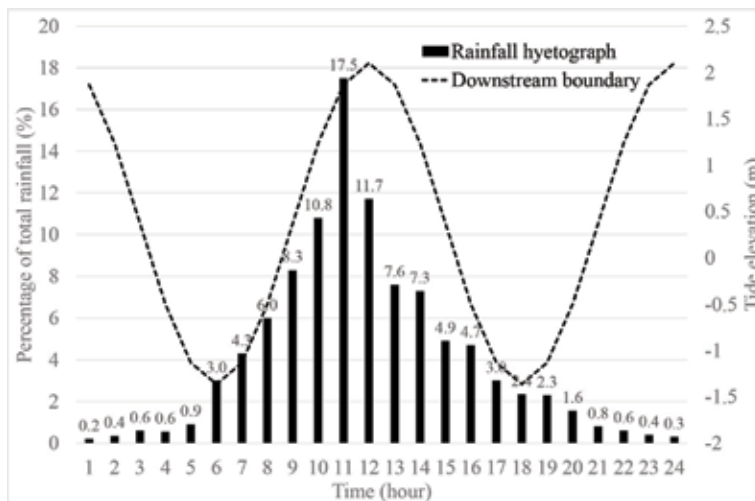


**Figure 2.** Dimensionless 24-hr design rainfall hyetograph and the downstream tide level for boundary condition [15].

elevation in 2012 was added by the cumulative land subsidence between 2012 and 2021 obtained by the land subsidence model under the conditions of with and without GWM.

4. *Roughness coefficient*: flow boundary roughness is categorized by the channel bed and overland surface. As almost all the drainage channels within the study area are man-made with gravel bottom and concrete siding, the nominal value of 0.02 for the Manning roughness coefficient was used according to Chow [16]. The roughness coefficient of the overland surface was determined by the land use listed in **Table 2**.

### 2.2.2 Land subsidence model

In this study, land subsidence is assumed to be caused by groundwater pumping. An uncoupled model consisting of a layered 3D groundwater solver and a 1D consolidation model was used to simulate land subsidence [17]. The layered 3D groundwater solver is first used to simulate depth-averaged groundwater flow and pore pressure head change due to groundwater extraction in every layer at each time step. The vertical soil displacement during each time step is then calculated by the 1D consolidation equation. The simulation model assumes (1) isotropic soil medium, (2) linear elasticity relationship between average effective stress and average displacement following Hooke's law, and (3) vertical displacements only. These assumptions, however, ignore the presence of the preconsolidation head, which implies that a decrease in pore pressure head due to groundwater extraction will always cause normal consolidation and is unable to consider overconsolidation and rebound (i.e., elastic range). This renders overestimation of land subsidence.

To simultaneously consider the inelastic/elastic behavior of land subsidence, Chang et al. [12] modified the 1D consolidation equation according to Leake [18] as

$$\Delta s_{l,k,t} = \begin{cases} \alpha C_c \left( \Delta h_{l,k,t}^p - \Delta h_{l,k,t-1} \right) + C_c \left( \Delta h_{l,k,t} - \Delta h_{l,k,t-1}^p \right), & \Delta h_{l,k,t} > \Delta h_{l,k,t-1}^p \\ \alpha C_c \left( \Delta h_{l,k,t} - \Delta h_{l,k,t-1}^p \right), & \Delta h_{l,k,t} \leq \Delta h_{l,k,t-1}^p \end{cases} \quad (1)$$

$$\Delta h_{l,k,t}^p = \text{Max} \left[ \Delta h_{l,k,t}, \Delta h_{l,k,t-1}^p \right] \quad (2)$$

where  $\Delta s_{l,k,t}$  = land subsidence within layer- $l$  at control point- $k$  during the  $t$ -th time period;  $\Delta h_{l,k,t}$  = drawdowns of layer- $l$  at control point- $k$  at the end of the  $t$ -th time period;  $\alpha$  ( $< 1$ ) = ratio of elastic to inelastic compaction per unit increase in drawdown;  $C_c = \rho_w g B / (2\mu + \lambda)$  with  $\rho_w$  = density of water,  $g$  = gravitation

Land use	$kn$
Agriculture	0.8
Built-up	10
Water conservation	0.2
Amusement and rest area	3
Transportation	1
Other	0.5

**Table 2.**  
 Relationship between the Nikuradse roughness coefficient  $kn$  and land use [15].

acceleration,  $B$  = layer thickness, and  $\mu, \lambda$  = Lamé constants; and  $\Delta h_{l,k,t}^p$  = difference between initial head and preconsolidation head at the end of the  $t$ -th time period. The positive value of  $\Delta h_{l,k,t}^p$  denotes that the initial head is higher than the preconsolidation head. The total land subsidence amount at the control point- $k$  can be determined by

$$\Delta s(k) = \sum_{l=1}^{NL} \sum_{t=1}^{NT} \Delta s_{l,k,t} \quad (3)$$

where  $NL, NT$  = the numbers of layer and time period, respectively. More detailed descriptions on the land subsidence model can be found in the studies of Chang et al. [11, 12].

In the process of developing the groundwater subsidence model for the study area, monitored data on pore pressure head and land subsidence during 2007–2009 were used to calibrate the model parameters such as hydraulic conductivity and soil compaction coefficients. Then, monitored data made in 2010–2011 were used for validation. The validated model was used to predict the cumulative land subsidence in the study area over a 10-year period during 2012–2021. Calibration and validation of pore pressure head and land subsidence in the study area were found quite satisfactory for pore water pressure and less satisfactory for land subsidence [13]. The reason might be because groundwater extraction alone is not the only cause for land subsidence. In addition, the 1D consolidation equation used in the land subsidence model cannot account for the body force and viscoelastic effects, which might have influences on land subsidence in thick aquitards. However, the validation results indicate that the simulation model can reasonably reproduce the general pattern of land subsidence in both time and space.

### 2.3 Optimal groundwater pumping model

Before developing a viable GWM for optimal pumping in the study area, insights were gained by applying the validated simulation model to examine the subsidence behavior under the existing pumping practice. The simulation results indicated that the levee freeboard and maximum inundation depth have a similar tendency in spatial variation affected by land subsidence. Both tend to become worsened in the near-shore low-lying area due to reduced difference between the sea level and levee crown elevation. Thus, continuing land subsidence would worsen the flood hazard in this area, and the results are consistent with those of Ward et al. [4] and Wang et al. [5]. On the other hand, outside the near-shore low-lying area, it was found that the freeboard and maximum inundation depth do not necessarily get worse. This is because the influence of the downstream boundary condition defined by the sea level is minimal. Instead, the relative variation of land subsidence in space becomes the dominant factor affecting the changes in freeboard and maximum inundation depth because it alters the slopes of drainage channels and the land surface.

By incorporating the above insights about land subsidence—flood hazard inter-relationship, an effective GWM model can be developed for reducing the undesirable pumping-induced land subsidence and flood hazard in the study area. For the near-shore low-lying area, one could reduce the land subsidence amount because flood hazard is highly related to the magnitude of land subsidence. For the region outside the near-shore low-lying area, one could reduce the relative variation of land subsidence in space to prevent flood hazard from worsening. The optimal groundwater pumping model can be formulated as

$$\text{Minimize max } [\Delta s(k_{uc})] \quad k_{uc} = 1, \dots, NUC \quad (4)$$

$$\text{Subject to } \Delta s(k_c) \leq \Delta s^*(k_c) \quad k_c = 1, \dots, NC \quad (5)$$

$$\sum_{j=1}^{NP} Q(j, t) \geq Q_D(t) \quad t = 1, \dots, NT \quad (6)$$

$$Q^L(j, t) \leq Q(j, t) \leq Q^U(j, t) \quad (7)$$

in which  $k_{uc}$  = the  $k_{uc}$ -th control point outside the near-shore low-lying area;  $k_c$  = the  $k_c$ -th control point within the near-shore low-lying area;  $NUC$  and  $NC$  = number of control points outside and inside the near-shore low-lying area, respectively;  $\Delta s(\bullet)$ ,  $\Delta s^*(\bullet)$  = cumulated and the maximum allowable land subsidence, respectively, at control points at the end of the management period;  $NP$  = number of pumping wells;  $Q(j, t)$  = pumping rate at the  $j$ -th well during the  $t$ -th time period;  $Q_D(t)$  = groundwater demand during the  $t$ -th time period; and  $Q^L(j, t), Q^U(j, t)$  = minimum and maximum allowable pumping rates, respectively, at the  $j$ -th well during the  $t$ -th time period.

The objective function Eq. (4) is to minimize the maximum land subsidence among all control points outside the near-shore low-lying area. The consideration of Eq. (4) can optimally reduce the magnitude and spatial variation of land subsidence outside the near-shore low-lying area. On the other hand, for any control point within the near-shore low-lying area, constraint Eq. (5) that directly limits the land subsidence can be imposed to prevent flood hazard from worsening due to the reduced levee freeboard.

### 3. Model application

To demonstrate the positive contribution of GWM to flood hazard reduction in land subsidence prone areas, the optimal groundwater pumping model developed by Chang et al. [13] is applied here to a selected study area in Taiwan.

#### 3.1 Description of the study area

The study area chosen has a catchment area of 267 km<sup>2</sup> located in the northwest part of Yunlin County, Taiwan (see **Figure 3**). The northern boundary of the study area is defined by the Zhuoshui River, the longest river in Taiwan, and the western boundary is adjacent to the Taiwan Strait. The study area covers nine townships and has four drainage systems consisting of Shihtsoliao, Yutsailiao, Makungtso, and Chiuhuwei. The mean annual rainfall in the study area is about 1200 mm of which about 80% of rainfall occurs between May and September due to monsoons and typhoons (see **Table 3**). Despite the fact that the mean annual rainfall in the study area is less than half of the average value in Taiwan (i.e., 2500 mm), the study area is still highly susceptible to flood hazard due to its low lying and flat terrain.

**Figure 4** is the topographic map of the study area, which shows its ground elevation ranging from -1.0 to 28 m with reference to the mean sea level. The east-to-west average land surface gradient is less than 1/1000 indicating that the surface runoff produced by heavy rainfall can be easily trapped in the study area. Furthermore, ground elevation in the downstream part of the study area is lower than the average spring high tide of 2.1 m. This implies that flood water in the drainage channels from a rainstorm event may not be effectively drained into the Taiwan Strait due to the backwater effect.

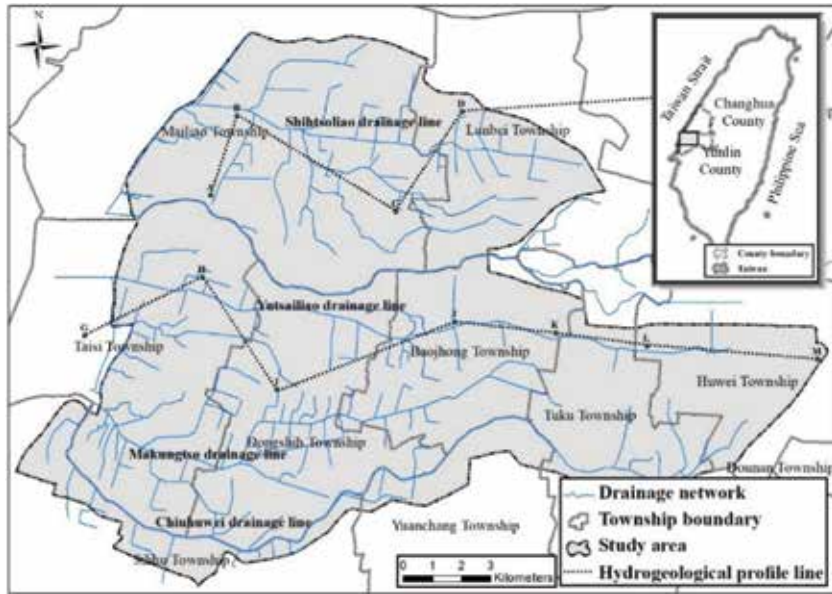


**Figure 3.**  
Geographical location of the study area.

Month	Jan	Feb	Mar	Apr	May	Jun
Rainfall (mm)	19.6	35.2	50.3	78.2	159.3	269.5
Month	Jul	Aug	Sept	Oct	Nov	Dec
Rainfall (mm)	209.5	221.6	100.8	16.7	18.1	14.8
Annual Avg (mm)	1176.8					

**Table 3.**  
Mean monthly rainfall amount in the study area.

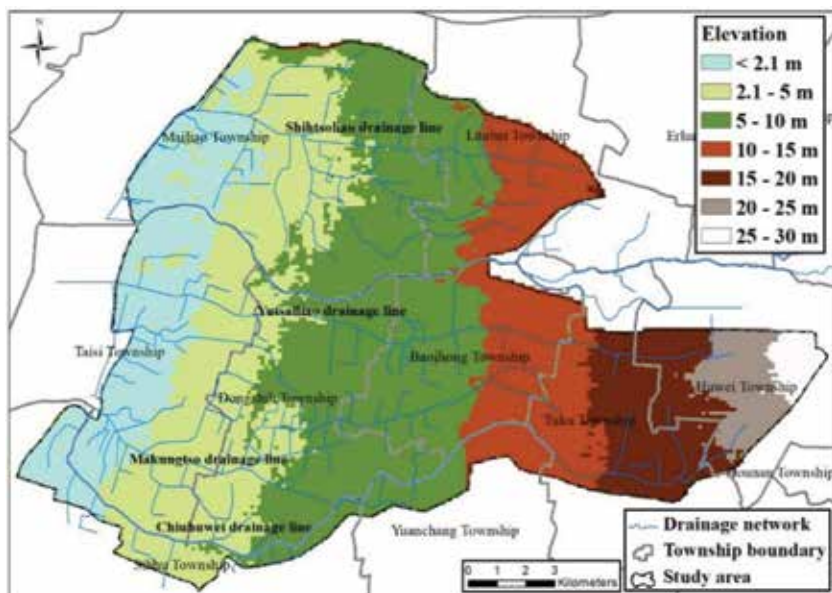


**Figure 4.**  
Spatial distribution of ground elevation in the study area.



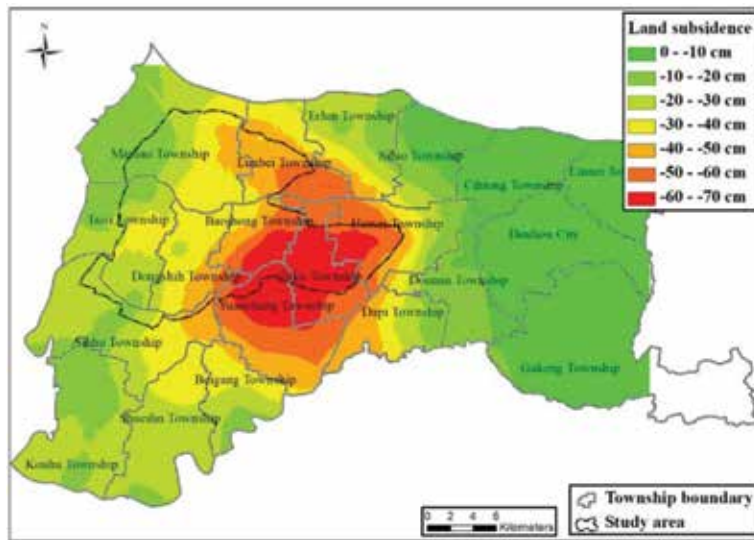


**Figure 5.**  
Contour map of cumulative land subsidence in 2002–2011 in the study area.

Yunlin County is an important region for agriculture and freshwater fish farming in Taiwan. The two activities require a tremendous amount of fresh water, especially the latter. Due to the lack of sufficient and stable surface water supply in the area, groundwater pumping is widely used to secure fresh water. According to the record, groundwater constitutes 30% of agricultural water usage and almost 100% of domestic use in Yunlin County. **Table 1** lists the average groundwater extraction and recharge for the nine townships in the study area which shows that annual average groundwater extraction significantly exceeds the annual natural groundwater recharge. Since groundwater has been excessively pumped for more than 30 years in the general area of Yunlin County, serious land subsidence problem has been created. **Figure 5** shows the cumulative land subsidence during 2002–2011 in Yunlin County with negative values representing the ground elevation being lowered.

The study area is highly susceptible to flooding due to low lying and flat terrain. Progressive land subsidence further exacerbates flood hazard. To mitigate flood hazard in the area, the Water Resources Agency (WRA) of Taiwan had spent more than 3 billion \$NT (approx. 0.1 billion \$US) during 2006–2013 to strengthen and heighten the sea wall and levee of drainage channels, construct the polder protection system, and upgrade the pumping stations and tidal gates. Because groundwater extraction in the area was not effectively controlled and managed, the land subsidence continued to erode away the effectiveness of flood protection infrastructure systems with time.

## 3.2 Effect of optimal GWM on land subsidence and flood hazard

### 3.2.1 Land subsidence

After the optimal pumping strategy is obtained, the right-hand branch of the analysis framework (see **Figure 1**) is implemented to evaluate the effect of GWM. **Figure 6** shows the change in the land subsidence amount under the conditions of with and without GWM. A positive-valued change means that the land subsidence is reduced under the optimal pumping scheme. **Figure 6** indicates that, while satisfying the groundwater demand of each township, the optimum pumping

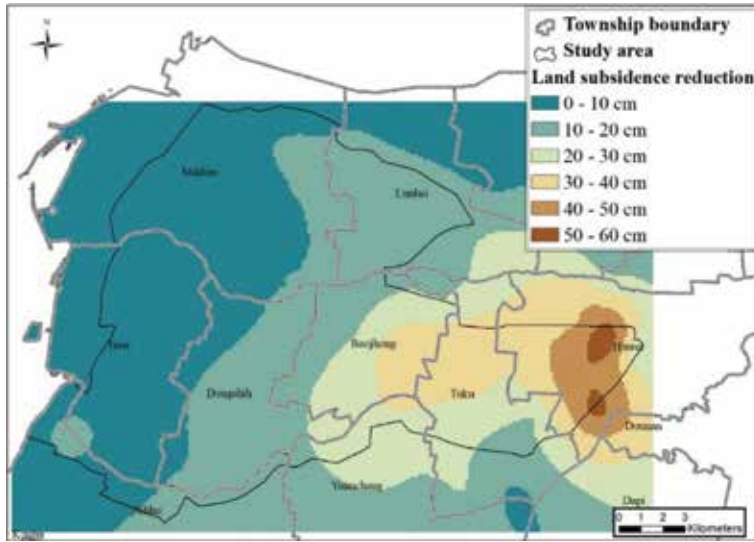


**Figure 6.** Reduction in cumulative land subsidence due to GWM in the study area.

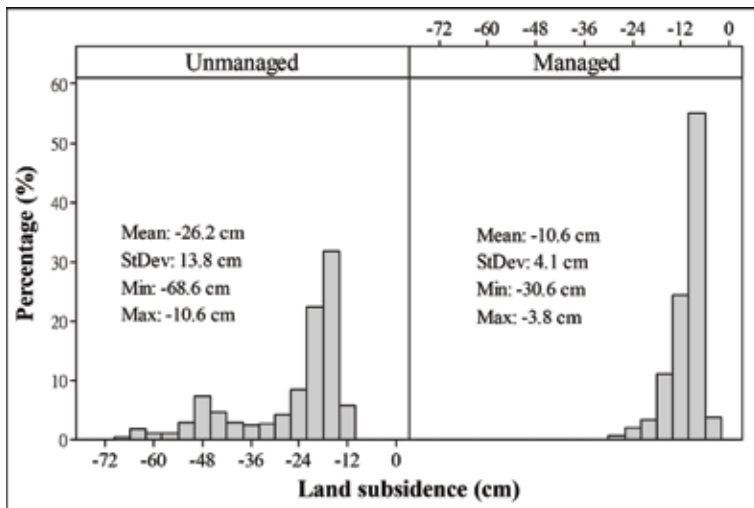


**Figure 7.** Histograms of the cumulative land subsidence in 2012–2021 under the conditions of with and without GWM.

strategy could greatly reduce the land subsidence in the study area. The most reduction in land subsidence ranging from 40 to 60 cm occurs in Huwei and Tuku townships where the land subsidence was the most serious without GWM.

**Figure 7** shows the histograms of cumulative land subsidence during 2012–2021 under the conditions of with and without GWM. Without GWM, the histogram on the left shows that the magnitude of land subsidence in the study area varies between  $-10$  and  $-68$  cm with the standard deviation of 13.8 cm. On the other hand, under the optimum pumping strategy, the histogram on the right shows that the range of land subsidence variation is greatly narrowed, and the standard deviation is reduced to 4.1 cm. Both **Figures 6** and **7** indicate that the magnitude and the spatial variation of land subsidence in the study area can be significantly reduced through optimum management of groundwater pumping.

### 3.2.2 Levee freeboard

Under the optimal GWM, **Figure 8** shows the change in the freeboard after a 10-year land subsidence where the study is subject to a 100-year design rainstorm. The solid black line in **Figure 8** is the contour of cumulative land subsidence over 2012–2021 with a contour interval of 2 cm. **Figure 9** further shows the histogram of the difference in the 2021 freeboard between the conditions of with and without GWM. The change with the positive value represents that the freeboard with GWM is greater than that without GWM when subject to a 100-year design rainfall. An

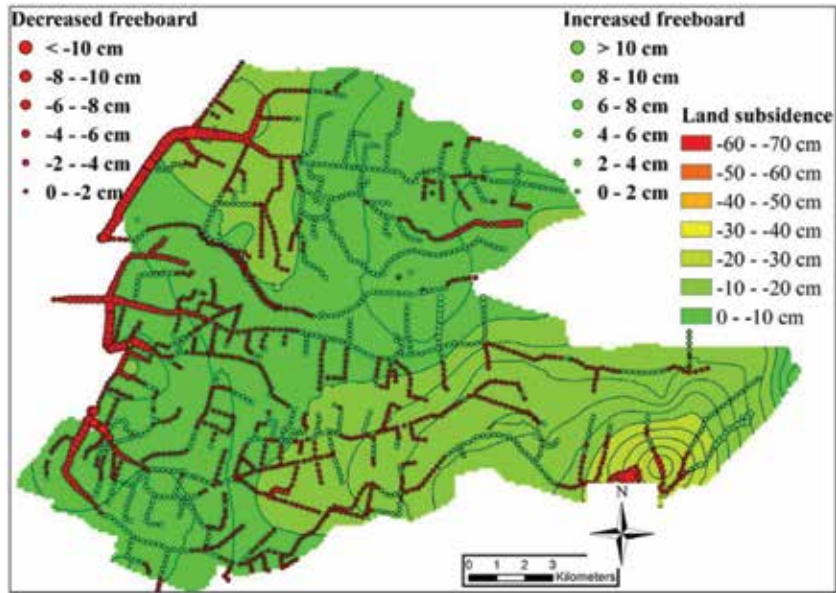


**Figure 8.** Change in the levee freeboard after a 10-year land subsidence under the 100-year design rainstorm with GWM.

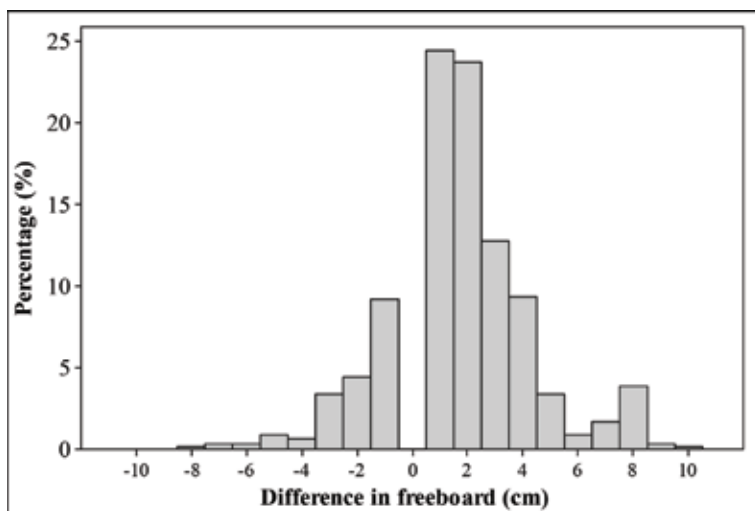


**Figure 9.** Histogram of the difference of the levee freeboard in Year 2021 between conditions of with and without GWM under the 100-year design storm.

increase in the freeboard indicates overflow potential from drainage channel systems that is reduced through GWM. The most significant difference reaches 8–10 cm which occurs in the near-shore low-lying area (see **Figure 8**). The results clearly indicate that GWM can prevent the levee freeboard from decreasing and thereby sustain the effectiveness of the existing flood protection system over the management period. Even if it is required to upgrade the protection level in some areas, GWM can render a smaller scale for upgrading work and lower capital cost.

### 3.2.3 Maximum inundation depth

**Figure 10** shows the difference in the maximum inundation depth in Year 2021 with and without GWM under the 100-year design rainstorm. The effect of GWM on the inundation depth is observed to be similar to that on the levee freeboard. It was found that the inundation depth in the near-shore low-lying area increases with 2021 land subsidence even with GWM. However, the range of increase is narrowed because the optimum pumping strategy greatly reduces the land subsidence in this area. The most reduction in inundation depth reaches 4–6 cm which occurs in the downstream of Yutsailiao and Chiuhuwei drainage lines (see **Figure 10**). The inundation depth could further be reduced if the maximum allowable land subsidence in Eq. (5) is set in a more restrictive manner. However, a more restrictive land subsidence control policy would result in a less amount of groundwater pumping which means that the current demand for the near-shore townships may not be satisfied.

Outside the near-shore low-lying area, the optimum pumping strategy can effectively prevent the inundation depth to be changed because of the reduced spatial variation of land subsidence. An exception is found at the farthest upstream from the Chiuhuwei drainage line where the inundated area grows larger with GWM because the land subsidence cone is moved to this area under the optimum pumping strategy. However, the gradient of land subsidence near this area under the condition of GWM is not as large as that of without GWM. Therefore, the increase in the inundated area would not greatly influence the flood hazard and the effectiveness of the existing flood protection system.

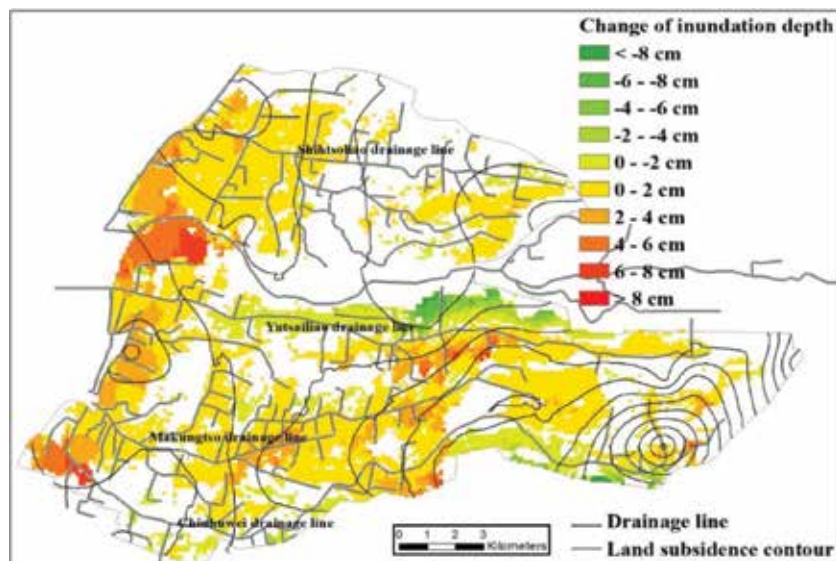


**Figure 10.** Change in maximum inundation depth after a 10-year land subsidence with GWM under the 100-year design rainstorm.

### 3.2.4 Flood damage reduction

To assess land subsidence-induced flood risk cost in the study area, representative relationships between inundation area and flood damage for several economic crops, aquacultural produces, and buildings were established and are shown, respectively, in **Figures 11–13** according to past flood events. Then, by applying the flood inundation model on different land surface topographies in the study area under the conditions of with and without GWM and the design

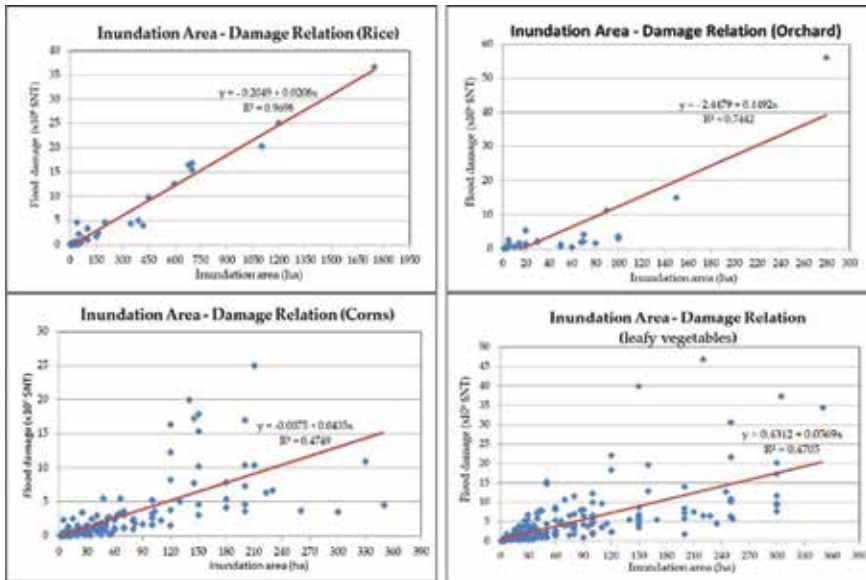


**Figure 11.**  
 Flood damage relationships for different agricultural produces.

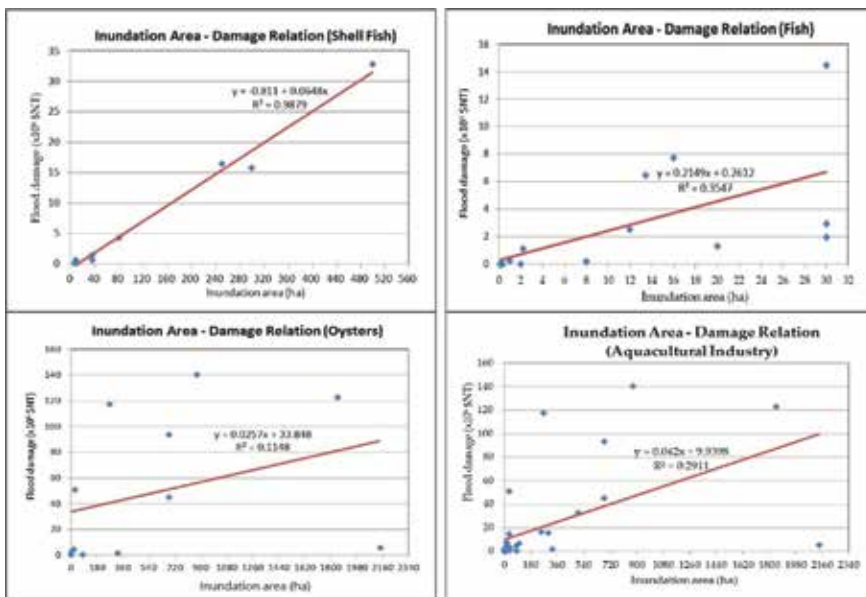


**Figure 12.**  
 Flood damage relationships for different aquacultural products.

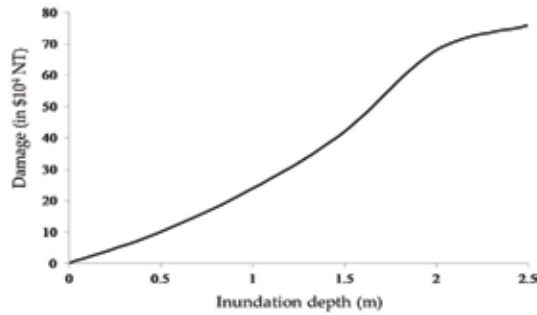


**Figure 13.**  
Damage-inundation depth relationship for buildings in the study area.

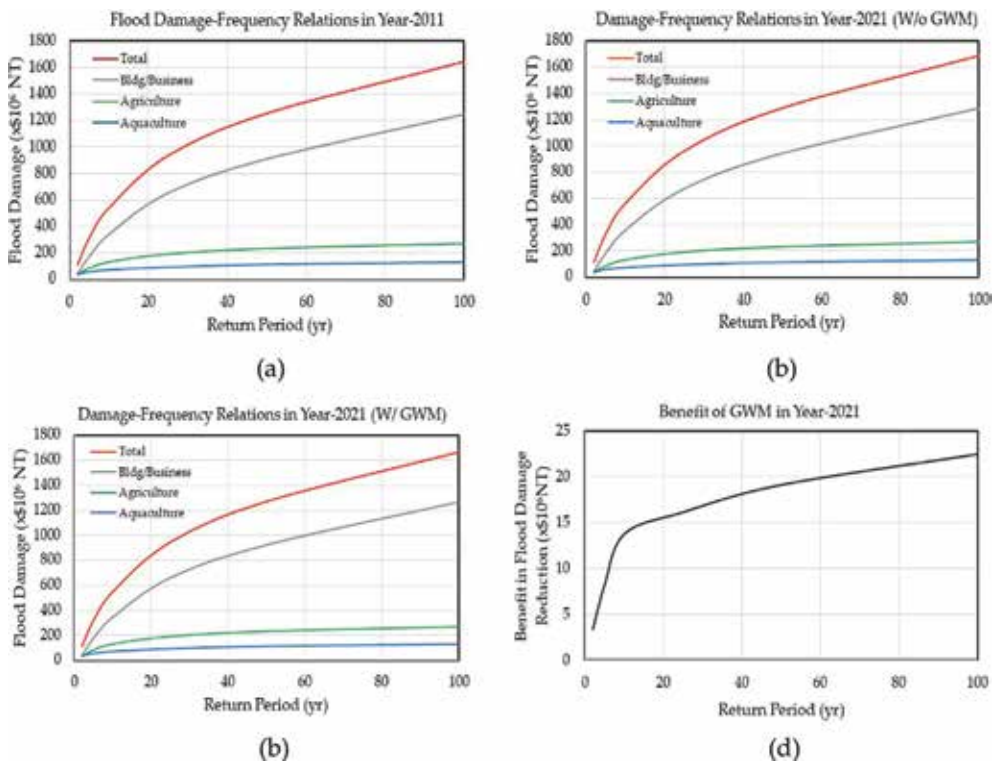


**Figure 14.**  
Flood damage-frequency relationships under different scenarios. (a) In Year 2011. (b) In Year 2021 W/o GWM. (c) In Year 2021 W/ GWM. (d) Difference between w/o and w/ GWM.

rainstorm of different frequencies, areal extent and maximum water depth of inundation can be determined. These hydraulic modeling results, jointly with land use maps and inundation-damage relationships, allow the establishment of damage-frequency relationships as shown in **Figure 14(a)–(c)**. **Figure 14(a)** is derived according to Year 2011 land topography of the study area which serves as the initial condition for the 10-year GWM period. **Figure 14(b)** and **(c)**, respectively, is based on Year 2021 land topography as the consequence of with and without implementing GWM. To assess the economic merit of implementing GWM, the benefit due to inundation damage reduction in Year 2021 can be obtained as the difference between inundation damage with and without GWM, that is,

$$B(T|2021) = InunDmg(T, w/o GWM| 2021) - InunDmg(T, w/GWM| 2021) \quad (8)$$

in which  $B(T|2021)$  = benefit of GWM (in terms of inundation damage reduction) in Year 2021 under a T-year rainstorm;  $InunDmg(T, w/GWM|2021)$  and  $InunDmg(T, w/o GWM|2021)$  = inundation damage in the study area with and without GWM, respectively, while subject to the T-year rainstorm. Based on **Figure 14(b)** and **(c)**, one can obtain **Figure 14(d)** showing the benefit-frequency relationship for implementing GWM in Year 2021. Then, the annual expected benefit by GWM in Year 2021 can be calculated by

$$E(B|2021) = \int_1^{\infty} B(T|2021) \left( \frac{1}{T^2} \right) dT \quad (9)$$

where  $E(B|2021)$  = annual expected benefit of GWM for the year at the end of the 10-year management period 2012–2021. Note that land subsidence is a continuous process that progresses over the GWM period. It is anticipated that, from the initiation of GWM in Year 2012, the task will begin to accrue flood damage reduction (FDR) benefit over each individual management year with an increasing rate. The present worth of cumulative expected FDR benefit over the 10-year management period can be obtained as

$$PW(EB) = \sum_{t=2012}^{2021} E(B|t) \times \left( \frac{1}{1+i} \right)^{t-2011} \quad (10)$$

in which  $PW(EB)$  = present worth of cumulative expected FDR benefit;  $E(B|t)$  = expected FDR benefit by GWM for Year- $t$ ; and  $i$  = interest rate. The term  $E(B|t)$  can be evaluated by Eqs. (8) and (9) for each individual year according to the flood inundation simulation results using the estimated land surface topography under the condition of with and without GWM. This would require hydraulic inundation simulation for each individual year, and the computation effort could be quite extensive.

To simplify the computation for economic merit assessment, it is assumed that the yearly FDR benefit increases linearly from zero in 2011 to  $E(B|2021)$  over a 10-year management period. That is, annual expected FDR benefit increases at an annual rate of  $E(B|2021)/10$ . With this discrete uniform gradient cash flow pattern, the present value of the total expected FDR benefit accrued over the 10-year management period,  $PW(EB)$ , can be computed as

$$PW(EB) = \left( \frac{E(B|2021)}{10} \right) \times UGPV(n, i) \quad (11)$$

where  $UGPV(n, i)$  = uniform gradient present worth factor, which can be computed by [19]:

$$UGPV(n, i) = \frac{(1+i)^n - (1+ni)}{i^2(1+i)^n} \quad (12)$$

in which  $n$  = length of management period, that is,  $n = 10$  in this application.

According to the total inundation damage-frequency relationships shown in **Figure 14(a)–(c)** and Eq. (9), the estimated annual expected inundation damages for Year 2011, Year 2021 (w/o GWM), and Year 2021 (w/GWM) are 213.695, 223.527, and 218.406 M\$NT (million New Taiwan dollars), respectively. Therefore, the incremental inundation damage in Year 2021 due to pumping-induced land

subsidence over a 10-year management period of with and without GWM are, respectively, 9.833 and 4.712 M\$NT. The benefit of GWM in Year 2021 associated with the expected FDR in the study area is  $E(B|2021) = 9.833 - 4.712 = 5.121$  M\$NT. Assume that the interest rate is 4.5% and the annual expected benefit by GWM follows a linear increasing pattern from 0 (in Year 2011) to 5.121 M\$NT (by Year 2021), the value of the uniform gradient present worth factor in Eq. (12) is  $UGPW(n = 10, i = 4.5\%) = 32.74$ . The corresponding present worth of the total benefit by GWM accrued in the study area over the 10-year GWM, by Eq. (11), is 16.768 M\$NT or equivalent to an annual benefit of 2.119 M\$NT amortized in 10 years.

By comparing the total amount of inundation damage amount in the study area (in the order of 200 M\$NT annually), the GWM benefit associated with FDR does not appear to be very impressive. This might be due to a relatively short management period of 10 years. For sustainable GWM, the period of management would generally be longer and it can be easily shown, by a similar analysis described above, that the economic benefit of GWM in terms of flood damage reduction would grow with the management period. Furthermore, **Figure 8** clearly shows that implementing GWM in the land subsidence prone area can sustain the design flood protection level of drainage systems by preventing the freeboard from decreasing. This implies that potential huge saving in the capital cost can be realized because the lower levee height in many parts of the study area would be sufficient if an effective GWM policy is in the place. Also, the maintenance cost for levee systems could be reduced as fewer existing levee segments require height upgrading because the mandated freeboard can be upheld or even improved by GWM.

#### 4. Conclusions

Groundwater is an important source of water supply, especially in regions where surface water supply is insufficient or not stable. However, the lack of proper management for groundwater extraction and usage in land subsidence prone areas could create a number of undesirable consequences such as damaging building structures, aggravating flood inundation hazards, and diminishing effectiveness of flood control facilities. This chapter presents a methodological framework demonstrating how a subsidence-focused GWM model can be formulated and applied to obtain an optimal pumping strategy that reduces the negative impact of land subsidence in a coastal region in western Taiwan which is experiencing serious land subsidence and associated flood hazards. Numerical results clearly show that, through the use of an optimal GWM model with an explicit consideration given to subsidence control, one is able to ease off uneven land surfaces and reduce seriousness of land subsidence and flood damage as well as sustain the flood protection level of drainage systems by maintaining a suitable freeboard. All these features provide strong evidence that GWM can play an important role, along with other engineering measures, in providing a sustainable solution to flood inundation problem in land subsidence prone areas.

#### Acknowledgements

This study was support by the Water Resources Planning Institute, Water Resources Agency, Ministry of Economic Affairs of Taiwan.



## Conflict of interest

No potential conflict of interest is present in this chapter.

## Nomenclature

$B$	layer thickness
$E(B t)$	expected FDR benefit by GWM in Year- $t$
$g$	gravitation acceleration
$i$	interest rate
$InunDmg(T, w/GWM t)$	inundation damage in the study area with GWM while subject to the T-year rainstorm
$InunDmg(T, w/o GWM t)$	inundation damage without GWM while subject to the T-year rainstorm
$k_{uc}$	the $k_{uc}$ -th control point outside the near-shore low-lying area
$k_c$	the $k_c$ -th control point within the near-shore low-lying area
$NC$	number of control points inside near-shore low-lying area
$NL$	number of layers in groundwater aquifer
$NP$	number of pumping wells
$NT$	number of groundwater management period
$NUC$	number of control points outside near-shore low-lying area
$Q(j, t)$	pumping rate at the $j$ -th well during the $t$ -th time period
$Q_D(t)$	groundwater demand during the $t$ -th time period
$Q^L(j, t)$	minimum pumping rates at the $j$ -th well during the $t$ -th time period
$Q^U(j, t)$	maximum allowable pumping rates at the $j$ -th well during the $t$ -th time period
$UGPW(\bullet)$	uniform gradient present worth factor
$\alpha$	the ratio of elastic to inelastic compaction per unit increase in drawdown
$\Delta s_{l, k, t}$	land subsidence within layer- $l$ at point- $k$ during the $t$ -th time period
$\Delta h_{l, k, t}$	drawdowns of layer- $l$ , point- $k$ at the end of the $t$ -th time period
$\rho_w$	density of water
$\Delta h_{l, k, t}^p$	difference between initial head and preconsolidation head at the end of the $t$ -th time period
$\Delta s(\bullet)$	cumulated land subsidence at control points at the end of the management period
$\Delta s^*(\bullet)$	maximum allowable land subsidence at control points at the end of the management period
$\mu, \lambda$	Lame constants

## **Author details**

Yin-Lung Chang<sup>1</sup>, Jinn-Chuang Yang<sup>1</sup>, Yeou-Koung Tung<sup>1\*</sup>, Che-Hao Chang<sup>2</sup>  
and Tung-Lin Tsai<sup>3</sup>

1 Disaster Prevention and Water Environment Research Center, National  
Chiao-Tung University, Hsinchu, Taiwan

2 Department of Civil Engineering, National Taipei University of Technology,  
Taipei, Taiwan

3 Department of Civil and Water Resources Engineering, National Chiayi  
University, Chiayi, Taiwan

\*Address all correspondence to: yk2013tung@gmail.com

## **IntechOpen**

---

© 2018 The Author(s). Licensee IntechOpen. This chapter is distributed under the terms of the Creative Commons Attribution License (<http://creativecommons.org/licenses/by/3.0>), which permits unrestricted use, distribution, and reproduction in any medium, provided the original work is properly cited. 

## References

- [1] Phien-wej N, Giao PH, Nutalaya P. Land subsidence in Bangkok, Thailand. *Engineering Geology*. 2006;**82**(4): 187-201
- [2] Nicholls RJ, Hanson S, Herweijer C, Patmore N, Hallegatte S, Corfee-Morlot J. Ranking port cities with high exposure and vulnerability to climate extremes: Exposure estimates. In: OECD Environment Working Papers, No. 1. OECD Publishing; 2008
- [3] Marfai MA, King L. Tidal inundation mapping under enhanced land subsidence in Semarang, Central Java Indonesia. *Natural Hazards*. 2008; **44**(1):93-109
- [4] Ward PJ, Marfai MA, Yulianto F, Hizbaron DR, Aerts JCJH. Coastal inundation and damage exposure estimation: A case study for Jakarta. *Natural Hazards*. 2011;**56**(3):899-916
- [5] Wang J, Gao W, Xu SY, Yu LZ. Evaluation of the combined risk of sea level rise, land subsidence, and storm surges on the coastal areas of Shanghai, China. *Climatic Change*. 2012;**115**(3-4): 537-558
- [6] Gambolati G, Teatini P, Gonella M. GIS simulations of the inundation risk in the coastal lowlands of the Northern Adriatic Sea. *Mathematical and Computer Modelling*. 2002;**35**(9-10): 963-972
- [7] Freeze RA, Gorelick SM. Convergence of stochastic optimization and decision analysis in the engineering design of aquifer remediation. *Ground Water*. 1999;**37**(6):934-954
- [8] Gorelick SM. A review of distributed parameter groundwater management modeling methods. *Water Resources Research*. 1983;**19**(2):305-319
- [9] Gorelick SM, Zheng C. Global change and the groundwater management challenge. *Water Resources Research*. 2015;**51**(5):3031-3051
- [10] Phillips SP, Carlson CS, Metzger LF, Howle JF, Galloway DL, Sneed M, Ikehara ME, Hudnut KW, King NE. Analysis of tests of subsurface injection, storage, and recovery of freshwater in Lancaster, Antelope Valley, California. U.S. Geological Survey Water-Resources Investigations Report 03-4061. 2003. pp. 93-100
- [11] Chang YL, Tsai TL, Yang JC, Tung YK. Stochastically optimal groundwater management considering land subsidence. *Journal of Water Resources Planning and Management*. 2007; **133**(6):486-498
- [12] Chang YL, Huang CY, Tsai TL, Chen HE, Yang JC. Optimal groundwater quantity management for land subsidence control. In: Proceedings of the IASTED International Conference on Environmental Management and Engineering, 4-6 July 2011; Calgary, A. B., Canada. pp. 38-45
- [13] Chang YL. The influence of hydrologic and topographic uncertainties on inundation risk in Southwest coastal area. Water Resources Planning Institute, Water Resources Agency, Ministry of Economic Affairs, Taiwan. Report: MOEAWRA1020238. 2013 (in Chinese)
- [14] Deltares. SOBEK, User Manual. Delft, The Netherlands: Deltares; 2014
- [15] WRPI. Handbook for Planning of Regulation and Environment Rehabilitation of Drainage System. Taiwan: Water Resources Planning Institute, Water Resources Agency; 2006. (in Chinese)

[16] Chow VT. Open Channel Hydraulics. McGraw-Hill; 1959

[17] Tsai TL. The development and application of model of regional land subsidence due to groundwater overpumping [thesis]. Hsinchu, Taiwan: National Chiao Tung University; 2001. (in Chinese)

[18] Leake SA. Interbed storage changes and compaction in models of regional groundwater-flow. *Water Resources Research*. 1990;26(9):1939-1950

[19] Park CS, Sharp-Bette GP. *Advanced Engineering Economics*. Wiley; 1990. p. 740

# Evidence-Based Contingency Planning to Enhance Local Resilience to Flood Disasters

*Miho Ohara, Naoko Nagumo, Badri Bhakta Shrestha and Hisaya Sawano*

## Abstract

The Sendai Framework for Disaster Risk Reduction 2015–2030 addresses the importance of “Enhancing disaster preparedness for effective response and to ‘Build Back Better’ in recovery, rehabilitation and reconstruction” as the fourth priority action. One of the practical tools to achieve effective preparedness for flood disaster response is evidence-based contingency planning, which is based on scientific approaches such as flood simulation and quantitative risk assessment. This method, however, is not always feasible to disaster-prone areas in Asia due to the lack of data on natural and social conditions. This chapter proposes a method with six steps for local communities to conduct contingency planning by assuming the dynamic change of inundation using flood simulation, assessing flood risk with key indicators, deciding response strategies against the identified flood risk and developing a contingency plan beforehand. This method was first applied to one of the Asian flood-prone areas, Calumpit Municipality in the Pampanga River basin of the Philippines, to verify its effectiveness in areas where the availability of natural and socio-economic data is limited.

**Keywords:** contingency planning, disaster response, flood, risk assessment, simulation

## 1. Introduction

Preparing a contingency plan before disasters is essential to increase the capacity of personnel in charge of disaster response and enhance local resilience to disasters. The Sendai Framework for Disaster Risk Reduction 2015–2030 [1], adopted at the Third United Nations World Conference on Disaster Risk Reduction in 2015, addresses the importance of “Enhancing disaster preparedness for effective response and to ‘Build Back Better’ in recovery, rehabilitation and reconstruction” as the fourth priority action. More specifically, its paragraph 33 states that national and local governments shall prepare or review and periodically update disaster preparedness and contingency policies, plans and programmes with the involvement of the relevant institutions, considering climate change scenarios and their impact on disaster risk and facilitating, as appropriate, the participation of all sectors and relevant stakeholders [1].

In order to achieve effective disaster response, it is important first to assume possible disasters, then quantify expected disaster damage and conduct contingency planning based on the scenarios of the possible disasters. One of the practical tools to carry out this process is evidence-based flood contingency planning, which is based on scientific approaches such as flood simulation and quantitative risk assessment. This planning method, however, is not always feasible to disaster-prone areas in Asia due to the lack of data on natural and social conditions. To overcome such a challenge, the International Centre for Water Hazard and Risk Management (ICHARM) focuses on flood disasters and proposes an effective method for local communities to predict the dynamic change of inundation using flood simulation, assess flood risk with key indicators, decide coping strategies against the identified flood risk and develop a contingency plan beforehand. This method is first applied to one of the flood-prone areas in Asia, Calumpit Municipality in the Pampanga River basin of the Philippines, to verify its effectiveness in areas where the availability of natural and socio-economic data is limited.

## 2. Proposal of evidence-based flood contingency planning

The “ISO22301 Societal security—Business continuity management systems” specifies requirements for all types of organisations to plan, implement, review and improve a documented management system to prepare for, respond to and recover from disruptive incidents [2]. It requires the organisations to select business continuity strategy based on the outputs from the risk assessment and business impact analysis. The risk assessment aims to identify and evaluate the risk of disruptive incidents to the organisations, while the business impact analysis assesses the impacts of disrupting activities that support organisation’s services. To conduct evidence-based flood contingency planning in reference to the procedures employed in the ISO22301, six steps are proposed, as shown in **Figure 1**.

The first step of this planning is to understand the current conditions of the target communities such as topography, land use, population and structures, as well as

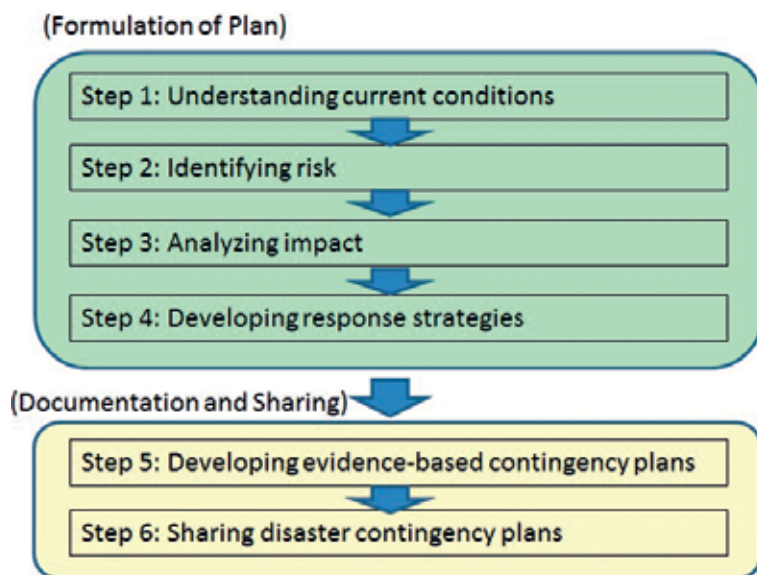


**Figure 1.** Six steps of evidence-based flood contingency planning.

past flood records in the area. At the second step, flood hazards and risks are identified through flood and inundation simulations conducted by national or provincial governments. Flood scenarios are presented with two key components, i.e. a flood inundation map and a time-series inundation water chart, to illustrate dynamic changes in inundation depth for residents to easily understand how the inundation may expand, linger and recede in their communities. The third step is flood impact analysis, in which the numbers of residents and houses at risk are estimated based on the average ground-floor height of houses, and possible problems the community may face due to the flood are identified. At the fourth step, the communities in the target area should develop a response strategy. Necessary actions should be discussed according to the time sequence of “before the flood”, “during the flood” and “after the flood”. The fifth and sixth steps are documentation and sharing of the plan among the community members. It is also important that the produced plan should be updated constantly through the Plan-Do-Check-Act cycle.

### 3. Case study area

Among the Asian flood-prone areas, a municipality called Calumpit was selected as the first case study area. It is in Bulacan Province in Pampanga River basin located northwest of Metro Manila in Central Luzon Island, Philippines. The municipality lies at the junction of several rivers, including Pampanga, Angat and Labangan, as illustrated in **Figures 2** and **3**. This topography makes Calumpit one of the most flood-prone municipalities in the Philippines. As of 2010, 101,068 people live in an area of 5625 ha, or 2.03%, of the province. The municipality has 29 barangays, the smallest administrative units. The recent largest flood was caused by Typhoons

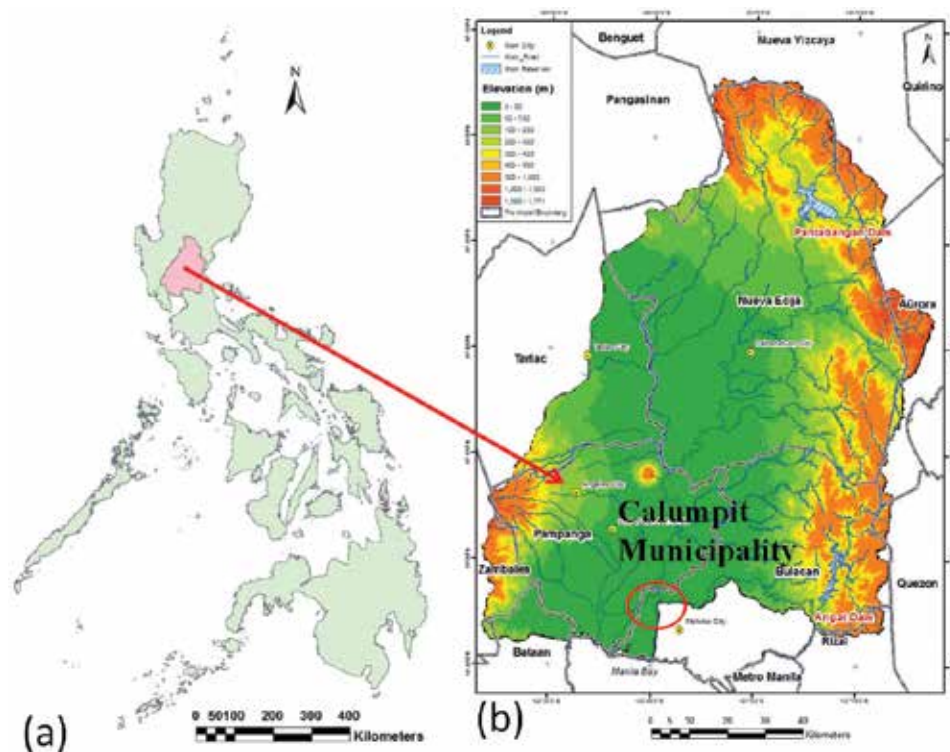


**Figure 2.** Location of Calumpit in Pampanga River basin. (a) Luzon Island and (b) Pampanga River basin).



**Figure 3.**  
*Land use map of Calumpit [4].*

Pedring and Quiel in September 2011, and a large area of the municipality suffered massive flood damage. Due to an inundation of 1.2–1.5 m deep, Calumpit lost its government functions, which consequently impeded emergency response.

The Philippine Disaster Risk Reduction and Management Act (Republic Act No. 10121) [3], enacted in 2010, provides for the development of policies and plans and the implementation of actions and measures related to all aspects of disaster risk reduction and management. It defines the National Disaster Risk Reduction Management Council (NDRRMC) as the national organisation to coordinate, integrate, supervise, monitor and evaluate disaster policymaking. It also mandates the establishment of the Disaster Risk Reduction and Management Office in every barangay, municipality, city and province.

Calumpit has the Municipal Disaster Risk Reduction Management Council (MDRRMC) and the Barangay Disaster Risk Reduction Management Council (BDRRMC) in its 29 barangays. The act defines MDRRMCs and BDRRMCs to perform functions such as designing and coordinating disaster risk reduction and management activities, supporting risk assessments and contingency planning activities at the local level [3]. Following this act, the MDRRMC of Calumpit published a contingency plan [4], which describes governmental emergency response in case of a flood. It assumes casualties, structural damage and impacts on livelihood, infrastructure and facilities in the worst-case scenario, based on the experience during Typhoons Pedring and Quiel in 2011. However, the scenario based on the past flood experiences makes it difficult to assume future floods of different scales which have never occurred before. It is therefore recommended to make contingency plans by quantifying a spatial distribution of expected damage and necessary needs in consideration of dynamic changes in inundation depth provided from flood inundation simulations performed for each community.

#### 4. Case study of evidence-based flood contingency planning

The proposed method was applied to Calumpit Municipality in Bulacan Province.



**Figure 4** illustrates overall activities related to the six steps to be proposed. The first and second steps were applied to the whole area of the municipality in April 2014. At the third and fourth steps, two flood-prone communities were selected as model sites, and their flood contingency plans were jointly developed through workshops with community leaders and members. In the workshops, the participants discussed problems they may face during the flood of each scale and proposed necessary response actions in order to make response strategies. The final workshop was held in March 2016, inviting all the community leaders in the municipality, and the experience in the workshops was shared among the participants. The following subchapters detail each step:

#### 4.1 Step 1: understanding current conditions

In areas where the availability of natural and socio-economic data is limited, administering interviews and questionnaires to local government officials, community leaders and local people is useful to understand the current conditions of their localities. In this study, interviews were conducted at MDRRMO and selected communities [5]. The surveys found that population census data at the barangay level was available, while the spatial distribution data of buildings was not. Then, a questionnaire survey was administered to all 29 barangay leaders to understand the building conditions in each barangay. The houses in the 29 barangays were classified and tallied according to construction types and storeys. Of those, 62.5% were a one-storey structure, while the rest were two-storey.

Interviews at the selected individual households were also conducted to understand recent flood damage, including the damage status of house structures, property and family members and their behaviours during the recent floods. During the interviews, the survey staff measured the heights of the first floor, ceiling and flood marks from the past floods with the permission of family members. From the household survey, it was found that the average first-floor height of the one-storey houses was 0.54 m from the ground, while that of the two-storey houses was 0.17 m, as shown in **Figure 5**. **Table 1** summarises the conditions of the houses at five inundation levels using the thresholds from the household interviews. Different damages to the livelihood of the residents are listed according to inundation levels. Inundation level 1 with a water depth of 0.17 m or lower did not inundate inside the house. At

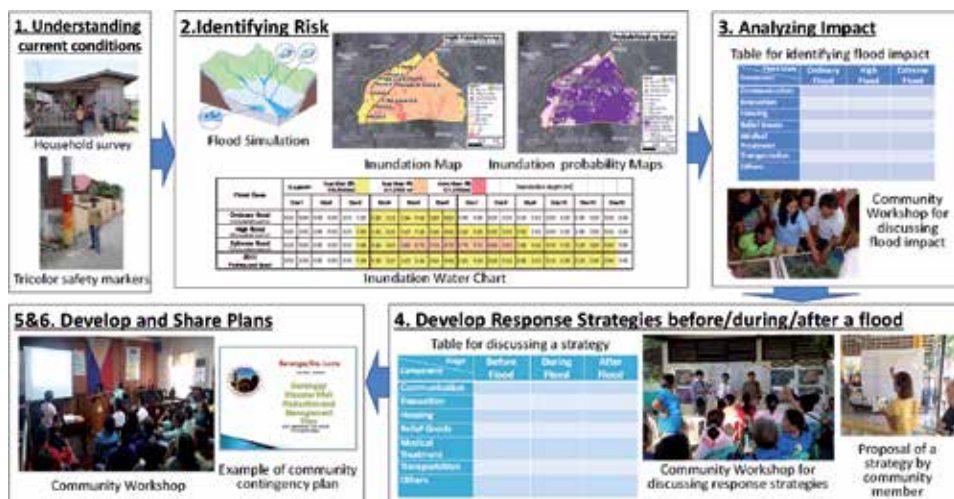


**Figure 4.** Activities at six steps of evidence-based flood contingency planning.

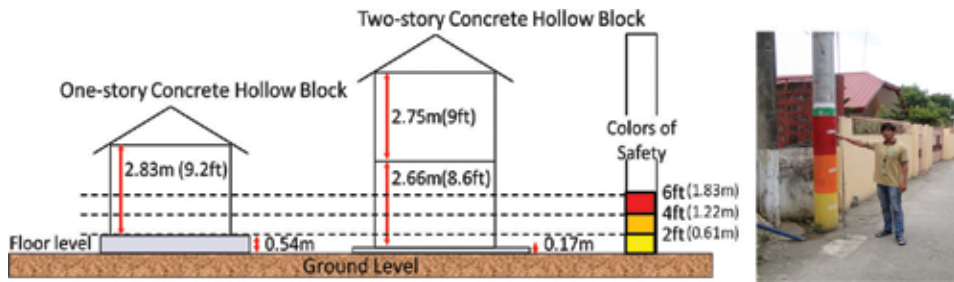


**Figure 5.**  
Threshold of inundation based on measurement results.

inundation level 2, the two-storey houses started being inundated. At inundation level 3, at which the water depth exceeds 0.54 m, both one- and two-storey houses suffered from inundation above the first floor, which suggests that the residents had to stay somewhere above the water level or evacuate to safer places near their houses.

The household interviews also found that the inundation above electric plugs caused severe damage to daily life. The height of electric plugs averaged 1.27 m and that of LP gas tanks 0.60 m. The residents usually move LP gas tanks to the second floor or to the rooftop to use them for cooking during an inundation. Inundation level 4 was set, based on the observed average height of electric plugs, as the condition cutting local people off from power. At inundation level 5, the inundation depth exceeds 2.83 m, the height of the second floor of a house. Under this situation, they could not find an evacuation space due to the rarity of buildings having three storeys or more, which means an inundation of this scale is likely to be a potentially life-threatening crisis for the residents.

Calumpit Municipality has its own community flood warning system called “colours of safety”. This system uses power poles painted in three colours (yellow, orange and red) by every 2 ft to visualise the level of danger and help residents make decisions on evacuation. At present, 193 electric poles in the municipality are tricoloured for this purpose. The residents are advised to evacuate before the water reached the red colour.

#### 4.2 Step 2: identifying flood risk

In this step, the expected flood inundation area was delineated by flood inundation simulation using the rainfall-runoff-inundation model (RRI model), developed

Level	Inundation Height (m)	One story house	Two story house
Level 1	0.0-0.17	No inundation	No inundation
Level 2	0.17-0.54	No inundation	Start Inundation
Level 3	0.54-1.55	Inundation	
Level 4	1.55-2.83	Inundation (Cannot use electricity)	
Level 5	Above 2.83	Inundation (A house is submerged)	Inundation (Inundation exceeds average height of second floor)

**Table 1.**  
Conditions of houses at each inundation level.

by ICHARM. The RRI model is a two-dimensional model capable of simulating rainfall, runoff and flood inundation simultaneously Sayama et al. [6]. The model deals with slopes and river channels separately. It applies a 2D diffusive wave model to flows on slope grid cells and a 1D diffusive wave model to channel flows. The software of the model can be downloaded from the ICHARM website [7] for free.

We used the RRI model that Shrestha et al. [8] locally customised to conduct flood simulation for the Pampanga River basin and performed hazard mapping for Calumpit Municipality, following the eight sub-step procedures [5] presented below:

Sub-step 1: acquisition of input data for the model.

Sub-step 2: acquisition of flood mark records.

Sub-step 3: flood inundation simulation during Typhoons Pedring and Quiel in September 2011 (grid, 200 m).

Sub-step 4: calibration of the model by comparing observed and simulated discharges in sub-step 3.

Sub-step 5: validation of the model by comparing the simulation results with flood mark records.

Sub-step 6: frequency analysis using rainfall data.

Sub-step 7: flood inundation simulation using design rainfall assumed with 10-, 30- and 100-year return periods.

Sub-step 8: development of inundation depth maps in Calumpit with 10-, 30- and 100-year return periods (grid, 5 m).

The simulation used the high-resolution digital elevation model (DEM) of 5 m grid, observed by the interferometric synthetic aperture radar (IFSAR) and provided by the National Mapping and Resource Information Authority (NAMRIA) in the Philippines without a fee. Inundation simulation for the River basin was first conducted using DEM data of 200 m grid created by IFSAR. After the flood inundation simulation, a grid of Calumpit with the inundation depth of 5 m was developed by obtaining the difference between the floodwater surface level of 200 m grid and the ground-level surface level of 5 m grid by IFSAR. As a result of the flood inundation simulation, three kinds of flood inundation maps with 10-, 30- and 100-year return periods were produced for ordinary, past largest and extreme floods. From the frequency analysis using past rainfall data, a return period of the flood caused by Typhoon Pedring in 2011 was estimated to be 28.3 years. The occurrence of flood inundation with a 30-year return period means the reoccurrence of the 2011 flood. **Figure 6** shows the inundation maps produced in this step.

Municipal personnel pointed out that the word “return period” is too technical for residents to understand. Thus, to help them understand the flood scale easily, floods were named according to their scales as “ordinary flood” for 10-year return period floods; “high flood” for 30-year return period floods, whose scale is roughly equal to the largest recorded flood in 2011; and “extreme flood” for 100-year return period floods.

Based on the flood simulation results, maps and a chart were created for each barangay, as shown in **Figure 7**. As mentioned above, Calumpit Municipality has its own community flood warning system called “colours of safety” in which power poles are painted in three colours by every 2 ft to visualise the level of danger and help residents make decisions on evacuation. The inundation maps for each barangay (**Figure 7b**) adopted this locally familiar tricolour system to show the inundation depth.

In addition to inundation maps with three different return periods, inundation probability maps, time-series inundation charts and resource maps were also developed for each barangay. The inundation probability map (**Figure 7c**) was created to help people understand the most frequently inundated areas, by combining the information of three inundation maps with 10-, 30- and 100-year return periods.

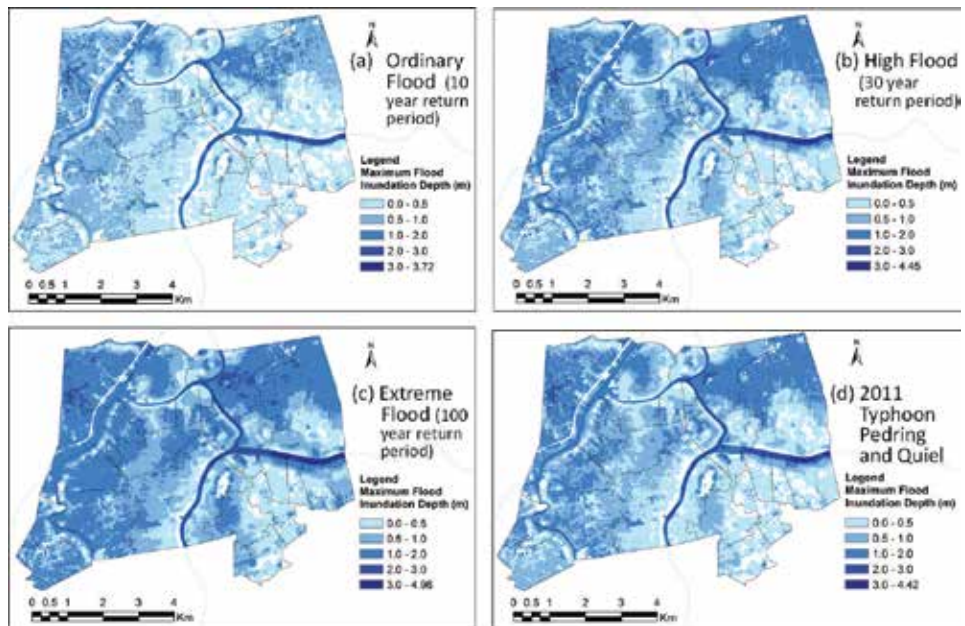


Figure 6. Maximum inundation depth maps.

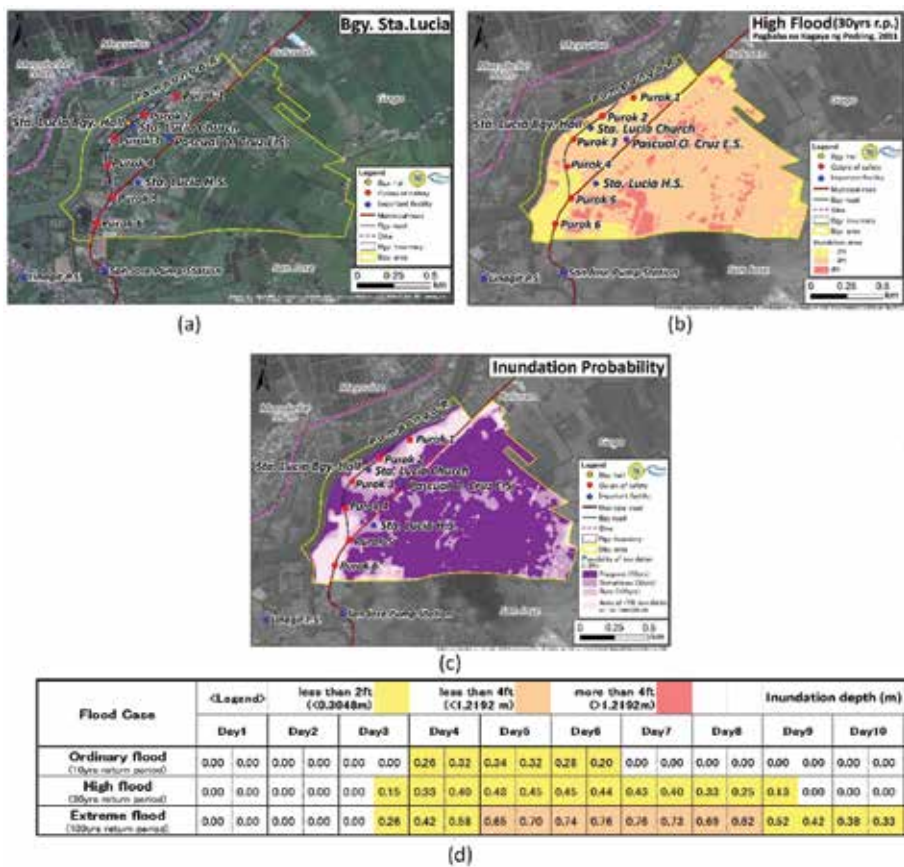


Figure 7. Maps and chart for each barangay (example of Barangay Santa Lucia).

The map shows the probability of inundation that may exceed 2 ft. (0.61 m) or higher, the depth almost equal to the height of the first floor of a one-storey house. The area in dark purple colour indicates that one-storey houses in the area may be inundated above the first-floor level in case of a 10-year return period flood. The time-series inundation chart (Figure 7d) shows the chronological development of inundation in a barangay using different colours. From this chart, people can understand how many days the area may be inundated according to different flood scales. In the resource map (Figure 7a), the locations of barangay halls, evacuation centres and electric poles for “colours of safety” were plotted.

In order to quantify flood risk at each community, the number of affected residents was estimated based on damage levels by overlaying inundation maps on the population distribution map of each barangay. Since most of the municipal area of Calumpit is used for agricultural purposes, we considered it reasonable to assume that the population is not uniformly distributed over the municipal area but disproportionately distributed in the built-up areas. For this reason, the built-up areas were identified. The identification of the built-up areas was made using satellite images because no digital land use maps were available. If accurate land use maps are available, they can be used for the purpose. The population in each barangay was assumed to be evenly distributed in its identified built-up areas. Then, the number of affected residents in each barangay was estimated according to inundation levels (Table 1). As a result, the total ratio of affected residents living in the area with inundation levels 3–5 was calculated to be 55.9% for a 100-year flood, while 34.6% for the past maximum flood case, as shown in Figure 8. That well over 55% of the population may suffer at inundation level 3 or above in a 100-year flood means both one- and two-storey houses are very likely to be inundated above the floor.

Figure 9 shows the estimated number of affected residents in each barangay in both flood cases. In case of a 100-year flood, more than 90% of the residents in barangays of Sapang Bayan, Corazon, Bulusan, Gugo and San Jose may suffer from an inundation of level 3 or above. They should prepare for prompt evacuation in case of such a severe flood. In this case study, only the number of affected residents was analysed due to a lack of spatial distribution data of buildings. If the data is available, the number of damaged houses and the repairing cost could be estimated. Moreover, the number of affected residents or those who need to evacuate outside their houses could be calculated more accurately based on the number of damaged houses.

### 4.3 Step 3: analysing flood impact

The third step is flood impact analysis, in which possible problem communities may face in the event of a flood are identified. The most important thing is for

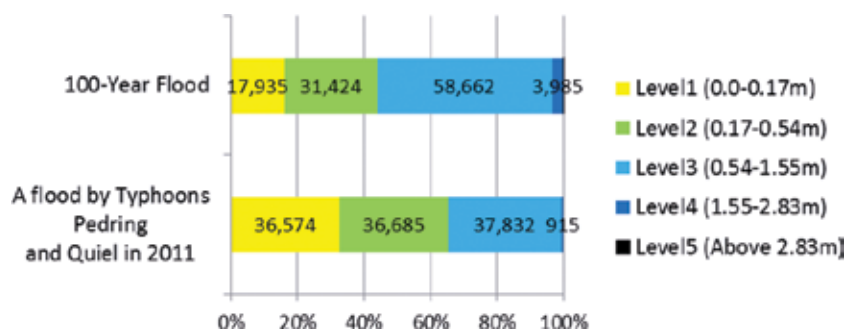


Figure 8. Estimated number of affected residents in Calumpit.

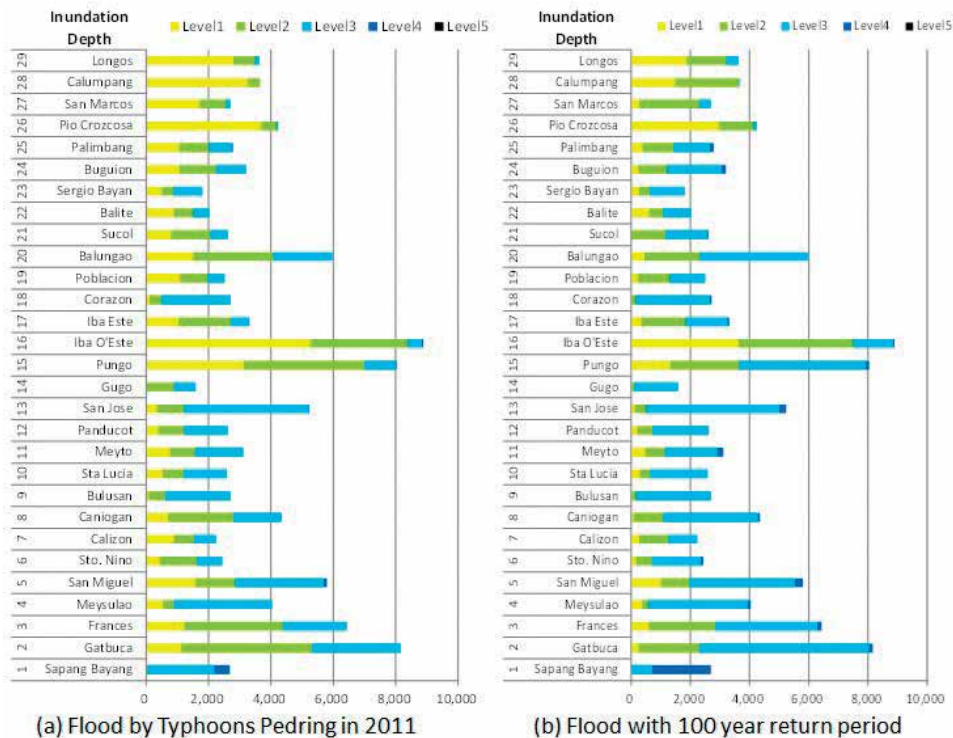


Figure 9. Estimated number of affected residents in each barangay.

communities to understand how flood impact becomes severer according to flood scales so that they can take sensible measures to increase disaster preparedness by themselves. Two flood-prone barangays were selected as model sites to develop flood contingency plans with barangay leaders and members through workshops. The participants of the workshops discussed problems on key components, such as information communication, evacuation, housing, water, food, relief goods, medical treatment and transportation, for three flood patterns identified in step 2: ordinary flood, high flood and extreme flood.

Table 2 summarises the impact of floods identified at the workshops in the two barangays. In case of high flood, many houses may be inundated, and the residents may experience various types of damage to their livelihood, while only non-elevated houses may be inundated in ordinary foods. The participants anticipated problems associated with information acquisition, capacities of evacuation centres, supplies of water, power, relief goods, availability of medical treatment and transportation. In case of extreme flood, they anticipated difficulty in repairing houses as a considerable number of inundated houses may well mean the shortage of construction materials. A photo in Figure 10 shows a scene of a workshop.

#### 4.4 Step 4: developing response strategies

At this step, necessary actions associated with the flood impact on each key component identified in step 3 are discussed at each community according to the time sequence of “before the flood”, “during the flood” and “after the flood disaster”. For this purpose, the second workshop was held at each of the two barangays. At the workshop, the participants were requested to share opinions on necessary actions by

Flood Scale	Ordinary Flood	High Flood	Extreme Flood
Component			
Information Communication		-No battery charge for telephone/mobile phone -Lack of information about inundation /damage situation.	
Evacuation		-Fast speed of rising water during inundation. -Evacuation center doesn't have enough capacity.	
Housing	-Only non-elevated houses get inundated.	-Difficulty in cleaning houses -Many houses get inundated.	-Difficulty in cleaning houses -Many houses get inundated. -Need of more construction materials for repairing houses.
Water, Food, Relief Goods	-No/less water supply. -No electricity.	-No water supply, no electricity -Delay of relief goods -Relief goods get wet. -Need of portable restroom	
Medical Treatment		-Need of medical mission, providing medicines for leptospirosis, fever etc.	
Transportation		-Difficult to go to center area because access road to the elevated road are inundated.	
Others		-Damage of Rice field -Delay in education in school	

**Table 2.**  
*Impact of floods on barangay identified at workshops.*

writing them down on Post-its and show them to other participants. Then, the actions presented by the participants were sorted out into two categories: actions that a barangay should implement immediately as self-help and mutual support and requests that a barangay should make to municipal, provincial or national governments as public assistance. This activity will help clarify actions to be taken by themselves and requests to be made to higher administrative organisations. **Tables 3 and 4** summarise the results of the discussions at the two barangay workshops on what they should do before, during and after the flood and what they should request. The participants found the importance of response strategies on actions such as informing water levels regularly to the municipal office, leading residents to evacuate quickly to a safer place, keeping relief goods dry, saving children and seniors and supporting residents in getting back to normal life quickly.

Although self-help and mutual support among residents are the priority for community disaster management, actions available for them are often limited due to budget and manpower constraints. At the series of workshops, the participants listed the requests they would like to make to higher administrative organisations, as shown in **Table 4**. **Figures 11 and 12** are photos taken at workshops.



**Figure 10.**  
*Workshop at Barangay Bulusan.*

Time Key Component	Before Flood	During Flood	After Flood
Information Communication	-Communicate with MDRRMO(Municipal Disaster Risk Reduction and Management Office)	-Inform water level at "Colors of safety" regularly to MDRRMO. -Keep communication with outside of the Barangay by using generator for charging battery for mobile phone. -Inform obtained information to Barangay people.	-Identify water level, duration, source of flooding.
Evacuation	-Make residents evacuate quickly to safer place -Quantify vulnerable individuals /families	-Make residents evacuate quickly to safer place -Quantify affected individuals /families	
Housing			-Support residents to clean houses for getting back to normal life quickly.
Water, Food, Relief Goods		-Get/provide relief goods and keep them dry.	
Medical Treatment		-Save children and elder people	
Transportation		-Use Bangka	

**Table 3.**  
Results of discussion on actions to be taken in the barangay.

Time Key Component	Before Flood	During Flood	After Flood
Information Communication	-Strengthen communication with MDRRMO -Provide 2-way radio	-Needs for getting information from MDRRMO about flood status during power outage	
Evacuation		-More evacuation space	
Housing	-Quick procedures for getting building permission for upgrading to second story house.		-Provide construction material for house repair quickly
Water, Food, Relief Goods		-Needs for food, water supply, generator, soap, battery, flash light, etc. -Needs for portable C.R.	
Medical Treatment	-Needs for medicines such as leptospirosis, etc.	-Needs for medicines such as leptospirosis, cold, fever, diarrhea, etc. -Needs for medical mission	
Transportation		-Needs for motorized Bangka (small boat)	
Others	-Needs for deep excavation of rivers		

**Table 4.**  
Results of discussion on requests to higher administrative organisations.

#### 4.5 Step 5: developing a contingency plan

After performing steps 3 and 4, the selected two barangays developed a contingency plan by themselves based on the results of steps 1–4. During the plan development, ICHARM provided them with necessary maps explained in the previous sections and several suggestions to barangay members in charge of the plan. **Table 5** is the final contents of their developed plans. Following the message from the barangay leader in the first chapter, the basic information and explanation of risk identification and the contingency plan are presented. In the chapter on risk identification, the inundation maps and chart in **Figure 7** are included, and the impact due to three types of floods discussed in **Table 2** is explained. The chapter





**Figure 11.**  
 Workshop at Barangay Santa Lucia.



**Figure 12.**  
 A resident presenting an opinion on Post-its to other participants at the workshop.

Category	Contents
1.Message	-Message from Barangay Leader
2.Basic Information	-Barangay Profile (Population etc.)
3.Risk Identification	-Past flood -Inundation maps -Time series Inundation chart -Number of vulnerable people -impact due to three floods
4.Contingency Plan	-Organization chart -Resource map -List of equipment -Response strategy -Sectoral Plan -Annual activity plan

**Table 5.**  
 Contents of contingency plan.

of the contingency plan consists of six parts: an organisation chart, a resource map which shows the locations of the important facilities in the area (**Figure 7**), a list of equipment, a response strategy as a result of step 4 (**Table 3**), a sectoral plan for each section to follow in order to achieve necessary actions listed in step 4 and an annual activity plan.

#### **4.6 Step 6: sharing a contingency plan**

In the final step, the main focus is to share the developed contingency plan among community members and with other municipalities. Inviting the leaders and related members of the 29 barangays and Calumpit Municipality, a workshop was held to share all the activities. As the project had drawn much local attention, over 100 people attended the meeting. The representatives from the two model barangays introduced their contingency plans and explained how they developed a barangay contingency plan by themselves, as shown in **Figure 13**. At the end of the workshop, ICHARM provided printed maps developed in step 2 to all the 29 barangays so that every barangay could also make an evidence-based contingency plan of their own (**Figure 14**).



**Figure 13.**  
*Presentation on contingency plan from representatives from two barangays.*



**Figure 14.**  
*Participants of final workshop in Feb. 2016.*

## 5. Conclusions

This study proposed an effective method to implement evidence-based flood contingency planning for local communities by assuming the dynamic change of inundation using flood simulation, assessing flood risk with key indicators and deciding response strategies against the identified flood risk before a flood occurs. The method was applied to a flood-prone municipality called Calumpit in the Pampanga River basin of the Philippines as the first case study to verify its effectiveness in areas where the availability of natural and socio-economic data is limited. The case study revealed that the proposed method can be successfully applied to data-limited regions. However, the method needs testing in different flood-prone communities for further verification.

As for the limitations of the study, the process of risk identification through flood inundation simulation was conducted by ICHARM although this process should be completed by the provincial or national governments of the country. In order for them to carry out the risk identification process by themselves, training of flood simulation and risk assessment should be provided for managers and engineers in flood risk management.

## Acknowledgements

This study was conducted in cooperation with the Municipal Disaster Risk Reduction and Management Office (MDRRMO) of Calumpit and the Philippine Atmospheric Geophysical and Astronomical Services Administration (PAGASA). We would like to express our deepest appreciation to Calumpit Municipality Mayor Jessie P. De Jesus and the officers of MDRRMO. We would also like to extend our sincere gratitude to the officers in the Pampanga River Basin Flood Forecasting and Warning Center (PRBFFWC) and the headquarters of PAGASA for their support during the field activities. We also owe a great debt to the National Mapping and Resource Information Authority (NAMRIA) for providing high-resolution DEM data (IFSAR) in the step of risk identification under the MOU between NAMRIA and ICHARM. Last but not least, we thank all persons involved for their kind support in conducting this study.


## Author details

Miho Ohara\*, Naoko Nagumo, Badri Bhakta Shrestha and Hisaya Sawano  
International Centre for Water Hazard and Risk Management (ICCHARM) Under  
the Auspices of UNESCO, Public Works Research Institute (PWRI), Tsukuba, Japan

\*Address all correspondence to: [mi-ohara@pwri.go.jp](mailto:mi-ohara@pwri.go.jp)

## IntechOpen

---

© 2018 The Author(s). Licensee IntechOpen. This chapter is distributed under the terms of the Creative Commons Attribution License (<http://creativecommons.org/licenses/by/3.0/>), which permits unrestricted use, distribution, and reproduction in any medium, provided the original work is properly cited. 

## **References**

- [1] UNISDR. Sendai Framework for Disaster Risk Reduction 2015-2030; 2015
- [2] ISO22301. Societal Security-Business continuity management systems; 2012
- [3] Congress of the Philippines, The Philippine Disaster Risk Reduction and Management Act of 2010 (Republic Act No. 10121); 2010
- [4] Calumpit Municipality. Calumpit Municipal Disaster Risk Reduction and Management Contingency Plan; 2014
- [5] Ohara M, Nagumo N, Shrestha BB, Sawano H. Flood risk assessment in asian flood prone area with limited local data–Case study in Pampanga River basin, Philippines. *Journal of Disaster Research*. 2016;**11**(6):1150-1160. DOI: 10.20965/jdr.2016.p1150
- [6] Sayama T. Rainfall-runoff-inundation analysis of the 2010 Pakistan flood in the Kabul River basin. *Hydrological Sciences Journal*. 2012;**57**(2):298-312
- [7] International Centre for Water Hazard and Risk Management (ICHARM). Available from: [http://www.icharm.pwri.go.jp/research/rri/rri\\_top.html](http://www.icharm.pwri.go.jp/research/rri/rri_top.html) [Accessed: August 1, 2018]
- [8] Shrestha B, Okazumi T, Miyamoto M, Sawano H. Development of flood risk assessment method for data-poor River basins: A case study in the Pampanga River basin, Philippines. In: *Proceeding of 6th International Conference on Flood Management (ICFM6)*; 2014

# Fitting a Generalised Extreme Value Distribution to Four Candidate Annual Maximum Flood Heights Time Series Models in the Lower Limpopo River Basin of Mozambique

*Daniel Maposa*

## Abstract

In this paper we fit a generalised extreme value (GEV) distribution to annual maxima flood heights time series models: annual daily maxima (AM1), annual maxima of 2 days (AM2), annual maxima of 5 days (AM5) and annual maxima of 10 days (AM10). The study is aimed at identifying suitable annual maxima moving sums that can be used to best model extreme flood heights in the lower Limpopo River basin of Mozambique, and hence construct flood frequency tables. The study established that models AM5 and AM10 were suitable annual maxima time series models for Chokwe and Sicacate, respectively. This study also revealed that the year 2000 flood height was a very rare extreme event. Flood frequency tables were constructed for the two sites Chokwe and Sicacate in the lower Limpopo River basin of Mozambique and these tables can be used to predict the return periods and their corresponding return levels at the sites and their neighbourhood. It is our hope that these long term forecasts will complement the short term flood forecasting and early warning systems in the basin in reducing the associated risk and mitigating the deleterious impacts of these floods on humans and property.

**Keywords:** moving sums, annual maxima, lower Limpopo River, generalised extreme value

## 1. Introduction

This chapter has its significance in disaster reduction in an economically challenged flood disaster prone developing country. The lower Limpopo River basin of Mozambique is one of the basins in Southern Africa that have not been deeply studied in terms of application of extreme value statistics. The basin suffers from extreme natural hazards that alternate between extreme floods and severe droughts. A lot of geoscientific work aimed at short-term forecasts and flood warning systems has been done in the basin. The present study is intended to complement the geoscientific work in the basin through shifting attention to long-term forecasts.

The combination of these two approaches is hoped to go a long way towards disaster reduction and mitigation efforts in the basin.

## 2. Background of the study

Hydrological extreme events such as floods and droughts have accompanied mankind throughout its entire history and these events are cyclic in nature. The twenty-first century, however, has been marked by an unusual number of natural disasters worldwide, among these events are the recent hurricane Matthew that devastated the Caribbean Islands of Haiti, parts of Jamaica and United States of America [1], the recent Nepal 2015 giant earthquake that killed more than 8000 people and injured more than 19,000 people [2], flooding and landslides in Brazil in 2011 and flooding in Mozambique and other parts of Southern Africa in 2000.

Natural disasters such as floods often pose an intolerable threat to society, hence a holistic approach is needed to understand such phenomena, predict such catastrophic events and mitigate the impact of these natural disasters. The lower Limpopo River in Mozambique has a history of worst floods and droughts than all other national and international rivers in Mozambique. The most catastrophic and expensive of these reported natural disasters in Mozambique were the year 2000 floods which killed a total of more than 700 people and caused economic damages estimated at US\$500 million. It is argued by the International Federation of Red Cross (IFRC) that aid money can buy more than seven times as much humanitarian impact if spent before a disaster rather than on post-disaster relief operations [3].

The chairman of the 2014 International Disaster and Risk Conference (IDRC) held in Davos, Switzerland, August 2014, Dr. Walter J. Ammann pointed out that the frequency and intensity of natural hazards such as floods and earthquakes are on the rise in these recent years [3]. In a separate study, a unique survey of 139 national meteorological and hydrological services carried out by the World Meteorological Organisation (WMO) in 2013 revealed that floods were the most frequently experienced extreme events worldwide over the course of the decade 2001–2010 [4]. Some studies have also shown that floods and droughts account for 90% of all the people that are affected by natural disasters [5]. According to Munich Re [6] the statistics of natural disasters for the year 2013 was dominated by floods that caused several billions of United States of America dollars in losses. Irina Bokova, the Director-General of UNESCO [7] stated that:

*Every year, more than 200 million people are affected by natural hazards, and the risks are increasing – especially in developing countries, where a single major disaster can set back healthy economic growth for years. As a result, approximately one trillion dollars have been lost in the last decade alone. This is why disaster risk reduction is so essential. Mitigating disasters requires training, capacity building at all levels, and it calls for a change of thinking to shift from post-disaster reaction to pre-disaster action –this is UNESCO’s position.*

The present study considers floods in the lower Limpopo River basin of Mozambique. The lower Limpopo River basin is characterised by extreme natural climatic conditions alternating between extreme floods and severe droughts. Droughts affect the country on an average of 7–8-year cycle and are usually associated with the El Nino phenomenon which affects Southern Africa [8]. The provinces of Gaza and Inhambane, which house the lower Limpopo River basin,

are among the drought-prone regions due to the action of thermal anticyclones. Droughts usually result in increases in the prices of basic commodities and food aid due to food shortages. Additionally, the number of deaths and diseases increase during the periods of drought [8].

On the contrary, floods in the lower Limpopo River basin are mainly associated with tropical cyclones. The provinces of Gaza and Inhambane are, also, the most affected by extreme floods due to their low-lying nature. Floods result in heavy losses to human lives and damage to infrastructure including bridges, houses, roads and schools. Among the cyclones that occurred in the basin in the recent past are Claudete in 1976, Angela in 1978, Nadia in 1994, Eline, Gloria and Hoday in early 2000s and Flavio in 2007. The year 2000 floods were due to cyclone Eline and were the most disastrous and expensive of all the floods in the basin [8].

While the characteristics of hydrologic extreme events depend on the regional climatic conditions and other factors, the magnitude, timing, duration, and frequency fall within predictable range and pattern over time. The annual maximum series (AMS), also known as block maxima [9], has long been employed in extreme value theory to estimate the distribution of extreme events such as flood flows, precipitation and wind speeds.

The main purpose of this paper is to identify suitable annual maxima flood heights moving sums time series models at Chokwe and Sicacate sites in the lower Limpopo River basin and to construct flood frequency tables for the basin at these sites in Mozambique. It is also our wish to suggest improvements in extreme flood frequency modelling of annual maximum flood heights in the basin.

The outline of the rest of the paper is such that Section 2 presents the research methodology, Section 3 presents the results and discussion of the findings, and finally Section 4 gives the concluding remarks.

### **3. Research methodology**

In this section we present the data source and fundamental principles of extreme value theory [9], as well as a brief discussion of some goodness-of-fit tests.

#### **3.1 Study sites, data and block maxima moving sums**

Hydrometric data has been collected in Mozambique since the early 1930s. However, due to war and other external factors there were periods in which no data were collected at some stations. For this study we obtained hydrometric data for the lower Limpopo River for the sites Chokwe (1951–2010) and Sicacate (1952–2010) from the Mozambique National Directorate of Water (DNA), the authority responsible for water management in Mozambique. The data obtained were daily flood heights (in metres) and were time series in nature.

In statistics of extremes there are two fundamental realisations used in flood frequency analysis namely block maxima and partial duration series commonly known as peaks-over-threshold (POT) [9]. The approach used in this study is block maxima. In hydrological studies, when sample sizes are large it is natural to block observations by years [9, 10].

Since in flood frequency analysis the years are natural blocks, the flood heights data in this study were blocked by years. Sequential steps were taken to obtain annual maxima data from the daily flood heights data series. Further sequential steps were taken to obtain the annual moving sums of 2 days (AM2), 5 days (AM5) and 10 days (AM10). A generalised extreme value (GEV) distribution

was then fitted to the annual daily (AM1) flood heights and their corresponding moving sums.

### 3.2 Generalised extreme value model

The GEV distribution is a well-known distribution in statistics of extremes. Comprehensive details of probability framework of block maxima and the practical reasons for using block maxima over POT are given in [9, 11]. Dombry [12] proved the consistency of maximum likelihood (ML) estimators when using block maxima approach.

The GEV cumulative distribution function,  $G$ , is given in Eq.(1) as:

$$G(\mu, \sigma, \xi; x) = \begin{cases} \exp\left(-\left(1 + \xi \frac{x - \mu}{\sigma}\right)^{-1/\xi}\right), 1 + \xi \frac{x - \mu}{\sigma} > 0, \xi \neq 0, \\ \exp\left(-\exp\left(-\frac{x - \mu}{\sigma}\right)\right), x \in \mathfrak{R}, \xi = 0, \end{cases} \quad (1)$$

where  $\mu$ ,  $\sigma$  and  $\xi$  are the location, scale and shape parameters, respectively. The parameters of the GEV in (1) are estimated by the ML method [11].

The log-likelihood function for the GEV in (1) is given in (2):

$$l(\mu, \sigma, \xi; x) = -k \log \sigma - (1/\xi + 1) \sum_{i=1}^k \log \left[1 + \xi \left(\frac{x - \mu}{\sigma}\right)\right]_+ - \sum_{i=1}^k \left[1 + \xi \left(\frac{x - \mu}{\sigma}\right)\right]_+^{-1/\xi}, \quad (2)$$

where  $k$  is the number of blocks (years) and annual maxima flood height  $x = (x_1, x_2, \dots, x_k)$ .

### 3.3 Anderson-Darling and Kolmogorov-Smirnov tests

The goodness-of-fit of the GEV model to the annual maxima flood heights moving sums time series models was verified using Anderson-Darling (A-D) and Kolmogorov–Smirnov (K-S) tests. The A-D test is sensitive to the tails of the distribution, while the K-S test is sensitive to the centre of the distribution [13]. The moving sums time series models were ranked from 1 to 4, with 1 being the best according to the particular test. A model that attains the lowest value of the total rank (sum of A-D rank and K-S rank) satisfies the criteria for the best annual maxima moving sums time series model. Where there is a tie in the total ranks for two or more models, then the rank value of the A-D test is used as a tie-breaker (with smaller value being best) since the main emphasis in extreme value theory is in fitting the tails.

## 4. Results and conclusion

This section presents the results of the study. **Tables 1** and **3** present the ML estimates of the parameters of the GEV distribution for Chokwe and Sicacate, respectively, for the models AM1, AM2, AM5 and AM10. **Tables 2** and **4** present results for the goodness-of-fit of the GEV distribution to the annual maxima moving sums time series models for Chokwe and Sicacate, respectively. **Table 5** presents the flood frequency tables of the return periods and their corresponding return levels for Chokwe and Sicacate based on the best fitting models.



Model	$\mu$	$\sigma$	$\xi$
AM1	4.2671	1.8242	-0.11031
AM2	8.4538	3.4794	-0.09947
AM5	19.671	7.9968	-0.07243
AM10	35.889	14.8720	-0.05874

**Table 1.**  
 ML estimates of the GEV distribution parameters for Chokwe (1951–2010).

Model	K-S	Cv	R	A-D	Cv	R	Total
AM1	0.054	0.172	3	0.237	2.50	4	7
AM2	0.051	0.172	1	0.234	2.50	3	4
AM5	0.052	0.172	2	0.185	2.50	1	3
AM10	0.062	0.172	4	0.218	2.50	2	6

Key: Cv stands for critical value, R stands for rank, K-S is Kolmogorov–Smirnov, A-D is Anderson–Darling.

**Table 2.**  
 Goodness-of-fit tests of the GEV distribution for Chokwe (1951–2010).

Model	$\mu$	$\sigma$	$\xi$
AM1	6.190	3.4587	-0.49005
AM2	12.267	6.8603	-0.48351
AM5	29.440	16.466	-0.45154
AM10	54.217	29.875	-0.38701

**Table 3.**  
 ML estimates of the GEV distribution parameters for Sicacate (1952–2010).

Model	K-S	Cv	R	A-D	Cv	R	Total
AM1	0.093	1.737	3	0.394	2.50	4	7
AM2	0.094	1.737	4	0.370	2.50	3	7
AM5	0.089	1.737	2	0.324	2.50	2	4
AM10	0.053	1.737	1	0.217	2.50	1	2

Key: Cv stands for critical value, R stands for rank, K-S is Kolmogorov–Smirnov, A-D is Anderson–Darling.

**Table 4.**  
 Goodness-of-fit tests of the GEV distribution for Sicacate (1952–2010).

Return period	20	50	100	200	500
Chokwe (AM5)	32.89	36.12	38.54	40.96	44.15
Sicacate (AM10)	103.58	115.66	124.72	133.75	145.66

**Table 5.**  
 Return periods (years) and their corresponding return levels (m) for the two sites.

#### 4.1 Time series plots of the data

**Figure 1** gives the time series plot of the annual daily maximum (AM1) flood heights data at sites, Chokwe, Combomune and Sicacate. The AM1 series for Chokwe is for the period 1951–2010, for Combomune is for the period 1966–2010, and for Sicacate is for the period 1952–2010. Since the original data series for Chokwe and Sicacate are comparable in terms of the starting period, only the two sites were considered for further analysis in this chapter. That is, the series for Combomune site was dropped for further analysis. Therefore, the results for this study are based on the two sites, Chokwe and Sicacate.

Furthermore, since the fundamental approach of this study is on the use of extreme value statistics using the block maxima, only the annual maximum value for each year was recorded and plotted in **Figure 1**. It is assumed that these AM1 data series are independent and identically distributed (iid) since they are blocked by years [9–12]. Similarly, it is also assumed that the annual maxima moving sums are also iid.

Since extreme value analysis is used in this chapter the data used in this chapter was not divided into training period, test period and forecasting period as these are not necessary in extreme value theory (EVT). In EVT special attention is paid to the estimation of the extreme quantiles and their corresponding return periods.

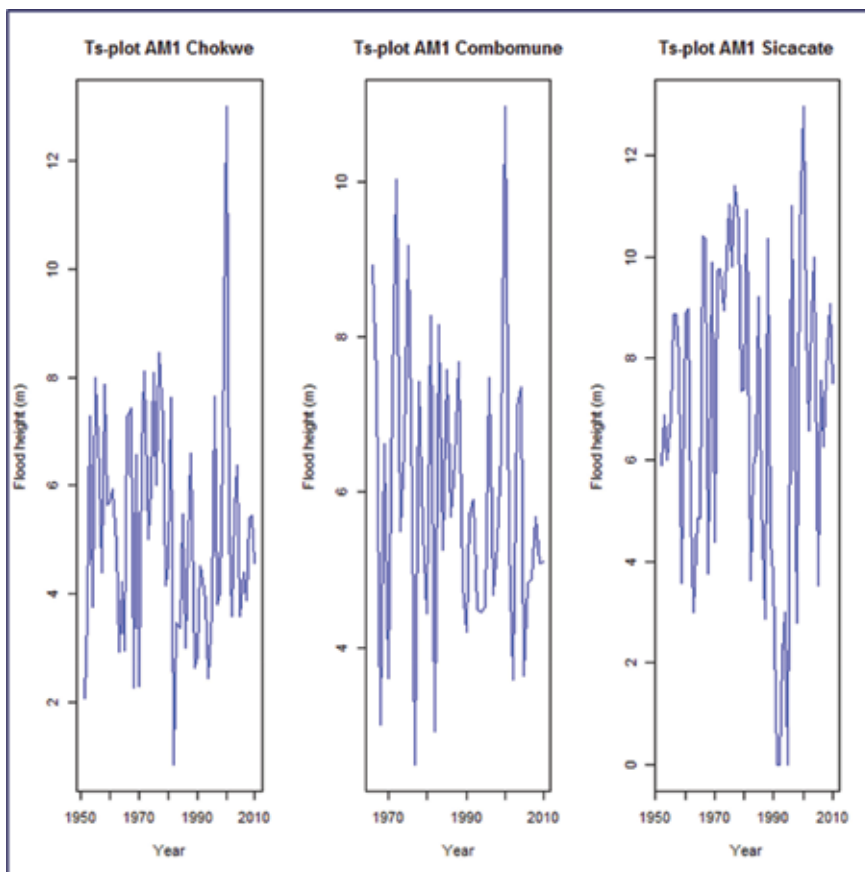


**Figure 1.** Time series plots of annual daily maximum (AM1) flood heights (in metres) at the three sites: Chokwe (1951–2010), Combomune (1966–2010) and Sicacate (1952–2010) along lower Limpopo River of Mozambique.

## 4.2 Chokwe models

The results in **Table 1** show that the shape parameter,  $\xi$ , is negative for all the models. This reveals that the distribution of floods in the lower Limpopo River basin at Chokwe site follows a short-tailed Weibull family of distributions. Further analysis on the values of the shape parameter at Chokwe site indicated that the distribution of floods at the site also belong to the Gumbel family of distributions since these values are not significantly different from zero ( $p$ -value  $> 0.05$ ) for all the models particularly AM2, AM5 and AM10.

Results in **Table 2** show that model AM5 had the lowest total rank of 3 suggesting that it is the best annual maxima moving sums time series model at the site of Chokwe. Consequently, forecasting at the site in this chapter is based on model AM5 for Chokwe.

## 4.3 Sicacate models

Results in **Table 3** show that the shape parameter,  $\xi$ , is negative for all the models at the Sicacate site. This suggests that the distribution of floods in the lower Limpopo River basin at Sicacate site follows a short-tailed Weibull family of distributions.

Results in **Table 4** show that model AM10 has the lowest total rank value of 2 which implies that it is the best annual maxima moving sums time series model for Sicacate site. Therefore, forecasting at Sicacate site in this chapter are based on model AM10.

## 4.4 Return level analysis

Flood heights (peaks) corresponding to return periods of 20, 50, 100, 200 and 500 years were estimated for flood disaster risk reduction in the basin (see **Table 5**). The best fitting annual maxima moving sums time series models AM5 and AM10 for Chokwe and Sicacate, respectively, were used to predict return levels for the selected return periods.

**Table 5** presents results for selected return periods and their corresponding return levels for Chokwe and Sicacate sites based on the best fitting models AM5 and AM10, respectively. The predicted return levels were compared with the observed annual maxima moving sums. It was found that only one annual extreme flood peak, the year 2000 flood height of 124.89 m, exceeded the 100-year flood level for Sicacate site. As for Chokwe site, the year 2000 flood height of 50.44 m, exceeded the 500-year flood level which explains why it was very destructive at the site. The 100-year flood level for Chokwe was exceeded by three observed extreme events with two coming in the mid-1970s and the third one being the year 2000 flood peak. These findings suggest that the return periods of extreme flood heights in the lower Limpopo River basin of Mozambique can be used as a proxy for the return periods of the summer flood intensity. Results in **Table 5** can also be used to construct flood frequency curves [14].

## 5. Concluding remarks

The principal aim of this study was to identify suitable annual maxima moving sums time series models for the lower Limpopo River basin and to construct flood frequency tables for the basin at the sites of Chokwe and Sicacate in Mozambique. This study has successfully identified the prevailing models at the two sites Chokwe

and Sicacate in the lower Limpopo River basin. Annual maxima moving sums of 5 days (AM5) and 10 days (AM10) were identified as suitable time series models for Chokwe and Sicacate, respectively. It was also found in this study that the year 2000 flood height was a very rare extreme event. Flood frequency tables were constructed based on the identified models. It can be concluded that the findings in this study are promising for this vulnerable part of the basin. The findings obtained in this study are aimed to make contributions in the long term forecasts of floods in the basin to complement the much established and sponsored short term forecasts in the region.

Future research studies in the lower Limpopo River basin of Mozambique may advance this study through hierarchical modelling for spatial extremes and Markov chain Monte Carlo methods to the location and scale parameters in a changing climate.

## **Acknowledgements**

We thank the Mozambique National Directorate of Water (DNA) in particular, Mr. Isac Filimone of DNA, who provided us with all the necessary data used in this study. We are also indebted to United Nations Office for the Coordination of Humanitarian Affairs-Southern Africa (OCHA) for providing us with weekly update reports of floods in Southern Africa, particularly for the lower Limpopo River basin of Mozambique. Finally we thank the University of Limpopo for providing the resources that facilitated the production of this article.

## **Conflict of interest**


The authors declare that there is no 'conflict of interest' in this study.

## **Author details**

Daniel Maposa  
Department of Statistics and Operations Research, University of Limpopo,  
Polokwane, South Africa

\*Address all correspondence to: danmaposa@gmail.com

## **IntechOpen**

© 2019 The Author(s). Licensee IntechOpen. This chapter is distributed under the terms of the Creative Commons Attribution License (<http://creativecommons.org/licenses/by/3.0>), which permits unrestricted use, distribution, and reproduction in any medium, provided the original work is properly cited. 

## References

- [1] CNN. Hurricane Matthew devastates the Caribbean Islands of Haiti and parts of Jamaica and United States of America. CNN News; 2016
- [2] CNN. At least 66 dead after another powerful earthquake hits Nepal. 2015. Available at: <http://edition.com/2015/05/12/asia/nepal-earthquake/>
- [3] IDRC Davos. Integrative Risk Management-The role of science, technology & practice. In: 5th IDRC Davos 2014, Programme & Short Abstracts, 24-28 August 2014, The IDRC Davos 2014 Conference Proceedings. Davos, Switzerland; 2014. Available at: <http://idrc.info/outcomes/conference-proceedings/> [Access: 10 December 2017]
- [4] WMO. Global Climate 2001-2010: A decade of climate extremes – Summary Report, WMO no. 119. Geneva, Switzerland: World Meteorological Organization; 2013
- [5] Smakhtin V. Managing floods and droughts through innovative water storage solutions. In: 5th IDRC Davos 2014, The IDRC Davos 2014 Conference Proceedings. 2014. Available at: <http://idrc.info/outcomes/conference-proceedings/> [Access: 10 March 2015]
- [6] Munich R. Floods dominate natural catastrophe statistics in first half of 2013. Press Release, 9 July 2013. Munich: Munich Reinsurance; 2013
- [7] Arya AS, Boen T, Ishiyama Y. Guidelines for Earthquake Resistant Non-engineered Construction. Paris: UNESCO; 2014
- [8] Maposa D, Cochran JJ, Lesaoana M. Fighting flooding in Mozambique. INFORMS: ORMS Today. 2015;42(2) April 2015 Edition
- [9] Ferreira A, de Haan L. On the block maxima method in extreme value theory: PWM estimators. The Annals of Statistics. 2015;43(1):276-298. DOI: 10.1214/14-AOS1280. Available at: <http://arxiv.org/pdf/1310.3222.pdf> [Access: 10 December 2017]
- [10] Maposa D, Cochran JJ, Lesaoana M. Modelling nonstationary extremes in the lower Limpopo River basin of Mozambique. Jamba: Journal of Disaster Risk Studies. 2016;8(1):a185. DOI: 10.4102/jamba.v8i1.185
- [11] Coles S. An Introduction to Statistical Modelling of Extreme Values. London: Springer-Verlag; 2001
- [12] Dombry C. Maximum likelihood estimators for the extreme value index based on the block maxima method. In: ArXiv: 1301.5611v1 [math.PR]. 2013. Available at: <http://arxiv.org/pdf/1301.5611.pdf> [Access: 15 December 2017]
- [13] Maposa D, Cochran JJ, Lesaoana M. Investigating the goodness-of-fit of ten candidate distributions and estimating high quantiles of extreme floods in the lower Limpopo River basin, Mozambique. Journal of Statistics and Management Systems. 2014;17(3):265-283. DOI: 10.1080/09720510.2014.927602
- [14] Maposa D, Cochran JJ, Lesaoana M. Construction of flood frequency curves in the lower Limpopo River basin of Mozambique using Bayesian and Markov chain Monte Carlo methods. In: Proceedings of the 60<sup>th</sup> International Statistical Institute (ISI) World Statistics Congress, 26-31 July 2015, Rio de Janeiro, Brazil. 2015. ISBN: 978-90-73592-35-3. Copyright ISI 2015. Available at: [www.isi-web.org](http://www.isi-web.org)



---

Section 2

# Flood Risk and the Urban Environment

---





# Flood Risk and Vulnerability of Jeddah City, Saudi Arabia

*Mohamed Daoudi and Abdoul Jelil Niang*

## Abstract

Coastal cities are often vulnerable and subject to the risks associated with floods, hence the need to sensitize decision-makers on the threats posed by climate hazards and uncontrolled urbanization. This study is part of this logic and aims to identify and map the flood zones of the city of Jeddah in order to reduce their vulnerability and to integrate them into the strategies of prevention and fight against the risks of flooding. The recent floods in 2009 and 2011 have caused heavy human and material losses that will permanently mark the collective memory of the inhabitants of the city. The multisource and diachronic data used as well as the methodology adopted made it possible to perform a multi-criteria spatial analysis by combining optical satellite imagery and radar DEM, topographic and geological maps, rainfall records, and available statistical data. Thus, risk factors have been identified and combined to understand and appreciate the gravity of recent disasters and provide planners and decision-makers with tools to assist in the effective and adequate management of the ever-changing urban space, in a context of climate change and increased anthropogenic pressure on coastal cities.

**Keywords:** natural hazards, flooding, multisource data, urban extension, Jeddah, Saudi Arabia

## 1. Introduction

Given the changing climate, rapid demographic growth, and significant urbanization, the risks of natural hazards have increased. Many regions of the world have seen devastating floods in recent years, as in the case of Saudi Arabia, which is part of the dry climate region. The city of Jeddah, located on the eastern coast of the Red Sea in the western region of the Kingdom, was hit by earthquakes in the southeast of the city, causing damage to life and property, which had social, psychological, economic, health, and environmental effects.

The urban explosion and the rapid growth of coastal cities mean that coastal cities are highly vulnerable to climatic hazards, which increase the risk of natural disasters [1]. In recent years, several regions of the world have experienced severe flood problems. This is the case of Saudi Arabia, a country characterized by arid climatic conditions, but which has, in recent years, faced severe flooding, particularly in the urban centers which are experiencing a strong expansion. Among these is the city of Jeddah, a cosmopolitan metropolis bordered by the Red Sea and Saudi Arabia's second largest city after the capital Riyadh in terms of population and economic development [2]. Its area was multiplied by 10 between 1972 and 2010. It is considered the door of the Muslims to the two holy places: Mecca and Medina. In 2009 and 2011, the city experienced floods (**Figure 1**) causing death and serious

damage at the social, psychological, economic, health, and environmental levels [3]. The roads were turned into torrents and saw dozens of cars washed away. The present work illustrates a spatial analysis of flood risk based on multisource data (satellite, DEM, cartographic and statistical) and aims to identify flood-prone areas to determine the vulnerability of the Jeddah area so as to avoid urban extension in risk areas and to develop adequate management of the environment.



**Figure 1.**  
*Floods in 2009 and 2011. Source: Internet.*

## 2. Study area

A cosmopolitan city, a major nerve center of the Red Sea and a dynamic port city, Jeddah is located in the Alhijaz region, on the Red Sea coast, developed on Tihamah coastal plain. It is the main urban center of the West (**Figure 2**). Its



**Figure 2.**  
*Study area.*

geographical location on the ancient trade routes and its status as a seaport and airport through which the vast majority of pilgrims travel to the two holy cities Mecca and Medina have made it the most cosmopolitan city in all of Saudi Arabia. While the population was estimated at nearly 1 million in the late 1970s, it rose to 1.4 million in 1986, exceeding 3 million in 2010 [4]. It now stands at nearly 3.5 million, with a rate of 3.5% according to the municipality of Jeddah, which represents 14% of the population of Saudi Arabia.

### 3. Geological and geomorphological framework

According to Monnier and Guilcher, the morphological setting is characterized by the Tihamah littoral plain with a maximum width of 40 km, located at the foot of the highly dissected Precambrian granitic mountains of Alhijaz whose peaks reach several hundred meters. The plain is surmounted by a crest of basalts forming part of a set of castings called harrats (lava flows today in inversion of relief), coming from mouths located at a hundred kilometers inside and going back to the old Pleistocene based on their stratigraphic relations [5] in [6]. The existence of geomorphological phenomena related to the eustatic variations of the Red Sea during the Pleistocene is noted. The stability (or geological instability) of the coastal plain is related to the earthquakes associated with the formation of the Red Sea. Most faults, diaclasses, and cracks take parallel and orthogonal directions to the Red Sea. Hydrologically, there are 24 watersheds in the context of the flooded area. Sixteen watersheds are directed toward the city of Jeddah to the west, and the rest flows in a southwesterly direction toward the great valley of *Wadi* Fatimah [7].

The study area is composed of Precambrian-Cambrian formations, overlain by a succession of Cretaceous-Tertiary sedimentary rocks and Tertiary-Quaternary basaltic lava flows and Quaternary-to-recent alluvial deposits (**Figure 3**).

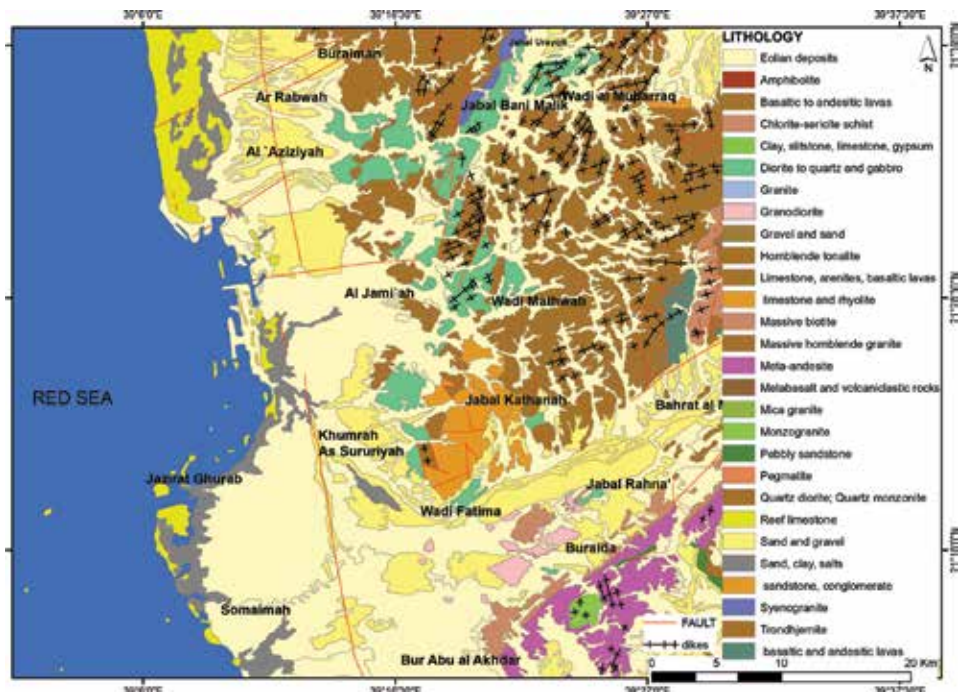


**Figure 3.**  
 Geological map of Jeddah city.

Volcanic lava tongues are associated with lineaments and ancient valleys. These lava formations follow the tracks of the paleovalleys and the direction of the movement of the water. The presence of volcanic languages and Quaternary sediments plays an important role in locating the population and human activities following the presence of springs and loose and fertile soil. The deltas of coastal *wadis* are affected by agricultural activities along the Red Sea coastal plain. **Figure 4** shows the geomorphological and topographic contexts of the city of Jeddah. This figure shows that the city extends on the outlet of several *wadis*, which in spite of the urbanization take back their old courses during strong and intense precipitations. Jeddah has developed all over the coastal plain and beyond, disrupting the normal flow of water.

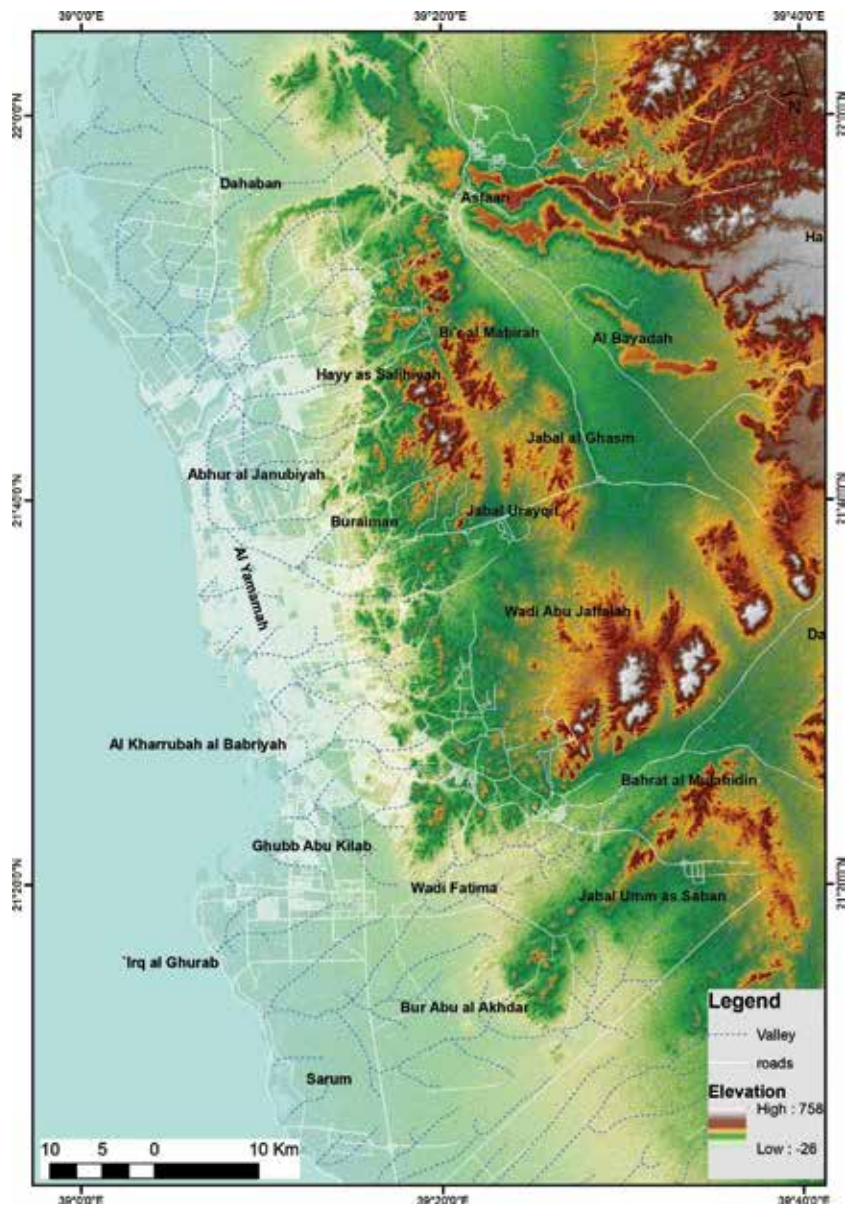


**Figure 4.** Geomorphological and topographic contexts of Jeddah city.

#### 4. Materials and methods

Remote sensing is a crucial tool for researching submersion areas and for assessing natural hazards. The present study is based on the processing of multisource and multirate satellite data, supplemented by cartographic documents and field observations. These different data were integrated in the same mapping projection system before proceeding to a series of digital treatments: digitalization, color composition, improvement, combined classifications using image texture, and fusion. **Figure 5** shows the different stages of treatment. Rainfall statistics were also used.

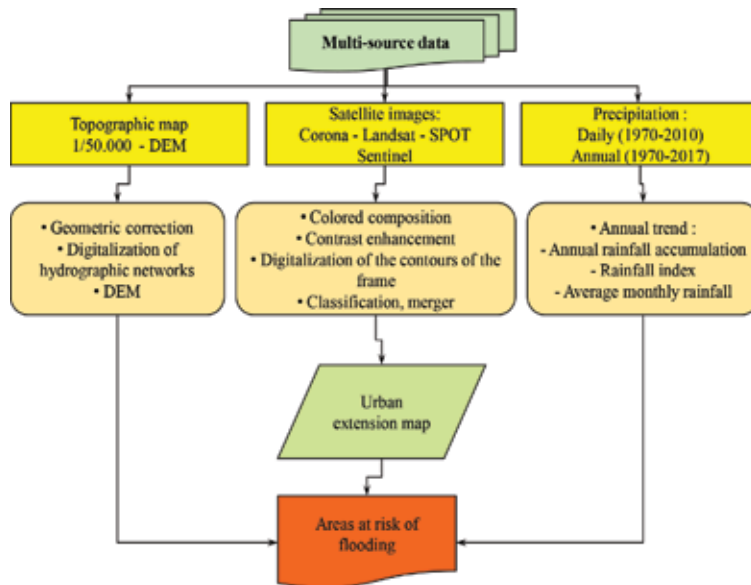


**Figure 5.**  
*Methodology of the study—Different stages of treatment.*

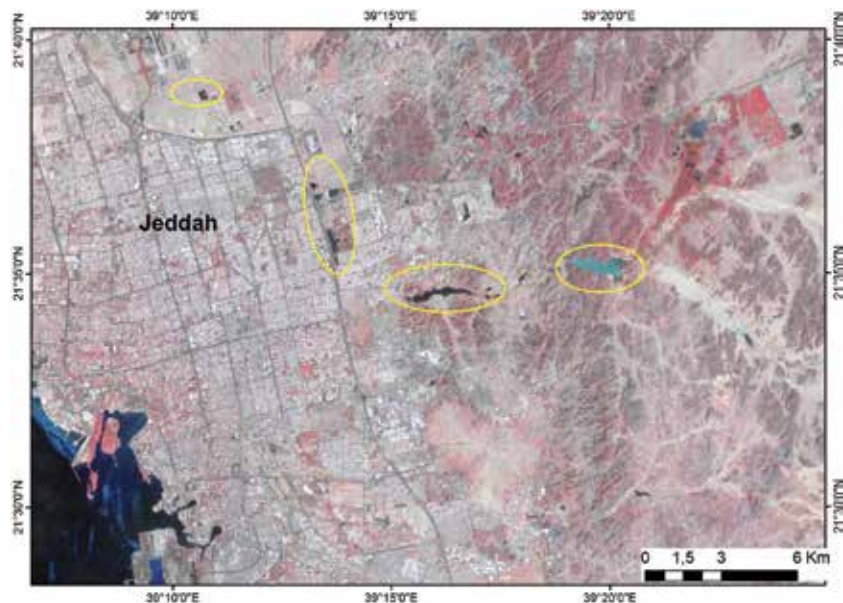


**Figure 6.**  
*Extract from Landsat ETM+ of February 1, 2011. There are only a few small water bodies (circled in yellow).*

It should be noted, however, that the data used do not allow for immediate monitoring of the catastrophic floods that occurred in 2009 and 2011. The lack of information on the intensity and duration of rainfall data that caused the floods does not allow for a detailed analysis of rainfall conditions. For this reason, we will limit ourselves to a general descriptive analysis of the 1970-2017 rainfall data sets for the Jeddah station. At the level of remote sensing data, we did not find SPOT or Landsat images within 3 days after the floods, whereas beyond this period the traces of flood are no longer visible on the satellite imagery, as shown in **Figure 6**. We note that phenomena are as violent as ephemeral. The only image in our possession that is close to the January 27 flood is a Landsat ETM+ acquired on February 1, 2011 (**Figure 6**). The data at our disposal nevertheless allow the monitoring and mapping of the most vulnerable areas.

## 5. Research findings and discussion

### 5.1 Variable and torrential rainfall

It can be seen from **Figures 7** and **8** that the rainfall pattern of the Jeddah area is characterized by a great interannual variability marked by the alternation between wet years (as in 1996, when 284 mm was recorded) and completely dry years, as in 1986 (where no raindrop was reported according to the data processed). As for the seasonality of the rains, it is observed that the precipitation is winter (they begin in October and end in April, **Figure 8**) [8]. These are the typical characteristics of the temperate and Mediterranean climate. This is not the monsoon regime that is generally active in July and September. We can also say that it is the month of November which records the maximum of precipitations and for which the services of civil protection must be more vigilant to envisage periods of water levels in *wadis* and floods. Analysis of daily rainfall (even if the latter do not cover the whole period) is revealing. It shows that the daily rainfall during the 2009 flood (70 mm) “Flash flood or crue eclair” are the largest in 24 hours since 1979. This extreme event combined with the urban growth experienced in the city in this period explains the severity and magnitude of the disasters recorded. The 1970s did not experience major floods, despite large amounts of precipitation falling (1972, 1973, 1978, and 1979); this is due to the absence of urban expansion in this period in risk areas (*wadi* beds). The year 1996 had an exceptional year-to-date, but did not do any damage because the rains fell over several days [9, 10].

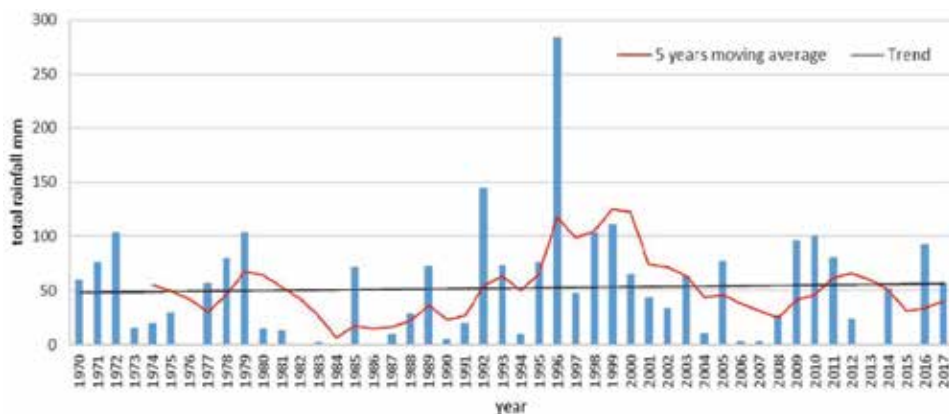


**Figure 7.** Annual total rainfall in Jeddah 1970–2017.

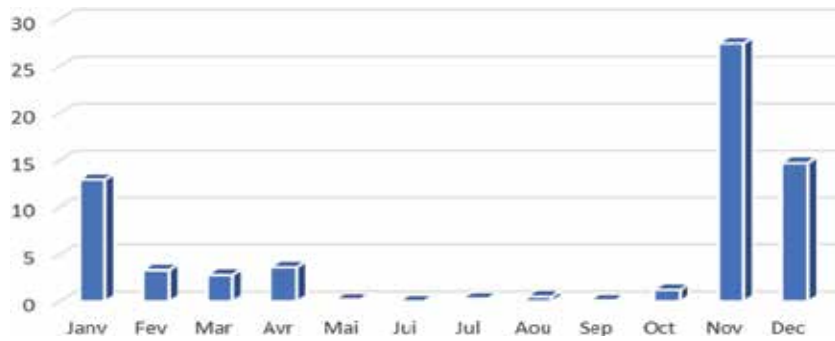


**Figure 8.**  
 Average monthly rainfall in Jeddah 1970–2014.

It has become clear that Saudi Arabia is located in new climatic trends, represented mainly by torrential rains. This was obviously marked by events of frequent natural disasters and especially intense rainfall in different parts of the territory [4]. Disasters recorded in 2009 and 2011 are caused by problems of urbanization combined with the frequency of precipitation that was recorded in less than 2 hours. The city of Jeddah does not have a truly effective system of sanitation and drainage, especially the southern part of the city where the houses are located in *wadi* beds and poorly built because they do not conform to technical standards. Significant rainfall events recorded in recent years and widely reported in the media are those of January 2011 “75.9 mm”; December, 2010 “65.6 mm”; and November, 2009 “70 mm” (Figure 9).

We put emphasis on the fact that anthropogenic pressure has aggravated the extent and scope of flooding, in particular the phenomenon of urban extension along the rivers in their lower reaches, as is the case, for example, in “*wadi* Assir, *wadi* Al Asla” (Figure 10) where homes were recently built without taking into account any assessment of natural disaster risks. A recommendation is made to apply similar studies for flood risk assessment in Saudi Arabia using the same method applied in this research.

Constructions in littoral zones result in a destruction of the environment. The sea is a space that is subject to planning and development for leisure activities. The population has no sense of the littoral environment; thus, it takes an education policy, aiming to enhance the image of the environment and to demonstrate the factors that could effectively contribute to stopping the destruction of nature [6]. The impact of urbanization and the delimitation of its extension is one of the

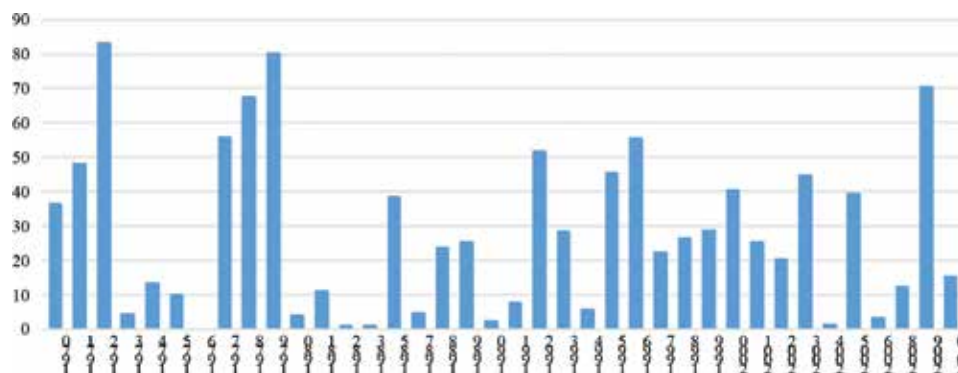


**Figure 9.**  
 Total daily maximum rainfall in Jeddah (1970–2010).



**Figure 10.** Urban extension along the wadis beds, flood 2009 (IKONOS image, after [7]).

fundamental concerns of the management and planning of space. The urban perimeter is an essential data in an analysis for the determination of the peripheral growth of large cities and to highlight the choice of the location of new constructions [11] in [12]. Beginning around 1980, an accelerated impact of construction of buildings, roads, port facilities, and recreational areas has affected the urban area of Jeddah. The area of the city increased from 6200 ha in 1966 to 9500 ha in 1972 and 68,500 ha in 1986; it reached 110,000 ha in 2018 (**Figure 11**).

The growth of the city is mainly toward the north along the plain of Tihamah. The urban expansion that started out in anarchy is nowadays planned. The first steps to be adopted were legislative, beginning with the regulation of the private and public uses of space and activities.

The demarcation of risk areas was established by spatial analysis. The map was made by combining the layers of urban extension zones and the hydrographic network (**Figure 12**). The approach to identifying flooded areas from satellite images was mainly applied using direct visual interpretation and field verification.

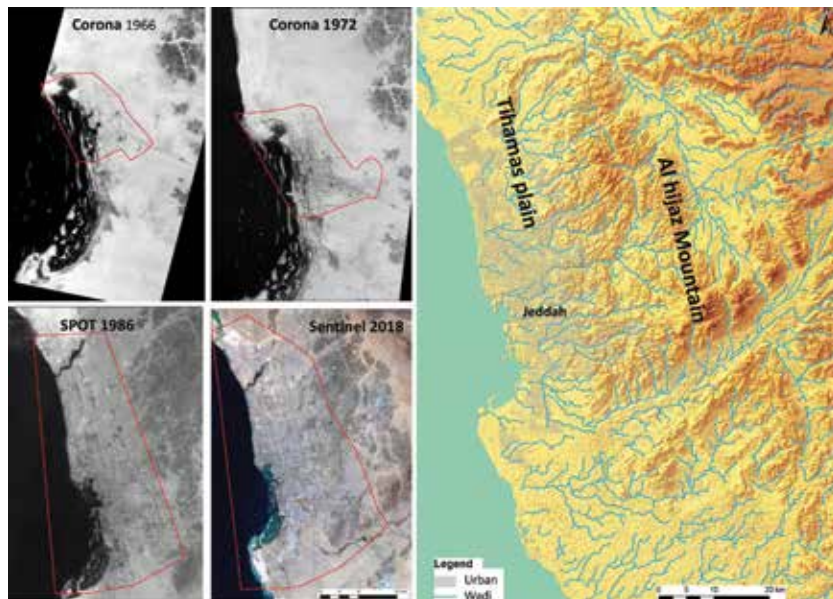


**Figure 11.** Urban extension of Jeddah city between 1966 and 2018 and its topographic context (from remote sensed data).



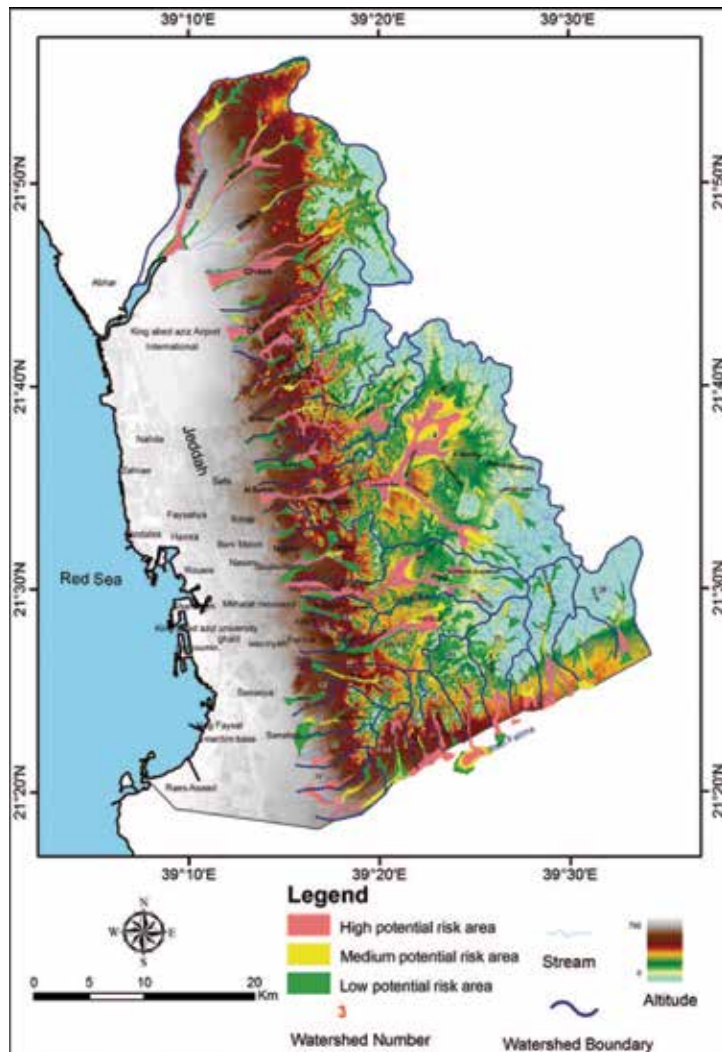


Figure 12.  
Natural flood and torrent risk map (after Al Saud M [14]).

As a result, a map showing risk areas with different levels of damage was produced. For this purpose, we have identified three flood risk zones: the first zone, representing the very high risk, refers to the direct contact strip between the *wadis* and the urban fabric. The second zone presents a high risk, which groups the zones next to the first, at the level of the third zone, which, with moderate risk, is located in the sectors bordering on the second zone. The proposed map is the result of a synthesis that should be completed and validated to adjust and take into account other risk factors. This research could therefore serve as a decision-making tool and constitute a discussion paper for a rigorous spatial planning of the city of Jeddah. Strengthening the legislative framework is necessary at the present time for appropriate management of natural risks [13].

## 5.2 Environmental impact assessment of floods

The rainfall that fell over certain areas of the study area was concentrated, but many of the natural-like areas of the affected area are still at risk if the same

phenomenon is repeated at a high rainfall and exceeds the 5-year moving average. Damage includes the destruction of thousands of cars, the displacement of hundreds of families, the evacuation of homes in the affected areas and the nearby neighborhoods during the crisis, in order to avoid possible future rains, the destruction of farms, and the emergence of mental disorders of people who lived the disaster. Losses were estimated at \$ 3 billion, resulting in damages of \$ 5.1 billion [3]. In this context, it was necessary to address the environmental impact assessment of the floods, to determine the size of the disaster and its geographic distribution, and thus to identify the factors and dynamics of the flow of water and drifting load, so that the appropriate solutions can be conceived and the right decision can be taken. The study is subject to global climate changes and specifically with the expectation of increased rainfall and simultaneous rainfall frequency in the coming years in extreme quantities [15].

The concept of environmental impact assessment emerged at the beginning of the 1960s and included all studies on the direct or indirect impact of any intervention on the environment based on a vision that includes planning and forecasting. The environmental assessment study of a project examines the potential or resulting environmental impacts, identifies appropriate actions to address adverse impacts and minimizes them, and achieves positive returns to the environment in line with existing standards. The environmental assessment process requires identifying all elements that can be classified, its structure in terms of basic data organization, prediction of impacts and changes, and providing solutions and recommendations [16].

The evaluation process has two main aspects: the first aspect is the interactive planning of a purely technical and administrative nature, while the second is participatory planning involving a technical and administrative part. The technical aspect includes study, interpretation, and prediction of the project. The management aspect focuses on the sound decision-making process, with ongoing field monitoring of the environmental impact of the project. The impact study is based on three methods: identifying impacts, developing strategies, and evaluating variables. The effects are identified using several methods, including ad hoc methods, checklist impacts, matrices, networks, overlays, and models.

#### *5.2.1 Multiple standards to support decision-making*

The environmental impact assessment process is based on several criteria—which allow for the appropriate decision of environmental solutions at four levels:

- The subject matter of the decision and the activities involved in the original problem.
- Analysis of results and preparation of standards.
- Decision modeling and operational methods.
- Procedures for investigation and preparation of diagnosis.

This typology can help to make decisions at four levels:

- Choose the best procedures.
- Sort them according to their own values.
- Sort by relevance.
- Describe and present results systematically and formally.

Decision-making is based on a multidisciplinary team comprising a reporter, a facilitator, a decision-maker, and an effective intermediary. On the other hand, it depends on the modeling of variables including business objectives, organizational variables, field information, and basic factors in the study. The decision is preceded by the so-called negotiation process between a multidisciplinary team on environmental impact assessment studies. The process goes through several stages: consultation, negotiation, confrontation, agreement, dialog, and discussion.

### *5.2.2 Disaster variables*

The flow of floods in deserts and arid regions is a product of the interaction of a number of factors and physical and human variables that overlap and affect each other at different degrees. In this context, the cause of the disaster floods in the city of Jeddah is due to a range of variables, including those listed below.

The high density of the hydrographic network and the absence of widening of the sewage for the flow quantities with the intensity of the descent of the springs; the intensity and the high rates of precipitation in short periods, which were in the form of convective and frontal storms and the absence of channels and waterways suitable to absorb the flowing quantities, in addition to the urban expansion of the city on the valleys; and the lack of a strong infrastructure to contain the rapid population growth. Moreover, these variables include the rise of the water table due to the leakage of sewage, irrigation, and rainwater with the high level of seawater.

### *5.2.3 Modeling the probability of occurrence of the hazard*

This process, carried out immediately after the floods, includes:

- A statistical report on the flow of floods (water height, speed, duration of flood, speed of water level rise, and flow times) from knowledge of the risks associated with the natural phenomenon, which depends on the combination of risks and the likelihood of occurrence, exceeding its natural limits.
- Hydrodynamic modeling of floods by choosing the appropriate method due to the multiplicity of models in this area. It is one-dimensional and multidimensional.

### *5.2.4 Modeling exposure to risk*

This type of modeling as summarized in **Figure 13** includes the following elements:

#### *5.2.4.1 Identification at risk*

This consists of identifying all at-risk elements by integrating accurate and correct multisource databases and mapping them according to the scale of the methodology of the study, followed by field outputs to complete some of the data deficiencies and to verify the completed cartographic documents.

#### *5.2.4.2 Social effects*

The social effects of the city's population, their family composition, their indigenous culture, and their psychological effects are based on three main factors that should be taken into account: the indicators of flood (FI), people at risk, and their

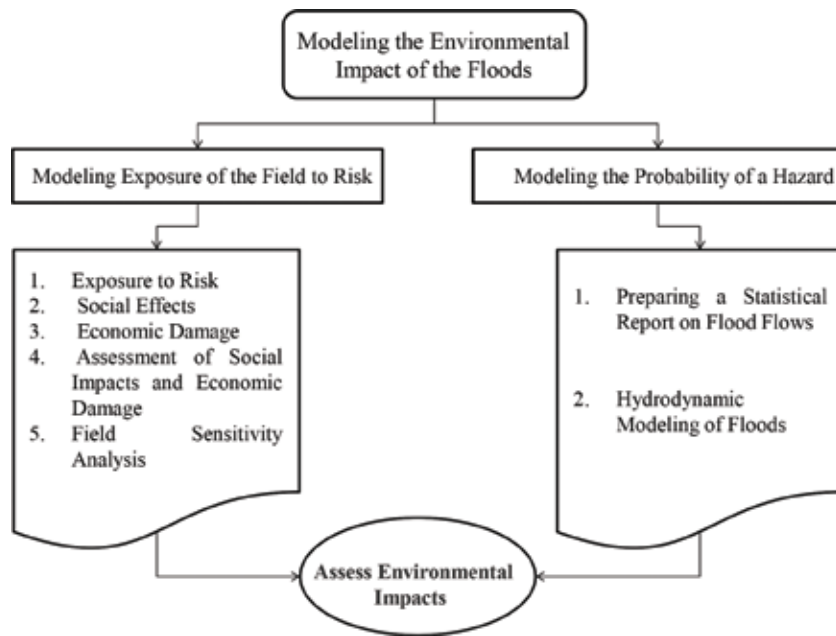


**Figure 13.**  
*Modeling the environmental impact of the floods.*

vulnerability (AC). These three factors are combined in the following mathematical equation:

$$SI = 0.5FI + 0.25 V + 0.25 AC \quad (1)$$

This process aims to assess the social impact index (SI) at various levels: “high, medium, and low” [17].

#### 5.2.4.3 Economic damage

The assessment of economic damage depends on the knowledge of the relationship between the losses caused by a particular type of property due to floods and flood indicators, especially the depth of water, its speed, duration, and pollution according to the basic spatial unit adopted in the research scale.

#### 5.2.4.4 Evaluation of social and economic impacts

The assessment of social and economic impacts requires the use of complementary data sources that allow for the identification of new characteristics identified in the presentation analysis of the estimated cost of property, the number of people living in the property, the sensitivity and social vulnerability, and the adaptive capacity of the affected society.

#### 5.2.4.5 Sensitivity analysis

In this context, a very important variable is needed, which affects the modeling of flood risk and the emergence of some uncertainty in the digital process of assessing the impact of floods on the environment, namely knowledge of the water level, which is due mainly to the lack of data needed for careful study of such topics.

### **5.3 Toward a future vision for assessing environmental impact**

In this context, the following points can be formulated:

- Raise awareness of environmental issues, establish a sense of individual and collective responsibility for maintaining and improving them, and encourage national voluntary efforts in this area.
- Make environmental planning an integral part of comprehensive planning for development in all industrial, agricultural, urban, and other fields.
- Adhere to the General Regulations of the Environment and the Implementing Regulations issued by the General Presidency of Meteorology and Environmental Protection in Saudi Arabia.
- Form a national emergency management body responsible for preparing for natural disasters, developing ready-made rescue programs, and taking precautions to deal with risks before and after they occur.
- Develop an early warning system based on modern technology, which is linked with relevant departments, such as traffic, civil defense, the secretariat, the governorate, the Ministry of Meteorology, and government and private hospitals, and inform the population in all available ways and means, including the use of mobile phones.
- Establish cooperation between officials and decision-makers to enhance preparedness and response, in order to deal with natural disasters.
- Develop awareness programs among the different segments of society, and activate its role to learn how to deal with disaster at the time of its occurrence.
- Implement periodic and continuous reviews of all systems and plans related to natural disaster management.
- Set up training courses for constituents and other community groups.
- Review and study all systems related to regional planning, especially with regard to the determination of the urban scope of each city to identify the lack of plans and their applications.
- Take advantage of the experiences of countries that are at risk, and cooperate with them when necessary.
- Activate the role of maintenance of equipment and rain streams in the seasons of precipitation.
- Give attention to the preparation of hydrological studies and the exploitation of their results in the completion of various development projects.
- Adopt some measures for existing buildings to reduce their risk of flooding [18]:
  - Ensuring the security of persons by establishing an area of refuge, facilitating the passage of the interests of rescue and debris, preventing the floating of waste on water, and checking the location of swimming pools and water basins.

- Sealing water leaks in buildings by installing water leakage barriers, processing sandbags, cracking, network packaging (electricity, gas, telephone, and water), closing ventilation outlets under flood levels, and using internal pumps to pump water.
- Facilitating the return to normal mode by creating the surroundings of the buildings, using thermal insulation of water, placing the electrical panels outside the water level, establishing a separation network for the flooded places, and completing a peripheral drainage.
- Application of environmental assessment methods including checklists, matrices, networks, GIS, and expert systems.

## 5.4 Measures taken in previous periods to address the problem of floods

### 5.4.1 Completion of floodwater channels

- The northern channel of the direction of sailing for the drainage of the Valley of El Assla and Mreikh (**Figure 14**).
- The central channel for the drainage of the valleys of Karaa, Mreikh, Ghia, Om Hableen, Dagbj, and Bariman.
- The southern channel of the drainage of the valleys of Kawes, Osheer, Methweb, Ghilil, and Khumra.

### 5.4.2 Construction of medium and trench dams

### 5.4.3 Dam Lake which was previously used in sewage

It was found that most of them obstructed the movement of water and were exposed to the intensity of evaporation and high temperature in the region, with a decrease in the level of water in general in the area surrounding the body of the dam, and desertification of most of the land in front of it. This is due to the increased risk of floods caused by the phenomenon of sedimentation behind dams. The lack of access to the sea has led to the deterioration of the marine environment, where many marine organisms, including benthic fish and crustaceans that feed on the sediment, have been affected [19] (**Figure 15**).



**Figure 14.**  
*Floodwater channels.*



**Figure 15.**  
*Dam Lake for sanitation.*

### **5.5 Some ways to reduce the risk of floods**

The valleys have devastating effects on urban facilities:

- Establishment of dams of various types and forms (surface and subsurface) on the main valleys or on the tributaries, especially in the places of danger revealed by hydrological studies, to reduce the runoff in the valleys and the use of water in times of extreme necessity.
- Rationalization of the construction of protection dams in major cities, which lack rainwater drainage channels and floods to regulate flow.
- Establishment of industrial channels to transfer runoff from hazardous areas to places where runoff water can be exploited.
- Cladding process using appropriate materials on the sides of roads or barriers to be provided around residential areas, farms, and installations.
- Geomorphological maps that illustrate the locations of risk and safety places on which any plan is developed.
- Treatment of the source of the problem of sedimentation in dams.
- Creation of different land use schemes away from hazardous areas, based on prior scientific studies.
- Benefit from this study in applying its proposals to similar areas in Saudi Arabia.

- Application of warning methods, including:
  - Using flash flood warning systems for sudden flooding by connecting rain and runway monitoring stations with automatic telephones and light signals to warn residents and road users.
  - Employing remote sensing and radar data to monitor the weather situation and identifying hazard areas.
  - Organizing awareness sessions and workshops, using awareness leaflets and warning plates, with guides and maps for road users, and methods to be used to avoid danger.
  - Making use of studies of the expected periods of flow, the expected volume of the flood, thereby informing the inhabitants of these areas in advance, in addition to the precautions to be taken by the citizens and the authorities responsible for them.

## **6. Conclusion**

This study looked at the vulnerability of the city of Jeddah to floods. Several risk zones have been identified. Spatial analysis of flood risk has led to the establishment of a two-dimensional, natural, and societal hazard profile. It has produced several valuable pieces of information that can be used as part of a geographical information system for monitoring the natural risks of the city of Jeddah. The vulnerability of the study area to the risk of flooding seems to have increased sharply following the uncontrolled and very rapid extension of the urban fabric but also to the irregularity of the annual precipitations. Regarding the state of flood risk in Jeddah, the study showed that by combining multisource and multi-species data, it is possible to obtain a good estimate of areas vulnerable to flood risk, monitored and validated by reliable fieldwork. It would also be necessary to establish risk levels for any new housing area and redevelop very-high-risk sites to avoid future disasters, taking into account climate change. This chapter also allows for the establishment of solid foundations for the study of environmental impact assessment, according to a methodology that takes into account all the variables and criteria that must be met in such studies, in order to model them and provide possible solutions to protect the danger zone and predict future exposure. This is not excluded in light of climate change and global warming, which cause catastrophic floods in most regions of the world.



## Author details

Mohamed Daoudi<sup>1\*</sup> and Abdoul Jelil Niang<sup>2</sup>


1 Department of Geography and GIS, Faculty of Arts and Humanities,  
King Abdulaziz University, Jeddah, Saudi Arabia

2 Department of Geography, College of Social Sciences, Umm Al-Qura University,  
Makkah Al-Mukarramah, Saudi Arabia

\*Address all correspondence to: [mdaoudi@kau.edu.sa](mailto:mdaoudi@kau.edu.sa)

## IntechOpen

---

© 2019 The Author(s). Licensee IntechOpen. This chapter is distributed under the terms of the Creative Commons Attribution License (<http://creativecommons.org/licenses/by/3.0>), which permits unrestricted use, distribution, and reproduction in any medium, provided the original work is properly cited. 

## References

- [1] Niang AJ. La résilience aux changements climatiques: Cas de la ville de Nouakchott. (Resilience against climate change: Case of Nouakchott City). *Geo-Eco-Trop.* 2014;**38**:155-168
- [2] Al SM. La transformation socio-spatiale à Djeddah (Arabie saoudite). Thèse de doctorat en Géographie. France: Université Paris IV - Sorbonne; 2010. p. 563
- [3] Momani N, Fadil A. Changing public policy due to Saudi City of Jeddah flood disaster. *Journal of Social Sciences.* 2010;**6**:424-428
- [4] Ewea HA. Hydrological analysis of flooding wastewater Lake in Jeddah, Saudi Arabia. *JKAU: Meteorology, Environment & Arid Land Agriculture Science.* 2010;**21**:125-144
- [5] Hacker P, Hötzl H, Moser H, Rauert W, Ranner F, Zötl JG. Region around Jeddah and its hinterland: Geology, geomorphology and climate. In: Jadd, Zötl JG, editors. *Quaternary Period in Saudi Arabia.* Vol. 2. Vienne-New York: Springer; 1984. pp. 107-122
- [6] Monnier O, Guilcher A. Le Sharm Abhur, ria récifale du Hedjaz, mer Rouge: Géomorphologie et impact de l'urbanisation. *Annales de Géographie.* 1993;**102**(569):1-16
- [7] Al Saud M. Assessment of flood hazard of Jeddah area 2009, Saudi Arabia. *Journal of Water Resource and Protection.* 2010;**2**:839-847
- [8] Subyani AM, Hajjar AF. Rainfall analysis in the contest of climate change for Jeddah area, Western Saudi Arabia. *Arabian Journal of Geosciences.* 2016;**9**:122. DOI: 10.1007/s12517-015-2102-2
- [9] Almathlouthi S. Fortes pluies dans la ville de Jeddah en Arabie Saoudite, causes et conséquences. *Revue de L'association des Géographes Tunisiens.* 2005;**17**:7-18. (in Arabic)
- [10] Yesubabu V, Srinivas CV, Langodan S, Hoteit I. Predicting extreme rainfall events over Jeddah, Saudi Arabia: Impact of data assimilation with conventional and satellite observations. *Quarterly Journal of the Royal Meteorological Society.* 2016;**142**:327-348. DOI: 10.1002/qj.2654
- [11] Tonye E, Akono A, Ndi Nyonguy A, Assako Assako RJ. Utilisation des données ERS1 et SPOT pour le suivi de la croissance périphérique de la ville de Yaoundé (Cameroun). In: Bannari A, editer. *Laboratoire de Télédétection et de Géomatique de l'Environnement, Département de géographie, Université d'Ottawa, Actes du Colloque international, Université d'Ottawa, Ottawa 10 au 12 mai. 1999.* pp. 83-98
- [12] Ould Sidi Cheikh MA, Ozer P, Ozer A. Risques d'inondations dans la ville de Nouakchott (Mauritanie). *Géo-Eco-Trop.* 2007;**31**:19-42
- [13] Daoudi M. Risque d'inondation et vulnérabilité de la ville de Jeddah, Arabie saoudite. *Geo-Eco-Trop.* 2014;**38**(2):259-270
- [14] Al SM. Flood control management for the city and surroundings of Jeddah, Saudi Arabia. In: Springer *Natural Hazards.* 2015. p. 169. DOI: 10.1007/978-94-017-9661-3\_12
- [15] IPCC, 2007: *Climate Change 2007: Synthesis Report.* Contribution of Working Groups I, II and III to the Fourth Assessment Report of the Intergovernmental Panel on Climate Change [Core Writing Team, Pachauri, R.K and Reisinger, A. (eds.)]. IPCC, Geneva, Switzerland, 104 pp

[16] Poutrel JM, Wasserman F. Comité scientifique Espace et cadre de vie France, Société d'études pour le développement économique et social. Prise en compte de l'environnement dans les procédures d'aménagement: Essai Méthodologique sur les Études d'impact. Collection Recherche Environnement, Broché, Diffusion la Documentation Française. 1977. p. 183

[17] Dewals BJ, Detrembleur S, Archambeau P, Erpicum S, Ernst J, Piroton M. Caractérisation micro-échelle du risque d'inondation : Modélisation hydraulique détaillée et quantification des impacts socio-économique. La Houille Blanche. 2011;2:28-34

[18] SPW. Inondations: Réduire la vulnérabilité des constructions existantes, Une publication du Service public de Wallonie, Belgique. 2014

[19] Daoudi M. A systematic approach to assess the impact on the environment: Flood risk model. Egyptian Journal of Environmental Change. 2015;7(2): 43-52. (in Arabic)



# Flood Risk Assessment in Housing under an Urban Development Scheme Simulating Water Flow in Plains

*Faustino de Luna Cruz, Oscar A. Fuentes Mariles, Judith Ramos Hernández and Jesús Gracia Sánchez*

## Abstract

Floods are increasingly occurring around the world more often, this implies analysing the risks connected to both human health and the environment, and to infrastructure and properties. The objective is to establish areas susceptible to flooding and their impact on the population through the effects on the unit of analysis “housing”. To simulate the floods and map the affected areas, the FluBiDi 2D model was used. Two conditions for one urban zone analysed within the Mexico Valley were compared: (a) with the current hydraulic infrastructure and (b) with the application of rectification of channels. The available information was the discharge getting into the catchment and the total of homes in 2015. Projections for 20-year and 50-year planning horizon were considered, and for the 50 years, an evaluation of a non-structural measure was applied. Results show that under the current infrastructure, the flood simulated had a flow depth of 20 cm, decreasing to 5 cm average with rectification of channels, and a decrement of 45% of the cost of housing risk. Applying the both structural and non-structural measures, the cost of vulnerable housing was reduced until 94%, thus, this a trustworthy tool for decision-making in urban developments.

**Keywords:** flood risk prediction, FluBiDi, 2D-hydraulic modelling, flood management, hydraulic vulnerability, urban development

## 1. Introduction

Floods are increasingly occurring around the world, and for some authors such as [1–3], climate change is one of the most important causes for them since it affects directly and indirectly the river network. Although the contribution of climate change is undeniable, also there is the human contribution to increase the frequency of floods. According to [4], human contribution includes its settlement in risk flooded zones, and, as consequence, cities with highly developed infrastructure and commodities could generate instability in the fluvial system due to the implementation of morphological adjustments in order to protect agriculture or cities on or around the floodplain [5, 6]. The different flood levels of damage along the

river are established according to the degree of the development of the region. A high-income region is more affected than a low-income region in terms of economic losses. However, low-income regions increase flood hazards since they have a poorly planned and managed infrastructure; thus, there is a growing population in a no suitable land such as floodplains and coastal and depressed inland areas, and economical losses are less than life losses [7]. When high- and low-income settlements are established in risk zones, some actions had been executed such as protective measurements as bank protection against migration, land protection constructing dam and levee systems and dredging [8]. However, these protective measures also have produced alterations in the channel and floodplain for a long time ago increasing the risk. Thus, it is necessary that flood control systems are matched with the river and floodplain changes and special care needs to be done to understand the causes and effects of the flood impact between natural and social environments in order to establish actions focused to minimise it [1, 7]. Ref. [9] considers that whether the purpose is the control of flood disasters, a flood risk management is clue, since it is the sum of actions to achieve the minimisation of the flood consequences. In general, [9] identifies two aspects that need to be addressed: the process of managing an existing flood risk and the planning of a system to reduce the flood risk. Generally, flood risk considered the probability of hazard (i.e. climatic change) and the exposure and vulnerability of the elements at risk (i.e. urbanised area) [1]. One way to predict flood hazards is as function of the computed probability of previous events known as return period ( $T_r$ ). Flood hazards (exposure) represent *the exceedance probability of potentially damaging flood situations in a given area within a specified time period* [10]. In the case of vulnerability, it can be defined as *the potential for loss* [11], which could be associated in an urbanised system to the loss of the ecosystem services in the area. Although [12] pointed that urbanisation is not a synonym of an increment in flood vulnerability, some relationships could be expected. Urbanisation implies in some degree the presence of infrastructure, in particular against natural extreme events. An alternative is to consider both flood structural and nonstructural measurements as content.

In [13], the need for a quantitative but also a qualitative flood risk analysis was established. The first one provides information of the potential damage in terms of direct economic lost calculated using stage-damage functions (houses, industries and infrastructure), a situation that in the second case could not be achieved since it involves cultural, ecological and indirect economic damages [14]. One way to communicate both qualitative and quantitative hazard and the associated risk is through flood risk maps. For [15] there are flood hazard maps, which help to identify flooded areas with different probabilities, complemented by parameters indicating flood intensity, such as flood depth or flow velocity. Also, flood risk maps help to identify weak points of the flood defence system or indicate a need for action, even if the flood protection system adopted failure during the flood [9]. In fact, flood risk maps incorporate flood hazard information related to properties and population and their vulnerability to the hazard [1]. It is important to mention that many people have no other place to live, but they are habitual to frequent floods without representing any kind of lost. [16] pointed out that maybe due to the familiarity with flood or the lack of flooding experience, property owners in floodplains are not aware of the risk of living in a flood-prone area. The authors analysed the risk associated in terms of cost to protect their lives and properties. For that they mentioned that [17] were some of the first to manage the consumer perception of risk looking at the personal experience, history of past flooding, level of risk existing and how each individual responds to the risks. [16] stated that there is few information related to the effects of flooding risk on property values,

the majority being focused to insurance by natural risk. They cited researches like [17–18] as the ones that use *property location vis-a-vis a floodplain* and the value of the property which reduces when it is in a flood-prone zone. However, in terms of economic aspects, it is only the responsibility of the house-owner and its perception of loss to have any insurance. This chapter looks at the property in terms of the economic loss as a function of the flood hazard zone location under three population growth rate scenarios at the north-east of the Valley of Mexico. The house prices were established according to the material used to build them and the impact when different flood intensity events (return periods) are applied. In order to achieve the flood risk map, a hazard map was created based on the identification of flood-prone areas and the impact in the implementation of a structural mitigation measure (hydraulic infrastructure) according to the hydrology, soil and climate, among other conditions of the study area. To identify the flood areas, the flood simulation was realised using the 2D mathematical model, FluBiDi (modelo de flujo didimensional), for different return periods previously calibrated using discharge data. The risk map contains the information about the consequences expected by the hazard (flood), specifically the influence of structural (channel rectification) and nonstructural mitigation measures (spatial econometric analysis of properties at risk).

## 2. FluBiDi mathematical model

In general terms, FluBiDi is a distributed 2D physical-based model for forecasting runoff developed by [19] and complemented by [20] the Institute of Engineering of National Autonomous University of Mexico (UNAM, in Spanish). Firstly, FluBiDi seeks to establish runoff for any site within a basin under study and determines the contribution volume of this site to the total basin runoff (including local rain). Secondly, FluBiDi provides an interpretation closer to reality since it incorporates several variables and parameters of the hydrologic cycle and basin characteristics based on the physical principles that scale changes are possible using parametric values [20]. As a 2D (dimensional) model, it represents floodplain flow as a two-dimensional field with the assumption that the third dimension (water depth) is shallow in comparison to the other two dimensions as [21, 22] noticed. FluBiDi, as most approaches solve the 2D shallow water equations, represents mass and momentum conservation in a plane and can be obtained by depth-averaging the Navier–Stokes equations. These equations are founded of the motion of viscous fluids involving parametrisation at a macroscale from the basic microscale equation in the vertical direction under the assumptions of hydrostatic pressure distribution and uniform velocity profiles. The development of the equations could be found at [23]. Thus, the momentum equations are.

$$\frac{1}{g} \frac{\partial u}{\partial t} + \frac{n^2 |u| u}{h^3} = -\frac{\partial h}{\partial x} - \frac{\partial Z}{\partial x} \quad (1)$$

$$\frac{1}{g} \frac{\partial v}{\partial t} + \frac{n^2 |v| v}{h^3} = -\frac{\partial h}{\partial y} - \frac{\partial Z}{\partial y} \quad (2)$$

where X and Y are forces by mass unit at the x and y directions ( $\text{m}\cdot\text{s}^{-1}$ ); u and v are the flow velocities in x and y directions, respectively ( $\text{m}\cdot\text{s}^{-2}$ ); and x and y are horizontal and vertical directions in the Cartesian system. The Manning-Strickler equation for friction slopes was included for computing roughness coefficient. Z is

the surface water level related to the land topography considering the rain contribution and infiltration losses.

Also, the governing mass continuity equation considers the rain contribution and infiltration losses, and if the inertia is not significant, it is given as.

$$\frac{\partial h}{\partial t} + u \frac{\partial hu}{\partial x} + v \frac{\partial hv}{\partial y} = r - f \quad (3)$$

The diffusive wave approximation neglects the local acceleration term and convective acceleration term in the momentum equations, and it is applicable in situations where Froude number is small [24]. Thus, FluBiDi defines the system considering dynamic, diffusive and kinematic wave properties for an overland flow in a basin.

The integral form of the shallow water equations to define schemes on different mesh types is considered for the numerical integration; thus, a finite volume method needs to be used for the governing Equations [23]. The surface integrals represent the conversion of the lineal integral into area integrals implying to contemplate the boundary of the region that involves some integrations (Green's theorem). Some schemes consider the homogeneous conservative part of the system and a discretisation of the non-conservative term with a "lateralisation" [25]. For that, it is necessary to take into account that the mesh could have known depth and velocity values and the border boundaries consider four points: one for the right side of the intercell ( $R$ ) and another for the left side ( $L$ ) and the other two for above and below the cell.

FluBiDi is born as a hydraulic mathematical model to simulate runoff based on rainfall, and, in almost all the similar models, it considers river basins exposed to high rainfalls that present an organised drainage net, increasing the water flow at the mainstream according to the amount and intensity of precipitation and the topography at the basin [26]. However, in very few cases, this situation is presented, although it is the best condition to calibrate the model. Ref. [27] indicated that the river gauge water level time series comparison is one of the best forms to test the model's performance. For FluBiDi, a river basin in the Tabasco state offered input and output discharges measured and the awareness of how it behaves becoming an excellent option to calibrate the model. FluBiDi version 1.6 offered utilities to achieve hazard maps using routines to simulate the hydraulic phenomena obtaining water levels, velocities and water extension. Surface water levels could be used as a variable at the boundary conditions in FluBiDi. This is an important contribution, since very few codes have the ability to delimit boundary conditions and most of them require the definition of input discharge and water level.

### 3. Model calibration

Teapa River basin (TRB) together with Jalapa and Tacotalpa Rivers originate the La Sierra River with a basin (SRB) area of 1799.4 km<sup>2</sup>. **Figure 1** shows the extension of the TRB. The TRB is an instrumented basin with hourly rainfall records, hourly water levels and flow gauging. Also, the TRB is subject to continuous historic floods being one of the most severe in 2007 with a  $T_r = 100$  years. Particularly, at the Teapa station, the total drained area is 476 km<sup>2</sup>, with records of average temperature of 25.9°C, with variations from 22.5° to 28.8°C during the year. The total annual average precipitation corresponds to 3133.4 mm, with average monthly variations of 105–520 mm [28, 29]. It is necessary to mention that the basin under study does not have any additional volume income to the precipitation; thus, the resulting flow corresponds only to the precipitation and the vegetation.



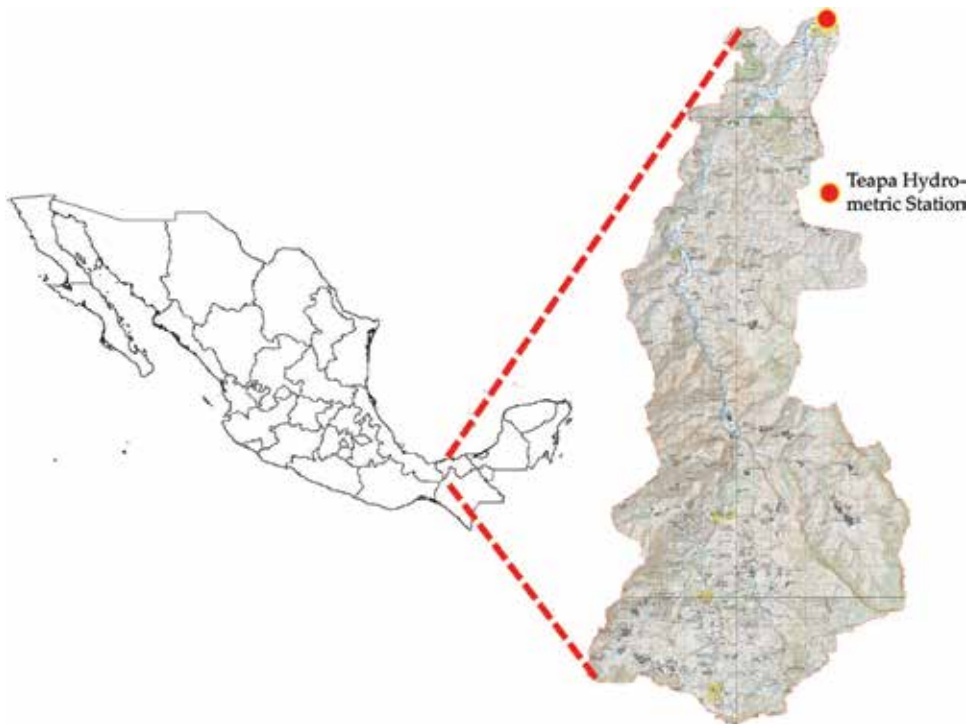


**Figure 1.**  
*Teapa River basin: Topographic relieve.*

The natural vegetation consists of high evergreen forest and medium subperennifolia forest (limits with Chiapas) and grasslands and secondary subperennifolia secondary forest, with some popal [28].

### 3.1 Data

Many authors such as [27] identify as a common method to calibrate a flood model the use of historic flood records. In particular, if these records were acquired just after the event has passed, the accuracy of the model will be guaranteed. Thus, the main application of FluBiDi in TRB is the flood simulation by the estimation of the flow that drains at the outlet of the basin. To simulate flood, records include the period from November 19 to 24, 2015. In general, 2015 was classified around the country as the 12th year with more rainfall since 1941 with 872 mm of total cumulated rain. The reason for that was a series of cold fronts (CF) that hit the region in 2015 starting with the CF-7 (October 16–17) which left heavy punctual rains in Tabasco varying between 90 and 300 mm and generating in the SRB severe floods, the Teapa town being one of the places that remained uncommunicated with 1 m of water height. Then, the CF-8 (October 22–29) affected seriously the region by the day 25th with a cumulate precipitation of 160.7 mm, and this value increased with the arrival of the CF-14 (November 21–24) to 223.7 mm. In December 14–20, the CF-21 took place leaving rains around 125.4 mm in Macuspana by day 18th, but at the end of day 19th, rains were maintained around 120 mm in Puyacatengo. The heavy rains of the CF-21 caused that the La Sierra River to overflow and partially flood 13 communities, some of them, Teapa again, reaching in some cases a water height of 50 centimetres and affecting at least 350 families according to the Institute of Civil Protection of the Tabasco State [30]. There were also economic losses including flooded grasslands, and other losses were associated with low sales, absenteeism and delay of workers.

### 3.1.1 Meteorology and hydrometric stations

Meteorological data was obtained from nine weather stations located in the area (see **Figure 5**): Puyacatengo, Teapa, El Refugio, Francisco I. Madero, Chapultenango, Tapilula, El Escalón, Arroyo Grande and Oxolotan [31]. Data are provided in the latency of 10 min/hourly/daily rainfall (mm), 10 min/hourly and daily temperature ( $^{\circ}\text{C}$ ), hourly/daily relative humidity (%), average daily wind speed ( $\text{m}\cdot\text{s}^{-1}$ ) and sunshine hours, among others. Also some daily evaporation records were obtained, but once they were compared with the effective precipitation, they have turned out to be negligible. These records could be used as an input to the model in order to simulate the event. In addition, the Teapa hydrometric station provides every 10 min continuous water level records obtained with an electronic system for real-time measurements and with quotation in the reference level bank of the hydrometric station. Daily water velocity using a hydraulic windlass method was acquired at 8 a.m. for each subsection in which the total section is divided using the divided channel method (DCM) [32].

It is important to know the spatial and temporal distribution of precipitation; thus, data for the nine weather stations were firstly grouped from 10 min to hourly rainfall values. **Figure 2** presents the analysis of spatial precipitation records for some hours, as well as the cumulative representation for the total modelling period of 6 days (144 hours).

The importance of the spatial-temporal analysis of precipitation can be observed since in the weather station (Chapultenango) rained the same or more than the cumulate rain for the total period of 7 days. In Chapultenango (see **Figure 4e, f**), the maximum rainfall value was around 250 mm for 1 h that corresponded to the maximum 24 h cumulative rainfall continuous value on November 23, whereas in the Teapa weather station, the maximum cumulated rainfall in 24 h was approximately 180 mm with less than 100 mm in 1 h.

**Figure 3** shows the comparison of records for water surface level and water elevation discharge curves. **Figure 5a** presents the relationship between the real-time water level measurements and the daily gauge in the period under study; the error was less than 2%. **Figure 5b** indicates the water level related to the discharge is 330 times, which is used to carry out an adjustment to a quadratic polynomial function. This polynomial function provides the final discharge ( $Q$ ) to the automatised water level measurements (without outliers present within the circle in **Figure 5b**). This provides from November 18 to 26, 2015, a total of 190 values of estimated discharges for 190 water surface elevations measured.

After reviewing the quality of rainfall information, it was considered that data ensure greater consistency to feed the mathematical model.

### 3.1.2 Topographic and thematic data

To apply the mathematical model, it is required to generate a mesh that represents the elevations and other topographic features (surface drainage system, slope and orientation) accurately. In this case, the digital elevation model (DEM) was obtained from the National Institute of Statistical and Geography (INEGI) Mexican Elevation Continuum [33]. Derived from the DEM (with a 30-m cell size), a mesh of 100 m per 100 m was resized in order to fulfil with the restriction for the modelled time required. Thus, for the new mesh, an interpolation technique was used where the main variable is the size against the calculation time. The merge of 100 m size is fed to the model in order to process it and recalculate variables such as slope, aspect, flow direction and basin limits.

A compendium of thematic maps, topography, climatology, edaphology, physiography, geology, hydrology, land use and vegetation, potential land use

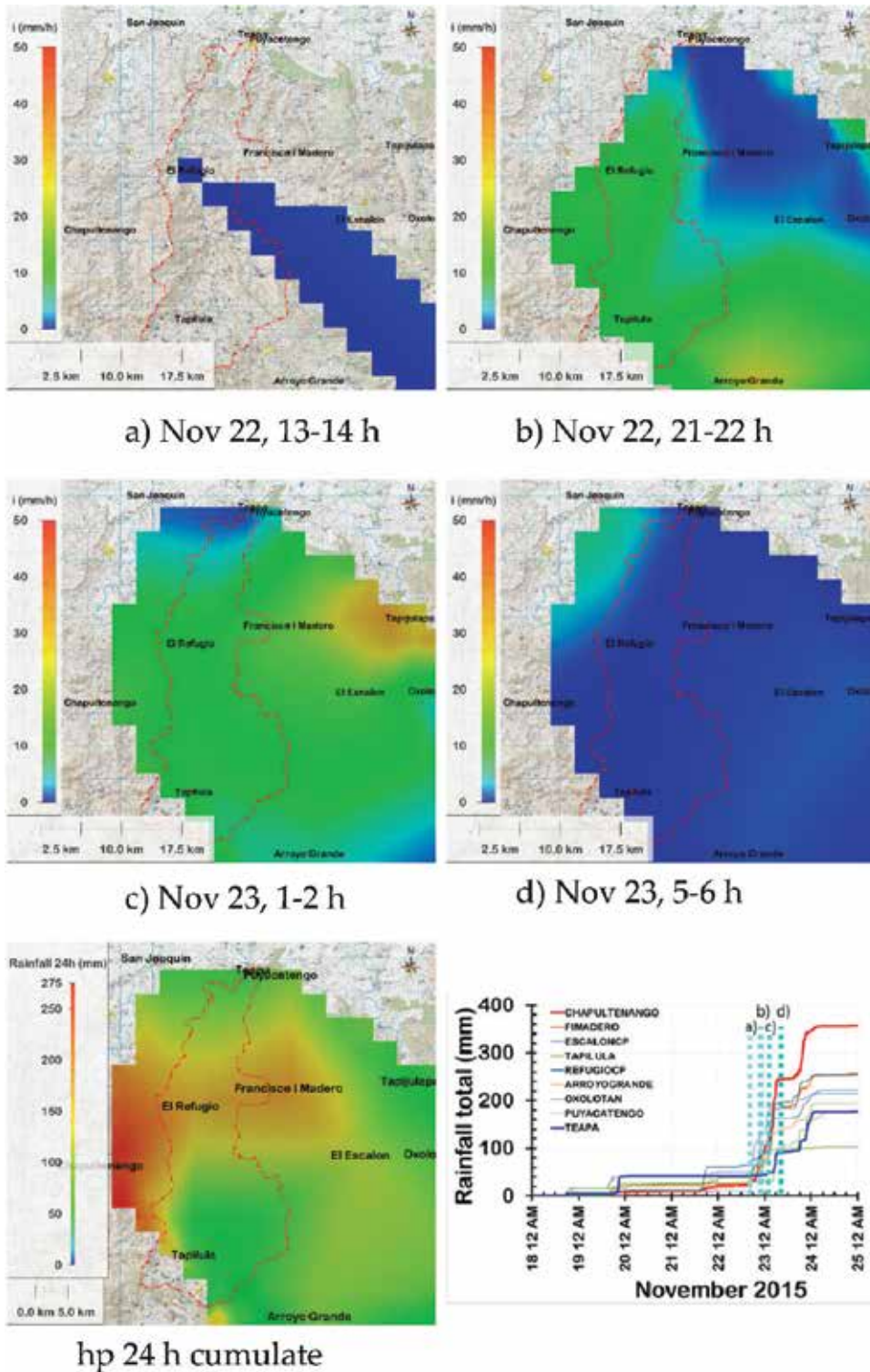


**Figure 2.**  
 Spatial analysis of precipitation from November 22 to 23, 2015.

and communication channels, were obtained from [33]. These maps and other information available from documents were integrated in a geographic information system (GIS), according to its continuous or discrete nature. In the case

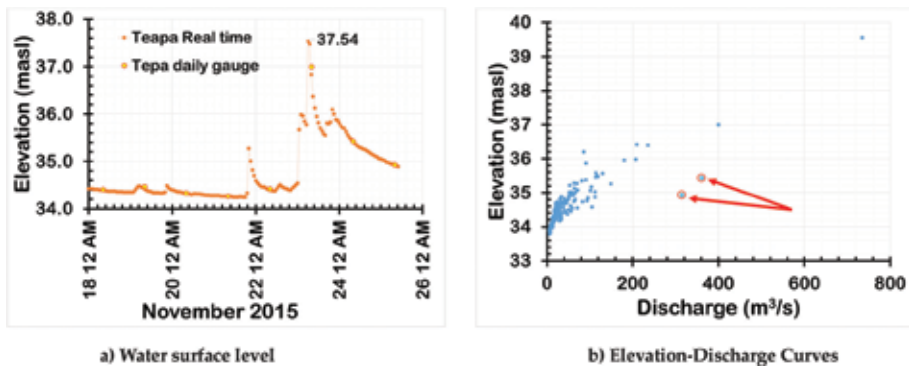


Figure 3. Water surface level and gauged records at the Teapa hydrometric station.

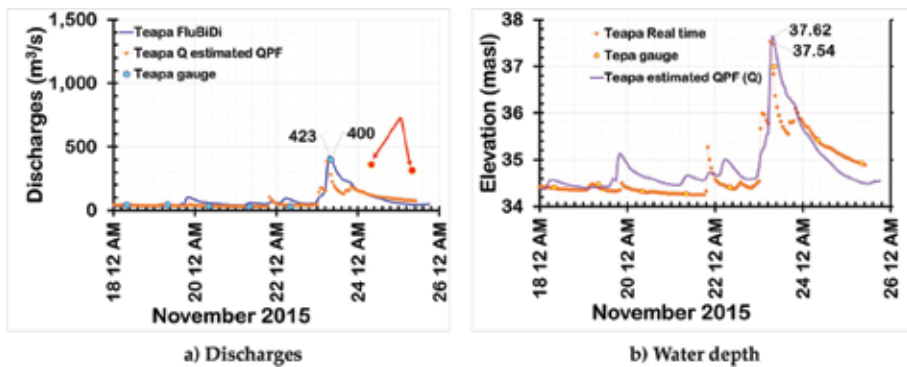


Figure 4. FluBiDi results calibrated. Red points mean data measured are wrong.

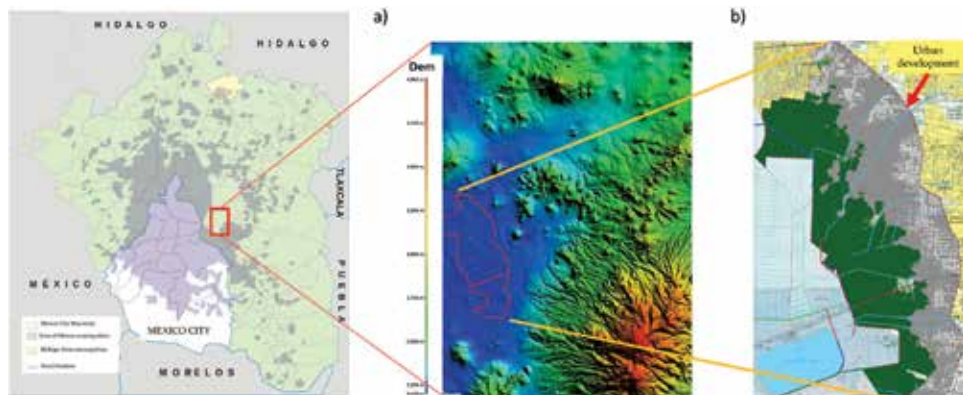


Figure 5. Study area in the Texcoco ex-lake at the ZMCM.

of the land use map, it is very important for mathematical modelling since it is the base information for the mesh of the Manning roughness coefficient “n”. It is necessary to mention that this coefficient can vary according to the time of the year; that is, for modelling in October–November, soil moisture increases to saturation; thus, the roughness coefficient also increases in a proportion of 0.03 and 0.05.

### 3.1.3 FluBiDi requirements

FluBiDi is configured to report flow depth and velocity data every hour, in order to compare results from the mathematical model with the correspondent real-time value measured at the hydrometric station. As response of the dynamic character of floods and the influence of water displacement downstream, FluBiDi provides flow equations in two horizontal dimensions, so water velocities correspond to its average value in vertical. For the simulation in the TRB, FluBiDi considers the contribution of water mass generated in the rainfall period that varies in time and space. Therefore, different hietograms are defined in different areas of the study domain. In the simulation of precipitation processes, it may be necessary to consider the infiltration of water in the no-saturate soil. Modelling infiltration is especially important to the transformation of rainfall into runoff. As it was mentioned, a mesh of the roughness coefficient of Manning “n” was obtained with the same resolution of grid from the DEM (100 m per 100 m side). The base flow was estimated in  $40 \text{ m}^3 \cdot \text{s}^{-1}$  that corresponds to the one estimated directly from the reading of water levels related to the volumetric discharge.

### 3.2 Results

FluBiDi is a mathematical model created to be used in real basins that is the case of the TRB with a drained area of  $476 \text{ km}^2$  and a volumetric flow rate of  $400 \text{ m}^3 \cdot \text{s}^{-1}$  reporting data at each hour with an interval of 5 seconds for the calculation time step, estimating that 24 hours of real time are mathematically processed in approximately 1 hour. In the model, it was the key to assess the maximum water level at the precise time when it is presented looking at the flood prevention. For this reason, in this calibration real precipitation data were used at the peak hours registered. Results are presented in **Figure 4** for November 24 at 6:00 am: an average volumetric discharge of  $423 \text{ m}^3 \cdot \text{s}^{-1}$  was obtained using FluBiDi, and the value obtained from the hydrometric station was  $400 \text{ m}^3 \cdot \text{s}^{-1}$ ; this implies a relative error (RE) of 5%. A median value of 34.766 in data measured and 34.764 in simulated was achieved, and a standard deviation of 0.64 and 0.66, respectively. The linear correlation is  $r = 0.87$ . The maximum water level has a difference around 8 cm of a total 4 m of water depth from 37.54masl head measured and 37.62masl head simulated.

In **Figure 6a** around November 24 and 25, there are two outliers that indicate the presence of a daily discharge relatively similar to the one observed on the 23rd. However, in **Figure 6b**, a water level increment similar to the one presented on November 23 was not reported. Therefore, as the volumetric rain coincides on the day of the maximum discharge and there are no other increases in subsequent water level days, it is considered that the gauge discharges may have an error in their methodology. If there is no rain, the discharge then maintains lower, and there is no transfer from another side because of the type of basin.

As shown, the model adequately predicts the discharge and water levels obtained from the precipitation recorded in the Teapa hydrometric station. This offers a very good agreement between FluBiDi and the measured values which guarantee an efficient rainfall-runoff relationship.

## 4. Application of model on an ungauged basin

Results from the calibration of FluBiDi were very satisfactory giving guarantee of the reliability of the model to be used with confidence in other basins with similar characteristics, even if it is ungauged at the output basin and without water depth references in the inundated zones. [27] mentioned three aspects that need to

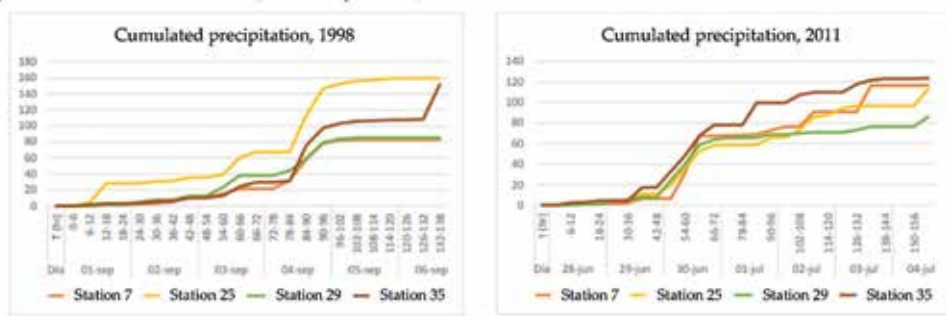


**Figure 6.**  
Mass curves for station in 1988 and 2011. Source: [35].

be addressed by the model to simulate large events: *the interchange of flow between the channel and floodplain, floodplain storage capacity and flow resistance across the floodplain* due to soil and vegetation conditions.

#### 4.1 Characteristics of the river basin

The study zone is located within the Valley of Mexico metropolitan area (zona metropolitana del Valle de México, ZMCM) at the west part corresponding to the Mexico State. The area involves the plain of the last ex-Lake of Texcoco, the largest one of an interconnected lake system during the prehispanic era. In **Figure 5**, the area of 92 km<sup>2</sup> can be shown with an average slope of 1% formed by an anthropic watershed defined by highways in the upper zone (the total contribution zone is 1020 km<sup>2</sup>). The study area is located in the subbasin “p” of Lakes of Texcoco and Zumpango of the hydrological region Panuco No. 26, and it corresponds to an endorheic basin without exit to the sea. Thus, all the rainfall becomes runoff and generates the lakes.

The Valley of Mexico is surrounded by mountains on all four sides creating a basin with only one small opening at the north. There main types of climate in the study area are subhumid temperate and dry temperate and both semi-cold semi-dry with rain in summer. The dry season is subdivided into two: dry hot (between March and May), with predominance of dry tropical air and high temperature, and dry cold (from November to February) characterised by polar-type air with low moisture content and temperature. The region receives anticyclonic systems, producing weak winds [34]. The expansion of Mexico City implicated the drying of the lakes and the expansion of the urban sprawl towards the lowlands. Thus, floods are a constant problem with inundated plains and urban settlements in a constant flood risk. In 2015, there were approximately 60,000 homes susceptible to flooding; these homes are dispersed in the grey and green area (**Figure 5b**).

#### 4.2 Data

In this case, the incoming flow to the system could be assigned to hydrograms coming from the upper part of the whole basin where some hydrometric stations are presented. The model was fed with eight hydrograms located each one in the river cut at the desire study area; they correspond to the vehicular bridges to cross the Texcoco-Tepepan highway over the riverbeds. Additionally, [35] provides local precipitation from four climatological stations (7, 25, 29 and 35) (**Figure 6**) located in the periphery but representative of the study area.

In 1988, there is a spatial difference in the rain observing between day 4 and 5 a cumulative rain of 24 h around of 90 mm in station 25, whereas in 2011 the spatial rain was almost homogeneous and of lower 24 h rain accumulating with 65 mm and with a mayor period of arriving. As result, it was determined that the rain is distributed in a homogeneous manner within the study basin, additionally to the size of the basin and the geomorphological characteristics. Therefore, a single station was proposed, which is the one that contributes with the hietogram fed to FluBiDi under a concentrated model of rain. Other consideration was to pose a hypothetical and very unfavourable event considering 5 consecutive rainy days. To this rain event, a statistical analysis was applied to four  $Tr = 20, 50, 100$  and  $200$  years. Additionally, historical events were considered: Derby 1988 and Arlene 2011. Results are shown in **Figure 7**, a recurrence of less than 20 years for the 5 continuous days of rain, which is the case of interest in areas with little slope.

As well as in the TRB calibration (Section 3), thematic data was available as well as topography and land use since it is a swamp area with some human settlements, soil and vegetation which are easily determined, but the hydrogeological conditions become very complex. The topographic information consisted in LIDAR (light detection and ranging) scale 1:10,000 with a grid resolution of 5 m per size [33]. The mesh generated from it to feed the model was integrated by 1900 rows per 1020 columns to cover all the study zone with a resolution of 10 mX10 m in order to consider 1 sec as time interval to run the FluBiDi model.

Unlike the TRB, for this case there was no information that allows a quantitative calibration. However, a qualitative calibration was carried out based on historical information of the rainfall generated by the remnants of the hurricane Derby in September, 1988, and the TS Arlene on late June and early July 2011. Both remnants left prolonged rainfall over much south central Mexico wherein Mexico City is affected by subsequent flooding damaging hundreds of homes and several roads. This information was compared with flood maps from INEGI showing the areas that could be inundated for the study area [33]. Additionally, there was social information extracted from newspapers related to the water depth occurred.

### 4.3 FluBiDi application

The discharge from the eight streams coming from the upper part of the basin was represented with its correspondent histogram and feed to the model as initial condition. At this point, the structural measure was incorporated to the flood

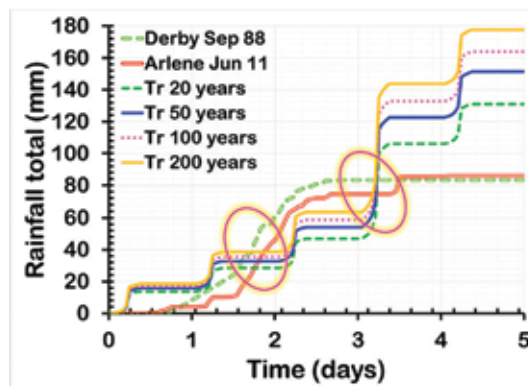


**Figure 7.**  
*Hp acumulada considerada en la modelación.*

simulation process. This structural measure of mitigation is based on rectified and lining of the riverbed to have a perfect geometry. Thus, the flood simulation was done under two conditions (**Figure 8**): (a) with the current hydraulic infrastructure and (b) with the rectification of channels. Results were used to carry out the risk assessment under a scenario of urban growth in 20 and 50 years from 2015.

The FluBiDi model was run 10 times: 5 with current conditions and 5 with mitigation measure, from which the water depths and velocity values were obtained to (1) current conditions, (2) Tr = 20 years, (3) Tr = 50 years, (4) Tr = 100 years and (5) Tr = 200 years making each of the cells an area of interest and also to the historical condition for the remnants of the hurricanes Derby and Arlene. The urban growth is evaluated through the number of houses settled in the area; thus, in 2015 it was of 18,569, and its expected increment was favoured by the possible construction at the east of the new international airport of Mexico City. The number of houses expected to increase is of 52,800 in a 20-year planning horizon and up to 158,500 homes in 50 years.

#### 4.4 Results

For each cell, it is possible to generate a limnigram as shown in the example of **Figure 9a** for a site in an area susceptible to flooding, but it is not the lowest, and some runoff is expected. **Figure 9b** shows the results of the model for the current infrastructure conditions, as well as the mitigation measures proposed for the four Tr analysed and the Arlene event in 2011.

Based on the hypothetical event and taking as reference Tr = 50 years, the maximum value under current conditions is 2232.1 masl passing with the mitigation measures at 2231.84 m. The major difference is that the inundated area takes at least 1 1/2 day to become flooded. Also, it is observed for Arlene that as a result of the mitigation work, the maximum flood levels decrease 28 cm (from 2232 to 2231.72) having the maximum value in 2 days later (from 2.3 to 4.3).

Due to the friendly output format from FluBiDi, results from the 10 mathematical simulations provided the envelope of maximum values of water depths for each cell and are presented in a map. Thus, one possible hazard scenario could be analysed throughout **Figure 10A** showing the current topographic conditions and **Figure 10B** considering the structural mitigation measure. Also, this kind of map was obtained for maximum velocities in each cell.

Comparing both maps, it was observed that the mitigation work effectively reduces those zones with higher elevations of water depth, although for lower elevation zones, water depths remain similar under both conditions. Channel rectification reduces that the river overspill; however, as this is a zone susceptible to inundation, it is impossible to eliminate the flood risk completely since there is the impact of the

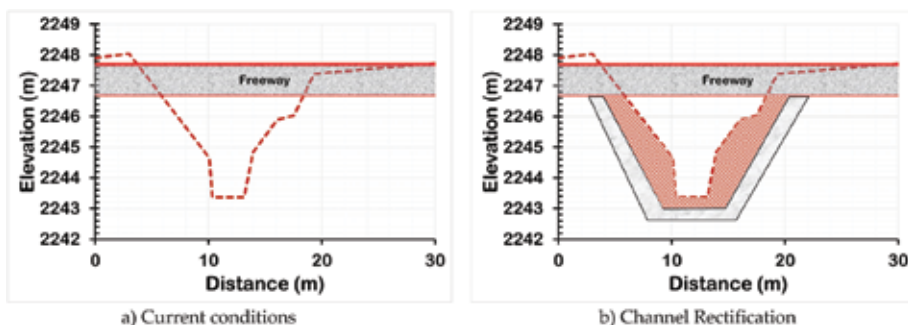


**Figure 8.**  
*Hydraulic infrastructure considered in the flood simulation using FluBiDi.*



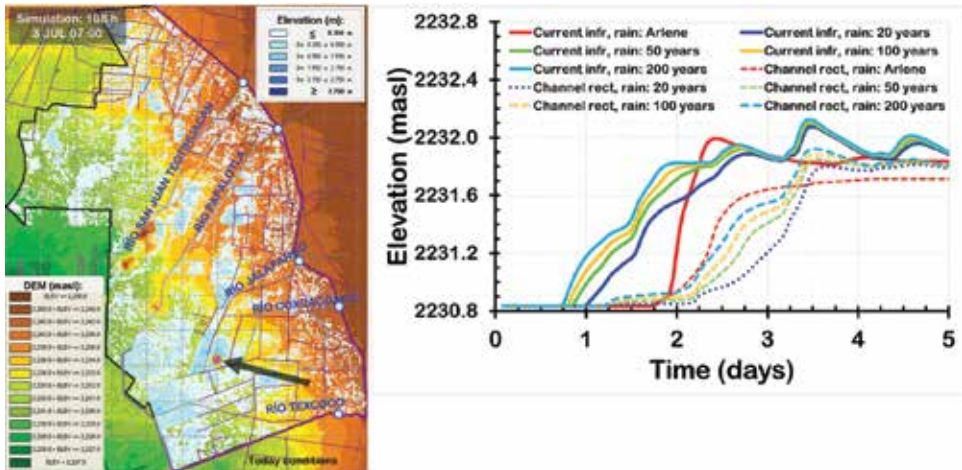


**Figure 9.**  
 Example of limnigrams for each cell.

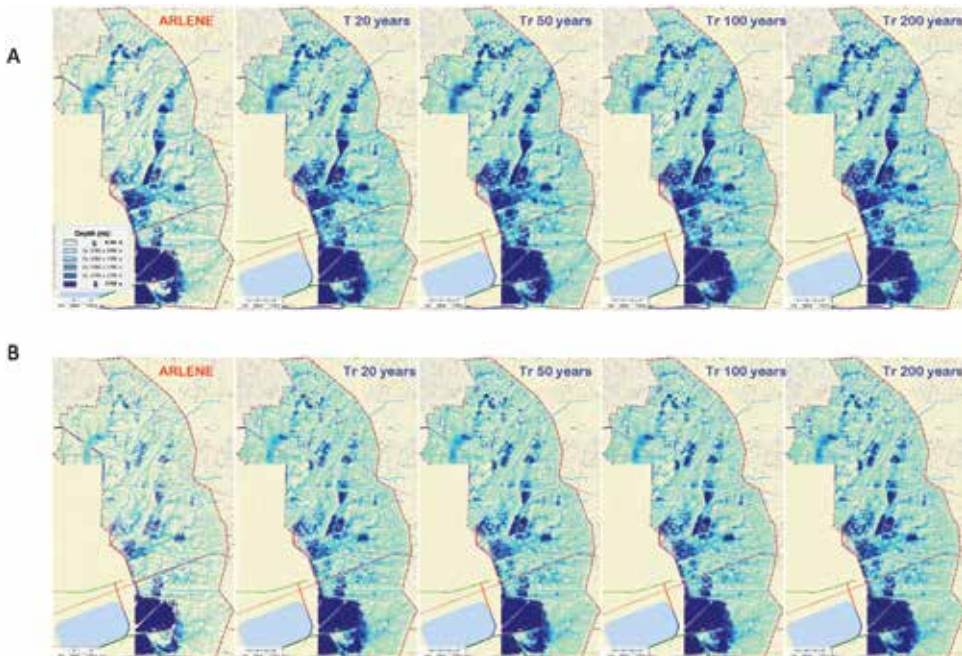


**Figure 10.**  
 Hazard flood maps considering as hydraulic infrastructure: (A) current conditions and (B) structural measure.

local rain. Thus, an important extension of the floodplain remains inundated although with a minor water depth as well as a small number of vulnerable houses; as long as people know there is an inundated zone, construction housing is limited. This situation leaves the necessity to improve water management in the study zone, and one option is to add a regulation associated to the amount of houses projected where the construction based on the hazard maps is allowed or not. In particular, for 50-year growth projection, the percentage of increment is 8.51 times the houses in 2015. Both measures, structural and nonstructural, were assessed in order to have a risk map. [7] mentioned that it is highly recommendable to use a nonstructural measure than a structural one. However, as it was observed here, the combination of both measures

improves results reducing considerably the probability of flood. Also, as [7] indicated, one finds that a better understanding of the system is crucial, since as a susceptible area to floods, it cannot be ignored and expected that there is no any flood risk. On the contrary it will continue but at different degree.

## **5. Flood risk analysis**

According to [36], maximum flood extent and water depth may be sufficient for hazard mapping and planning resources. However, velocity is essential in flood damage assessment; thus, in order to analyse the risk associated to flood events, a spatial economic analysis could be used since it considers the effects of floodplain hazard on property values (measure unit). In this case, the property values is related to the cost of the building that varies according to the socio-economic level of the people looking at the material cost and if the property is located within or without a flood-prone area. FluBiDi water depths and velocities were obtained for each instant calculation. Water depth was estimated for each cell of analysis considering an equidistance of 10 m; the guidance value corresponds to the maximum depth, since it is the one that causes the greatest damage in homes. Velocity was also available in each cell; being the premise that velocities are less than  $0.5 \text{ m}\cdot\text{s}^{-1}$ , this implies that there is no effect on the stability of the walls. Also, this means that floods in the area are slow and only walls and furniture in houses could be damaged. The criteria related to stability were confirmed using the Federal Emergency Management Agency Criterion, which provides a qualitative assessment of the stability of homes (with or without failure) which are located in the affected areas.

### **5.1 Dwellings**

The INEGI (2016) has a national housing inventory that indicates the spatial location of dwellings and the main road access if it is available. For the study area, there are 23,826 houses according to the 2015 inventory. Also, the Prevention Disaster National Centre (CENAPRED) provides regulations typifying five classes of dwellings according to the building material of walls and to the furniture inside. For each class CENAPRED established a curve to indicate the dwelling vulnerability in terms of flood hazards such as the water depth. This vulnerability is presented as an index in order to provide a quantifiable damage in monetary units. In a market study carried out, three dwelling groups were identified focusing on the average real estate costs: 330, 240 and 190 thousand pesos. These groups correspond to CENAPRED's type II housing: one-level houses with walls and roof of constructed material and concrete floor.

One important point to be considered is that the study area is located in the vicinity of a possible focus of major urban development due to the construction of the Mexico City new international airport. The hypothesis considers that the new settlement of houses will be developed in the lower areas. Two scenarios were predicted: for an inter-media dwelling growth in 20 years, an increment of 52,800 houses is assumed, whereas for a scenario of maximum saturation (50 years), 158,500 houses are considered.

### **5.2 Dwelling vulnerability**

Using the information obtained with the mathematical model for each cell and the maximum water depth, it is possible to associate the cell with the coordinate of the closest dwelling. This water level is the flood damage to the dwelling for each hydraulic infrastructure scenario at its respective Tr. **Table 1** presents the comparative summary for the 2015 houses and their degree of vulnerability under (a) channels at current conditions and (b) channels rectified.

Dwelling vulnerability comparison between current hydraulic conditions and rectified channels.

The rectification channels reduce the vulnerability at least in one-third, for the very high vulnerability and small differences were observed for very low vulnerability. For the other three categories, a proportional behaviour was observed reducing the number of housing as the degree of vulnerability increases. The same exercise was applied for the 20 and 50 years of urban growth projection. Also, the Arlene impact was analysed to the vulnerability being the one with less affectation to houses. Once the vulnerability index was estimated, the risk was computed based on the expected annual damage or “mathematical hope” of the occurrence of an event; this is represented by the area under the curve in **Figure 11**.

Results obtained indicate that for current houses, the risk decreases from 41 to 18 million \$-year<sup>-1</sup>, when the structural measure of channel rectification is implemented. For the 20-year projection of urban growth, the risk decreases from 280 to 102 M \$-year<sup>-1</sup> when carrying out the rectification of channels. For the 50-years scenario (housing saturation) reduction was from 700 to 275 M\$-year<sup>-1</sup> implementing the structural measure. These damage values are very useful for planning aspects in urban development, which can also be considered for insurance companies. **Figure 12** could be represented as maps as shown in **Figure 11**. For example, spatial dwelling at major or minor risk could be easily allocated in the map at the study area for the 50-year urban growth projection under the current hydraulic conditions.

As insurers consider the risk as the cost of the annual insurance premium, F represents a high number of homes but with a minor damage. Therefore, the value of the insurance in A is very high, and the owner will not opt for the policy. However, under present conditions there are few houses with grade A, and they do not settle in low areas. Though, it is quite favourable that in a 50-year project, the tendency is to inhabit low-lying areas, increasing the risk of flooding and the value of the policy. Even in the urban settlement growth without and with rectification, the number of vulnerable houses decreases from 32,686 to 20,441, respectively. This would represent a decrease in the risk measured in the cost of housing of up to 60%. Also, for the urban growth of 50 years, when the nonstructural measure is added to the structural one, the reduction in the cost of vulnerable housing goes to 94%. Thus, the above provides a tool for decision-making in urban development without risk to the population. This confirm the [27] conclusion that to have a risk map is essential to define the possible impact in the floodplain location on property prices. Moreover, it is necessary to mention that the evaluation was carried out only considering the damage in housing; thus, the damage avoided is greater if one considers

Vulnerability (biological)	Dwelling vulnerability (houses)				
	Arlene T 20 years	T 50 years	T 100 years	T 200 years	T 500 years
Extreme	292	618	697	454	895
High	290	304	360	465	421
Considerable	295	340	401	600	532
Moderate	481	322	1,025	1,057	1,124
Low	2,381	3,726	6,351	6,121	6,828
Vulnerability (structural)	Dwelling vulnerability (houses)				
	Arlene T 20 years	T 50 years	T 100 years	T 200 years	T 500 years
Extreme	51	236	222	243	221
High	82	272	282	273	260
Considerable	131	311	329	329	322
Moderate	312	326	427	361	1,005
Low	2,322	3,421	5,343	5,134	5,407

**Table 1.** Dwelling vulnerability comparison between current hydraulic conditions and rectified channels.

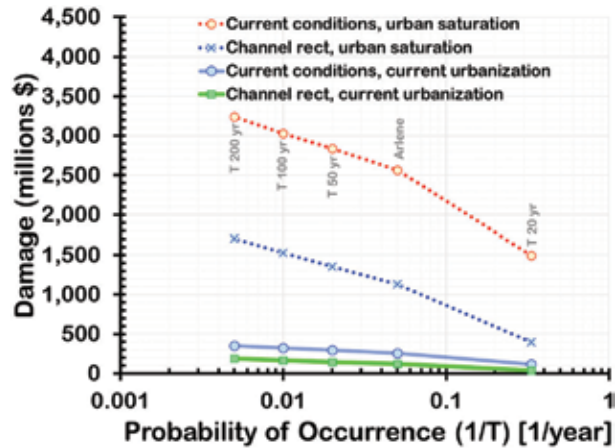


**Figure 11.** Risk computation for each  $T_r$  and Arlene events considering 2015 conditions and at 50 years of growth with and without rectification.

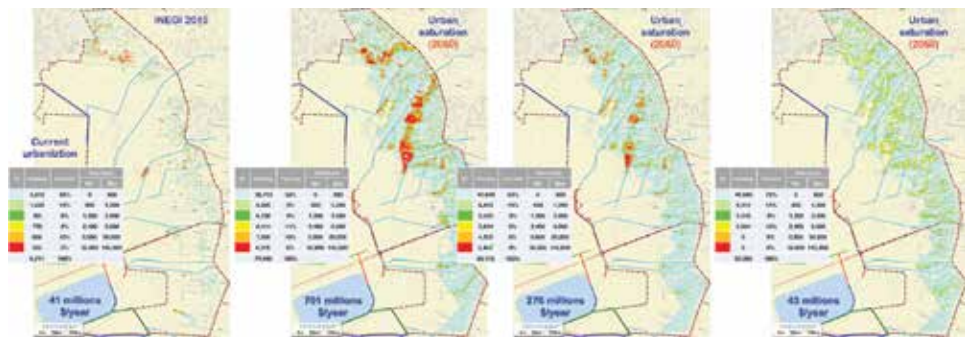


**Figure 12.** Risk with current infrastructure (a), for 50 years of growth without rectification (b), for 50 years of growth with rectification (c) and with nonstructural measure (d).

other buildings such as schools, hospitals, roads, businesses and other aspects that affect economically the area.

In particular, for a 50 years of growth projection where the percentage of increment is 8.51 times the houses in 2015, both measures (structural and nonstructural) were assessed to have the risk map. This agrees with [7], in the high convenience to use a nonstructural measure, even more than a structural one. However, as it was observed here, the combination of both measures improves results reducing considerably the probability of flood. Also, [7] indicated one can find that a better understanding of the system is crucial, since as a susceptible area to floods, it cannot be ignored and expected that there is no flood risk. On the contrary, it will continue but at a different degree.

## 6. Conclusions

Floods are very dynamic affecting the river and its floodplain particularly during its displacement downstream. This makes FluBiDi a good option to simulate flood events using a real topography under different conditions such as gauged and ungauged basins. The model calibration is a crucial activity, for planning and public safety. The method used for FluBiDi calibration was ideal since there were data

available constantly measured with different latency and accuracy. Results from the calibration were very satisfactory since discharge and water depth measured and simulated have less than 5% of error. This guarantees the reliability and robustness of FluBiDi.

Several tools were used (mathematical model, urban growth scenarios, hydraulic evaluation of mitigation measures, market studies of the type of housing) that together allow the planning of urban developments in flat areas that are associated with frequent floods. Flooding vulnerability in a basin with high developing urbanisation is potentially high when this urbanisation is located in flat areas, even if they are not subject to extreme climatic events. Achieving a harmony between society and the conditions of the ecosystem is relevant always recognising the interaction among exposure, sensitivity and adaptive capacity once flood vulnerability is analysed. This implies that it is possible that the development of the area is only a matter of living or using what one has. Thus, adaptation is possible in case of frequent floods, for example, to opt for the best type of house in order to reduce the risk such as stilt houses (raised on piles of wood or concrete), which are built primarily as a protection against flooding. These measures of adaptation, together with methods to control floods that happen in urban area, are ideal. These methods could consider different structural actions such as in this case it was the channel rectification as mitigation measure. However, also here it was demonstrated that effectively it is worth applying a structural measure, but in order to maximise results a nonstructural measure need to be applied reducing and, in some cases, removing the inundation risk. One important point to be considered is that the study area is located in the vicinity of a possible focus of major urban development due to the construction of the Mexico City new international airport. Planning, as a nonstructural measure, is perfectly a solution in urban growth development.

## **Acknowledgements**

The authors thank the National Water Commission (CONAGUA), in particular, the Technical General Sub-directorate for the available information on basins instrumented.

## **Author details**

Faustino de Luna Cruz<sup>1,2</sup>, Oscar A. Fuentes Mariles<sup>2</sup>, Judith Ramos Hernández<sup>2\*</sup> and Jesús Gracia Sánchez<sup>2</sup>

1 Programa de Maestría y Doctorado en Ingeniería, Universidad Nacional Autónoma de México, Ciudad de México, México

2 Instituto de Ingeniería, Universidad Nacional Autónoma de México, Ciudad de México, México

\*Address all correspondence to: [jramosh@iingen.unam.mx](mailto:jramosh@iingen.unam.mx)

## **IntechOpen**

---

© 2019 The Author(s). Licensee IntechOpen. This chapter is distributed under the terms of the Creative Commons Attribution License (<http://creativecommons.org/licenses/by/3.0>), which permits unrestricted use, distribution, and reproduction in any medium, provided the original work is properly cited. 

## References

- [1] Idris S, Dharmasiri. Mint: Flood risk inevitability and flood risk management in urban areas: A review. *Journal of Geography and Regional Planning*. 2015;8(8):205-209. DOI: 10.5897/JGRP2015.0510
- [2] Willner SN, Levermann A, Zhao F, Mint FK. Adaptation required to preserve future high-end river flood risk at present levels. *Science Advances*. 2018;4:eaa01914
- [3] Wohl EE. Hydrology and discharge. In: Gupta A, editor. *Large Rivers: Geomorphology and Management*. Chichester: Wiley and Sons, Ltd.; 2007. pp. 27-44
- [4] Criss RE. Increased flooding of large and small watersheds of the central USA and the consequences for flood frequency predictions. In Criss RE, Kusk TM, editors. *Finding the Balance Between Floods, Flood Protection, and River Navigation*, Centre for Environmental Sciences, St. Louis University. pp. 16-21. [Internet]. Available from: [https://www.researchgate.net/publication/316596045\\_A\\_brief\\_history\\_of\\_flooding\\_and\\_flood\\_control\\_measures\\_along\\_the\\_Mississippi\\_River\\_Basin](https://www.researchgate.net/publication/316596045_A_brief_history_of_flooding_and_flood_control_measures_along_the_Mississippi_River_Basin) [Accessed Aug 15 2009]
- [5] Biedenharn DS, Watson CC, Thorne CR. Fundamentals of fluvial geomorphology. Chapter 6. In: Garcia MH, editor. *Sediment Engineering: Theories, Measurements, Modeling and Practice: Processes, Management, Modeling, and Practice (ASCE Manual and Reports on Engineering Practice No. 110)*. Virginia: ASCE. 1st ed; 2008. pp. 355-386. ISBN-10: 0784408149, ISBN-13: 978-0784408148:
- [6] DRDE, editor. *Primer on Natural Hazard Management in Integrated Regional Development Planning*. Vol. 1. Washington DC: OAS (Organization of the American States); 1991. ISBN: 0-8270-3008-8
- [7] Jha A, Bloch R, Lamond J. *Cities and Flooding. A Guide to Integrated Urban Flood Risk Management for the 21st Century* 2011. New York: The World Bank; 2015 631 p. ISBN 978-0-8213-8866-2
- [8] Güneralp I, Marston RA. Mint: Process-form linkages in meander morphodynamics: Bridging theoretical modeling and real world complexity. *Progress in Physical Geography: Earth and Environment*. 2012;36(6):718-746. DOI: <https://doi.org/10.1177/0309133312451989>
- [9] Plate EJ. Mint: Flood risk and flood management. *Journal of Hydrology*. 2002;267:2-11 <https://www.sciencedirect.com/journal/journal-of-hydrology/vol/267/issue/1>
- [10] Merz B, Thieken AH, Gocht M. Flood risk mapping at the local scale: Concepts and challenges. In: Begum S, Stive MJF, Hall JW, editors. *Flood Risk Management in Europe. Innovation in Policy and Practice*, (Advances in Natural and Technological Hazards Research, 25). Berlin: Springer; 2007. pp. 231-251 <http://gfzpublic.gfz-potsdam.de/pubman/item/escidoc:237346>
- [11] Cutter SL, Boruff BJ, Shirley WL. Mint: Social vulnerability to environmental hazards. *Social Science Quarterly*. 2003;84(2):242-261. DOI: [http://danida.vnu.edu.vn/cpis/files/Papers\\_on\\_CC/Vulnerability/Social%20Vulnerability%20to%20Environmental%20Hazards.pdf](http://danida.vnu.edu.vn/cpis/files/Papers_on_CC/Vulnerability/Social%20Vulnerability%20to%20Environmental%20Hazards.pdf)
- [12] Indrawan I, Siregar RI. Mint: Analysis of flood vulnerability in urban area; a case study in deli watershed. *Journal of Physics: Conference Series*. 2018. DOI: 978:012036. DOI:10.1088/1742-6596/978/1/012036

- [13] Koivumäk AP, Lotsari E, Kayhko J, Saari A, Mint HH. Uncertainties in flood risk mapping: A case study on estimating building damages for a river flood in Finland. *Journal of Flood Risk Management*. 2010;**3**:166-183. DOI: 10.1111/j.1753-318X.2010.01064.x
- [14] De Moel H, van Alphen J, Aerts JCJC. Mint: Flood maps in Europe - methods, availability and use. *Natural Hazards and Earth System Sciences* 2009;**9**:289-301. DOI: [www.nat-hazards-earth-syst-sci.net/9/289/2009/](http://www.nat-hazards-earth-syst-sci.net/9/289/2009/)
- [15] van Alphen J, Passchier R. Atlas of Flood Maps, examples from 19 European countries, USA and Japan. Ministry of Transport, Public Works and Water Management, The Hague, Netherlands, prepared for EXCIMAP2007 [Internet]. Available from: [http://ec.europa.eu/environment/water/flood\\_risk/flood\\_atlas/index.htm](http://ec.europa.eu/environment/water/flood_risk/flood_atlas/index.htm) [Accessed: 2018-06-01]
- [16] Samarasinghe O, Sharp B. Mint: Flood prone risk and amenity values: A spatial hedonic analysis. *The Australian Journal of Agricultural and Resource Economics*. 2010;**54**. DOI: 457-475. Doi: 10.1111/j.1467-8489.2009.00483.x
- [17] Holway JM, Burby RJ. Mint: The effects of floodplain development controls on residential land values. *Land Economics*. 1990;**66**(3):259-271. DOI: 10.2307/3146728
- [18] Harrison J, Winterbottom S, Johnson R, editors. *Climate Change and Changing Patterns of Snowfall in Scotland*. Edinburgh: The Scottish Executive Central Research; 2001 48 p. <http://citeseerx.ist.psu.edu/viewdoc/download?doi=10.1.1.573.4260&rep=rep1&type=pdf>
- [19] Fuentes OA, Franco LE. *Modelo Matemático de Áreas de Inundación*. Cuadernos de Investigación No. 41. Mexico: Centro Nacional de Prevención de Desastres; 1997 37 p. <https://www.cenapred.gob.mx/es/Publicaciones/archivos/193-CUADERNODEINVESTIGACIONMODELOMATEMATICODEREADEINUNDACION.PDF>
- [20] De Luna F. *Modelo hidráulico de Flujo Bidimensional Para Estimar el Escurrimiento a Partir de la precipitación* [PhD Candidate Thesis]. Mexico: Universidad Nacional Autónoma de México; 2015
- [21] DHI. MIKE SHE User Manual. Hørsholm, Denmark: Danish Hydraulic Institute [Internet]. Available from: <https://www.dhigroup.com/> [Accessed: 2012-05-23]
- [22] Roberts CD, Palmer MD, McNeill D, Collins M. Mint: Quantifying the likelihood of a continued hiatus in global warming. *Nature Climate Change*. 2015;**5**(4):337-342. DOI: 0.1038/nclimate2531
- [23] De Luna F, Ramos-Hernández JG, Fuentes-Mariles OA, Gracia-Sánchez. Mint: FluBiDi a model to estimate flood based on runoff: Validation using extreme and natural basin conditions. *Hydrological Sciences Journal*. [Accepted]
- [24] Ogden FL, Lai W, Steinke RC. ADHydro: Quasi-3D high performance hydrological model. In: *Proceedings of SEDHYD 2015, 10th Interagency Sedimentation Conference, 5th Federal Interagency Hydrologic Modelling Conference April 19-23, Reno, Nevada, USA; 2015*. <http://acwi.gov/sos/pubs/3rdJFIC/index.html>. Accessed 03 June 2016
- [25] Costabile P, Costanzo C, Macchione F, Mercogliano P. Mint: Two-dimensional model for overland flow simulations: A case study. *European Water*. 2012;**38**:13-23. DOI: [http://www.ewra.net/ew/pdf/EW\\_2012\\_38\\_02.pdf](http://www.ewra.net/ew/pdf/EW_2012_38_02.pdf)
- [26] Gupta A. The hazardousness of high-magnitude floods. In:



Alcántara-Ayala I, Goudie AS, editors. *Geomorphological Hazards and Disaster Prevention*. Cambridge: Cambridge University Press; 2010 p. 291. ISBN: 978-0-521-76925-9

[27] Huxley C, Ryan P. Flood Modeling: How accurate is your model. In: *Floodplain Management Association Newsletter* [Internet. Accessed: 2018-05-10] Available from: [https://www.tuflow.com/Download/Publications/October2016\\_FMA\\_Newsletter\\_HuxleyRyan.pdf](https://www.tuflow.com/Download/Publications/October2016_FMA_Newsletter_HuxleyRyan.pdf)

[28] INEGI. Cuaderno Estadístico Municipal Teapa, Estado de Tabasco. 1st ed. INEGI: Agascalientes; 2000. 192 p. ISBN 970-13-3143-5

[29] Maza A. Cuenca Grijalva-Usumacinta Estudio de Gran Visión para las Obras de Protección de la Planicie, elaborado para la Subdirección General de Construcción, Gerencia Regional Sur. CONAGUA and Subdirección Técnica, Gerencia de Estudios de Ingeniería Civil, CFE, editors. 1997

[30] IPCET. Pronóstico Meteorológico [Internet]. Available from: <https://tabasco.gob.mx/pronostico-meteorologico> [Accessed: 2015-06-20]

[31] CONAGUA. Reporte de lluvias registradas [Internet]. <https://smn.cna.gob.mx/es/pronosticos/pronosticosubmenu/informe-meteorologico-especial-de-lluvias> [Accessed: 2013-04-21]

[32] Spada E, Tucciarelli T, Sinagra M, Sammartano V, Corato G. Mint: Computation of vertically averaged velocities in irregular sections of straight channels. *Hydrology and Earth System Sciences*. 2015;19:3857-3873. DOI: 10.5194/hess-19-3857-2015

[33] INEGI. 'Conjunto de datos vectoriales de uso de suelo y vegetación escala 1:250 000, serie V (capa unión)', escala: 1:250000. edición: 2a. [Internet].

2013. Available from: <http://en.www.inegi.org.mx/app/mapa/inv/default.aspx> [Accessed: 2018-05-10]

[34] INEGI. Cuaderno Estadístico Municipal Texcoco, Mexico. 1st ed. Agascalientes: INEGI; 2000. 184 p. ISBN 970-13-3271-7

[35] Romero GD. Caracterización de dos Eventos hidrológicos Ocurridos en los años 1988 y 2011 en el Valle de México [Thesis]. Mexico: Engineer Faculty, UNAM; 2017

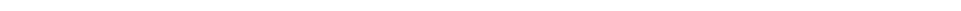
[36] Teng J, Jakeman AJ, Vaze J, Croke BFW, Dutta D, Mint KS. Flood inundation modelling: A review of methods, recent advances and uncertainty analysis. *Environmental Modelling and Software*. 2017;90:201-216. DOI: 10.1016/j.envsoft.2017.01.006





## Section 3

# Flood Risk and Agriculture





# Methodology for Agricultural Flood Damage Assessment

*Badri Bhakta Shrestha, Hisaya Sawano, Miho Ohara,  
Yusuke Yamazaki and Yoshio Tokunaga*

## Abstract

This chapter describes a method for assessing flood damage to the agricultural sector, specifically focusing on flood damage to rice crops. The chapter also includes the case studies of flood damage assessment conducted in the Asian river basins, the Pampanga River basin of the Philippines, and the Lower Indus River basin of Pakistan. The assessment was performed by defining flood damage to rice crops as a function of flood depth, duration, and growth stage of rice plants and using depth-duration-damage function curves for each growth stage of rice plants. In the case studies, flood characteristics such as flood depth, duration, and distribution were computed using a rainfall-runoff-inundation (RRI) model. Flood damage to rice crops was assessed for the 2011 flood and 100-year flood events in the case of the Pampanga River basin and for the 2010 flood in the case of Lower Indus River basin. The calculated values of agricultural damage were compared with reported data for validation of methodology, and it was found that the calculated damage reasonably agreed with reported data. The rice-crop damage assessment method described in this chapter can also be applied in other areas for flood risk assessment.

**Keywords:** flood damage, agriculture, damage curves, RRI model, Asian river basins

## 1. Introduction

The impact of floods is becoming greater due to their increasing frequency and scale and the concentration of population and socioeconomic activities in river basins [1]. Developing countries are particularly vulnerable to flood disasters because of limited resources to cope with them. Flood disasters cause serious damage to properties and livelihoods as indicated in **Figure 1**, which shows the estimated value of flood damage to agriculture and infrastructure and also the number of houses totally or partially damaged by floods in the case of Region III of the Philippines. For the assessment of flood disaster risk and the evaluation of risk mitigation measures, flood risk needs to be quantified as accurately as possible [2]. Flood damage assessment is thus essential for flood management to mitigate risk and also to quantify flood risk.

Flood damage can be assessed quantitatively based on the analysis of hazard, exposure, and vulnerability. By conducting flood damage assessment, the effectiveness of countermeasures in reducing the intensity of a flood hazard can be quantified by comparing simulated damage before and after the implementation of

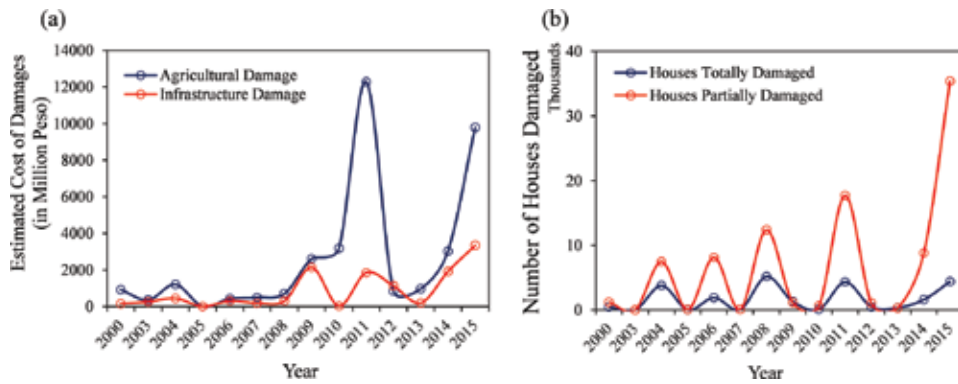


**Figure 1.**

*Agricultural, infrastructure, and house damage due to the past floods in Region III of the Philippines [Data source: Office of Civil Defense, Region III, Philippines].*

countermeasures. The quantification of the effectiveness of countermeasures is also essential in cost-benefit analysis to assess the effectiveness of preventive investment. For flood damage assessment, flood damage functions are generally derived from past flood damage data by relating flood characteristics, such as flood depth and flood duration, with damage [3]. Shrestha et al. [3] pointed out that past flood hazards and damage data and their relationships are very important for the development of an appropriate method as well as for validation of calculated results. In many countries, especially in developing countries where past damage data are very limited, more efforts should be made to improve a flood damage assessment method. Effort should also be focused on the collection of flood damage data for the development of damage curves, model validation, and adaptation of approaches [4]. It is thus essential to develop appropriate flood damage estimation methods for planning mitigation measures and preparedness activities in order to reduce flood damage in the future.

For flood damage assessment, numerous studies have focused mainly on flood damage to the residential, infrastructure, and industrial sectors, while less attention has focused on the agricultural sector [5, 6]. However, the agricultural sector is a major source of income in many developing countries in Asia and thus likely to play a major role in new flood management policies [6]. On the other hand, when a flood occurs, the agricultural sector of many developing countries is severely affected by flooding (**Figure 1**). Therefore, an appropriate methodology for assessing flood damage to the agricultural sector is essential. This chapter describes a method for assessing flood damage to the agricultural sector, specifically focused on flood damage to rice crops. Flood damage to rice crops is defined as a function of flood depth, duration, and growth stage of rice plants. The case studies of flood damage assessment in the river basins of Asia such as the Pampanga River basin of the Philippines and the Lower Indus River basin of Pakistan are discussed.

## 2. Categorization of flood damage

Flood damage refers to varieties of destruction and losses caused by flooding [7, 8], for example, harmful effects on humans; damage to buildings, residential properties, and other types of infrastructure; impact on lifeline and other public services; and losses of agricultural and industrial production [5, 7]. Flood damage is typically categorized as direct and indirect damage and further categorized as tangible and intangible damage depending on whether damage can be assessed in

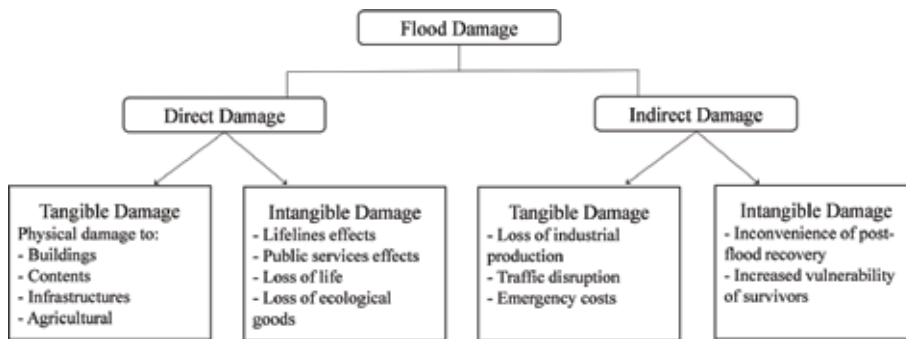


**Figure 2.**  
Categorization of flood damage [5, 6, 8, 9].

monetary values [5, 7, 8]. **Figure 2** shows the categorization of damage with some examples.

### 2.1 Direct and indirect damage

Direct damage is damage caused by direct physical contact of floodwaters [5, 8], such as flood damage to buildings and residential properties; losses of crops, livestock, and human lives; immediate health impacts; and losses of ecological goods. Indirect flood damage is damage which is not directly due to flood exposure but mainly caused by disruption of physical and economic linkages and other losses, such as loss of production at flood-affected factories and companies and costs of traffic disruption and emergency services [5, 6–8].

### 2.2 Tangible and intangible damage

Tangible damage is damage which can be easily specified in monetary values, such as damage to buildings, residential properties, assets, and agricultural crops and loss of production. Intangible damage is damage which cannot be specified in monetary values, such as casualties, health impacts, and damage to ecological goods and to all kind of goods and services [5, 7, 8].

## 3. Method for agricultural damage assessment

### 3.1 Framework of flood damage assessment

Flood risk and damage assessment are essential for flood risk management. The main purpose of flood damage assessment is to identify areas at risk where mitigation actions are necessary. This chapter describes a grid-based method for flood damage assessment considering three major factors of risk: hazard, exposure, and vulnerability. Flood damage assessment starts with the identification of the target area and items exposed to a flood hazard using the results of flood hazard simulation and moves on to the evaluation of damage that might occur to exposed items because of the vulnerability of each item. **Figure 3** shows the estimation process of agricultural flood damage assessment. Flood damage can be assessed by combining knowledge of a flood hazard and an item exposed to the flood with vulnerability. Flood characteristics such as flood depth and duration can be simulated using a

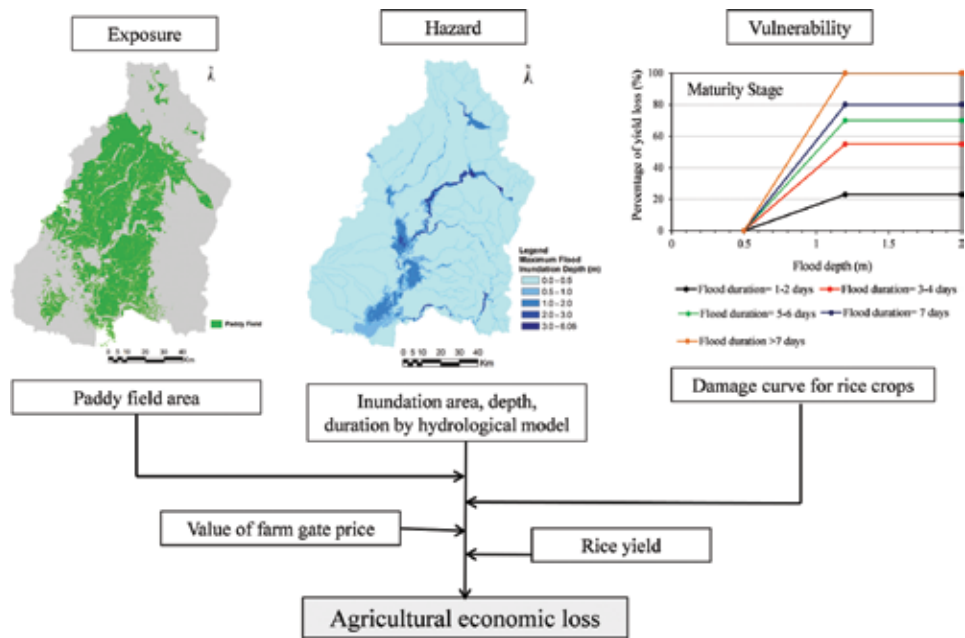


**Figure 3.** Estimation process of rice-crop damage caused by flooding.

hydrological model, and paddy areas can be extracted from land-cover and land-use maps to identify exposed paddy areas in the hazard-risk areas. Then, the yield loss caused by flooding can be estimated by applying flood damage curves and converted to economic value based on the value of farm gate price and rice yield.

### 3.2 Flood hazard assessment

The identification of flood hazard areas and the intensity of a hazard by hazard assessment is the first step for flood risk and damage assessment. Flood hazard assessment is conducted by applying a hydrological/hydraulic simulation model using hydrometeorological data, topographic data, land-use data, and operation rules of river management structures. Information on past flood hazards, such as rainfall, river water level, discharge volume, and inundation area and depth, is required to develop and calibrate a simulation model.

For the case studies in the Pampanga and Lower Indus River basins, the rainfall-runoff-inundation (RRI) model, developed by Sayama et al. [10], was employed to compute flood characteristics such as inundation depth and duration. The RRI model is a two-dimensional model capable of simulating rainfall-runoff and flood inundation simultaneously [11]. The model deals with slopes and river channels separately. The flow on the slope grid cells is calculated with a 2D diffusive wave model, while the channel flow is calculated with a 1D diffusive wave model. The details of the RRI model can be found in Sayama et al. [10] and Sayama [11]. The model parameters were calibrated to the past largest flood event cases. Flood hazard assessment was conducted for the past largest flood event and 100-year flood cases in the Pampanga River basin and for the past largest flood event case in the Lower Indus River basin. For the simulation of the target flood of a specific return period, statistical analysis was conducted to identify the magnitude of a hazard of the target scale.

Generally flood risk assessment is conducted for a probable future flood event of a specific return period or for the past largest flood event. The target scale differs by river according to the socioeconomic activities, expected flood damage, and history



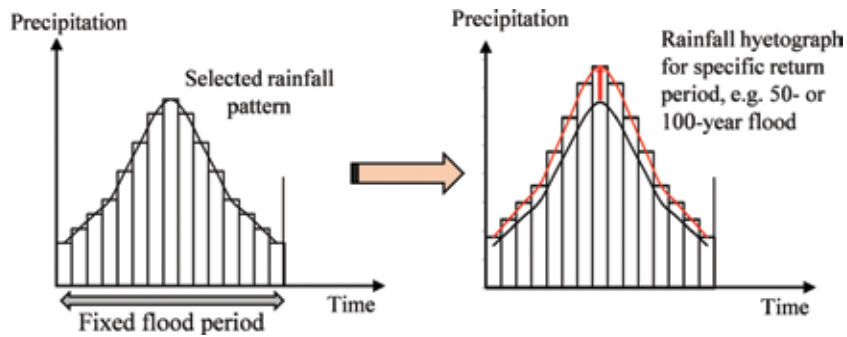


**Figure 4.**  
*Schematic figure for designing a rainfall hyetograph for a specific return period flood.*

of disasters in the basin. The magnitude of damage due to the target flood is an important factor in identifying the target scale for flood management and can be simulated in the process of risk assessment. To identify the magnitude of a flood of a specific return period, rainfall data should be used for statistical analysis as the primary information of the target natural hazard. Discharge volume is also applicable to statistical analysis if no overflows from the river occur in the upstream of the measurement point and the land use of the catchment area has not changed. The water level of the river is not appropriate for statistical analysis because the river cross section at the water-level observation point often changes in an alluvial floodplain.

As mentioned above, rainfall data is normally employed as a statistical sample for a study on the design flood scale. To assess a flood hazard of a specific return period, a rainfall hyetograph for a specific return period can be estimated by multiplying the selected rainfall pattern of a past flood event by a conversion factor, as shown in **Figure 4**. The conversion factor for each return period can be calculated as the ratio of the corresponding rainfall of the return period and the rainfall volume of the selected rainfall pattern. Normally, the rainfall pattern with the highest rainfall volume is selected among the past flood events for designing a rainfall hyetograph for a specific return period.

### 3.3 Identification of exposed paddy fields

After assessing hazard areas by a hydrological/hydraulic simulation, paddy areas exposed to the flood can be identified by overlaying the flood hazard areas and the paddy areas to assess flood damage to rice crops. The paddy-field areas can be extracted from a land-cover map prepared by using satellite images or land-use and land-cover maps prepared by a local government. Several freely available global land-cover data are presented in **Table 1**.

For the case studies, paddy fields were extracted using a land-cover map prepared by NWRB and JICA [12] for the Pampanga River basin of the Philippines and a global land-cover map prepared by the Global Land Cover by National Mapping Organizations (GLCNMO) [13] for the Lower Indus River basin. The details will be discussed in the section of case studies.

### 3.4 Agricultural damage assessment

#### 3.4.1 Depth-duration-damage function curves

After the identification of exposed paddy fields in the hazard areas, possible damage can be calculated using risk indicators. Each risk indicator represents the

Data description	Data provider	Specification	Website link
Global Land Cover Characterization (GLCC)	USGS	Spatial resolution: 30 arc-seconds	<a href="https://lta.cr.usgs.gov/glcc/globdoc2_0">https://lta.cr.usgs.gov/glcc/globdoc2_0</a>
Global Land Cover (GLCNMO)	ISCGM	Spatial resolution: 15 and 30 arc-seconds	<a href="https://globalmaps.github.io/">https://globalmaps.github.io/</a>
Global Land Cover-SHARE (GLC-SHARE)	FAO	Spatial resolution: 30 arc-seconds	<a href="http://ref.data.fao.org/map?entryId=ba4526fd-cdbf-4028-a1bd-5a559c4bff38">http://ref.data.fao.org/map?entryId=ba4526fd-cdbf-4028-a1bd-5a559c4bff38</a>
Climate Change Initiative Land Cover (CCI-LC)	European Space Agency	Spatial resolution: 300 m	<a href="https://www.esa-landcover-cci.org/">https://www.esa-landcover-cci.org/</a>
MODIS Land Cover	NASA/USGS	Spatial resolution: 500 m	<a href="https://lpdaac.usgs.gov/dataset_discovery">https://lpdaac.usgs.gov/dataset_discovery</a>

**Table 1.**  
*List of globally available land-cover data.*

vulnerability of each item by showing the correlation of the intensity of a hazard with damage quantified by a damage curve. Therefore, flood damage curves are important in flood damage estimation. To estimate flood damage to rice crops, depth-duration-damage function curves are normally used.

Flood damage curves can be mainly derived from two approaches: (1) using actual damage data of past floods and (2) using synthetic data (expert estimation or questionnaire surveys) [8]. In the former approach, flood damage curves are developed based on data and information of past hazards and resulting actual flood damage. Therefore, accumulation of data on hazards (inundation records) and flood damage is essential. In the latter approach, damage curves are derived from hypothetical analysis, information obtained from questionnaire surveys, or land cover and standardized typical property types.

**Table 2** shows the flood damage matrix for rice-crop damage published by the Philippines Bureau of Agricultural Statistics [14]. **Figure 5** shows the height of rice plants at each growth stage and its duration. Based on the flood damage matrix and the information on rice plant height at each growth stage, Shrestha et al. [16] proposed flood damage curves for rice crops as presented in **Figure 6**. Flood damage curves of rice crops vary with each rice growing stage. Based on the duration of each growth stage of rice plants and the information on a cropping calendar, the growth stage of rice plants during a flood event can be identified, and an appropriate damage curve corresponding to the growth stage of rice plants should be applied

Growth stage of rice plants	Days of submergence			
	1–2 days	3–4 days	5–6 days	7 days
Estimated yield loss (%)				
Vegetative stage	10–20	20–30	30–50	50–100
Reproductive stage (partially inundated)	10–20	30–50	40–85	50–100
Reproductive stage (completely inundated)	15–30	40–70	40–85	50–100
Maturity stage	15–30	40–70	50–90	60–100
Ripening stage	5	10–20	15–30	15–30

**Table 2.**  
*Flood damage matrix for rice crop published by the Philippines Bureau of Agricultural Statistics [14].*

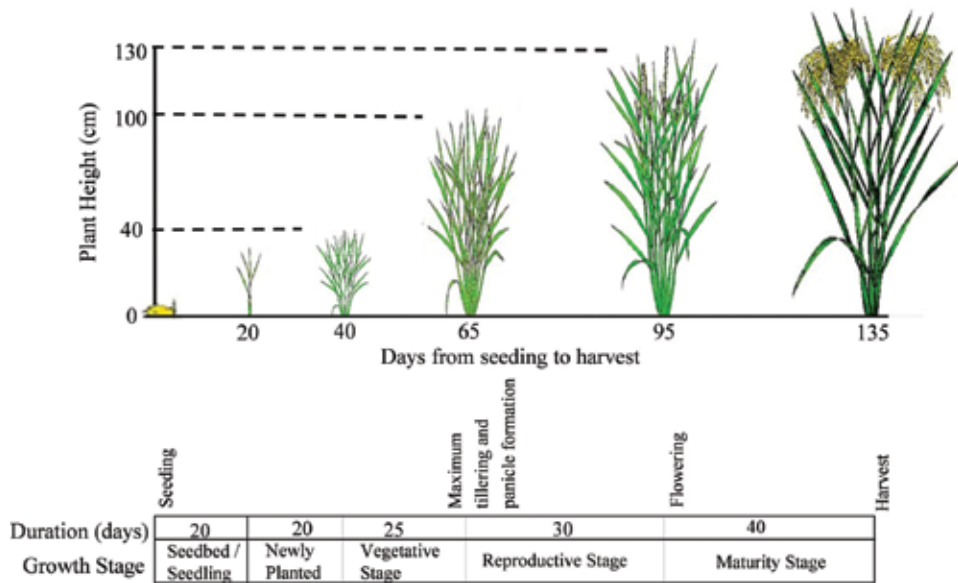


Figure 5. Height of rice plants at each growth stage and its duration [14, 15].

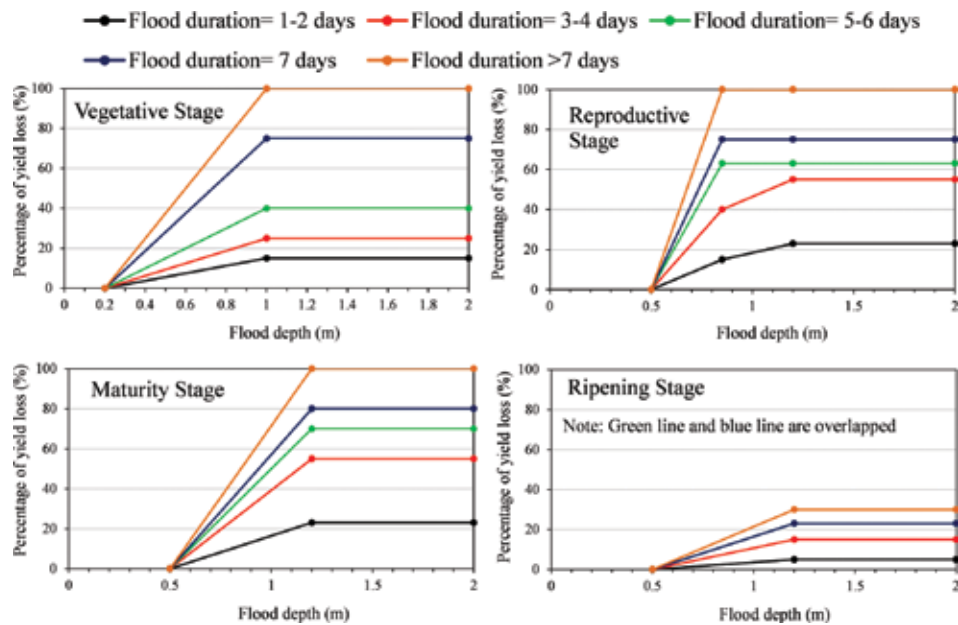


Figure 6. Depth-duration-damage function curves for rice-crop damage [16].

for damage estimation. For the case studies in this chapter, the flood damage curves for rice crops presented in **Figure 6** were used to estimate agricultural economical losses.

### 3.4.2 Damage estimation method

Flood damage to rice crops is defined as a function of flood depth, flood duration, and growth stage of rice plants and can be estimated by using the calculation

Growth stage of rice	Calculation method
Seedbed/seedling (20 days from rice plant germination)	Value of production losses = area affected $\times$ cost of input/hectare $\times$ yield loss
Newly planted stage (1–20 days after sowing)	
Vegetative stage (21–45 days)	
Reproductive stage (46–75 days)	Volume of losses = most recent yield/hectare $\times$ area damaged $\times$ yield loss
Maturing stage (76–115 days)	Value of production losses = volume of losses $\times$ most recent farm gate price

**Table 3.**  
*Calculation method of flood damage to rice crop for each growth stage of rice plants.*

method presented in **Table 3**. When flooding occurs during the early growth stage of rice plants, i.e., from the seedling to vegetative stages, at which no rice production is expected, farmers normally replant rice crops. In such a case, flood damage to rice crops can be estimated as losses of cost of input. On the other hand, when flooding occurs during the reproductive and maturity stages, at which rice production is usually expected, there is no time for replanting rice crops. In this case, flood damage to rice crops can be estimated as volume of production losses, i.e., yield loss, and then the value of production losses can be estimated based on farm gate price as calculation method presented in **Table 3**. The yield loss caused by flooding can be determined using a flood damage curve presented in **Figure 6**, according to flood depth and duration.

#### 4. Agricultural flood damage assessment in developing countries

The method for flood damage assessment for rice crops presented in this chapter was applied to assess agricultural damage in the river basins of developing countries in Asia. The method was verified by comparing calculated damage with reported data. In this section, the case studies of the assessment of flood damage to rice crops in the Pampanga River basin of the Philippines and the Lower Indus River basin of Pakistan are discussed.

##### 4.1 Pampanga River basin of the Philippines

The Pampanga River basin is located in the Region III of the Philippines, which is regarded as one of the most important river basins in terms of economic activities that influence the entire country. **Figure 7** shows the location of the Pampanga River basin. It is the nation's fourth largest basin and covers an area of 10,434 km<sup>2</sup>. The main river is about 260 km long.

In the case of the Pampanga River basin, the results of flood damage assessment for the past largest flood event as well as for a 100-year flood case are discussed. To assess flood damage to rice crop in the Pampanga River basin of the Philippines, flood characteristics such as flood depth and duration were computed using the RRI model. A digital elevation model (DEM) of a 450 m  $\times$  450 m grid size, derived from the Interferometric Synthetic Aperture Radar (IfSAR), was used in the RRI Model simulation. The IfSAR data was obtained from the National Mapping and Resource Information Authority (NAMRIA) of the Philippines. The flow accumulation and flow direction data, which are also necessary to input in the RRI model, were

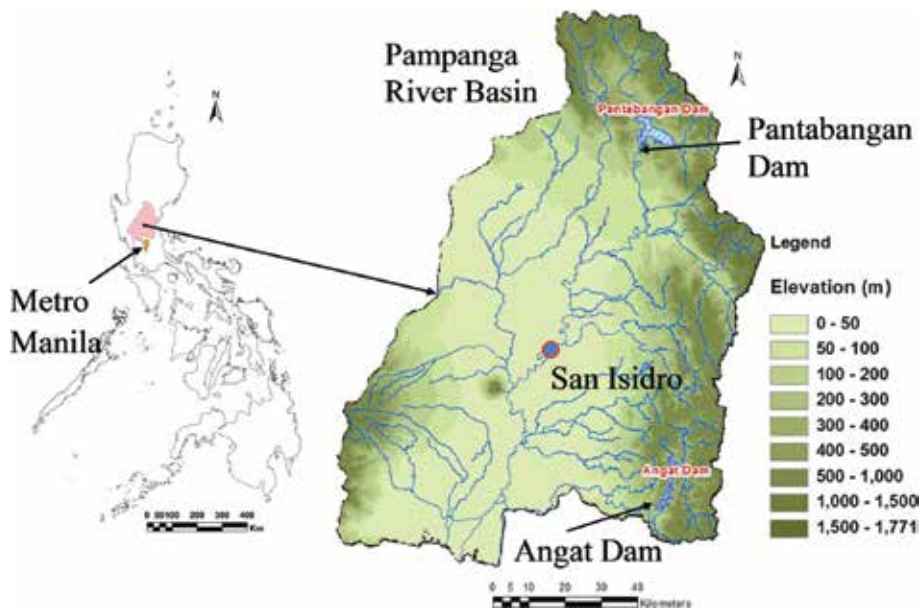


**Figure 7.**  
*Location of the Pampanga River basin in the Philippines.*

created using DEM in ArcGIS. Hourly rainfall and water-level data were collected from the Philippine Atmospheric, Geophysical and Astronomical Services Administration (PAGASA). The RRI model was calibrated and validated based on recent flood events by comparing the calculated and observed flood discharges at the San Isidro station in the basin. The flood event in September 2011 was the biggest flood in the basin in the last 30 years. The model parameters were thus calibrated to the September 2011 flood event. The calibrated parameters were validated with the 2015 flood event. **Figure 8** shows the comparison of the calculated discharge with the observed discharge at San Isidro gauging station for the flood events in 2011 and 2015 and also the comparison of the calculated flood inundation depths with the recorded flood depth in the barangays (villages) of Calumpit Municipality. The calculated results reasonably agreed with the observed data. The flood event in 2011 was due to Typhoons Pedring and Quiel. Typhoon Pedring was directly followed by Typhoon Quiel, and rice crops were severely damaged by this flood event. The flood event in 2015 was due to Typhoon Lando, which also damaged rice-crop areas in the basin.

To calculate the flood inundation depth and duration for a specific return period, flood frequency analysis was conducted by using 48-hour maximum annual rainfall data. Flood frequency analysis is essential for calculating expected damage. The main objective of flood frequency analysis is to relate the magnitude of extreme events to their frequency of occurrence through the use of probability distributions [17, 18]. The Gumbel distribution method was used for rainfall analysis. Since the rainfall volume of the September 2011 flood during Typhoon Pedring was the highest rainfall volume in the last 30 years, the rainfall pattern of the September 2011 flood (only for the Typhoon Pedring case) was selected for designing a rainfall pattern for a specific return period. **Figure 9** shows the results of flood frequency analysis using the Gumbel method and the estimation of a design hyetograph for an event of a specific return period such as a 100-year flood. To calculate flood characteristics for a 100-year flood, a design hyetograph for a 100-year return period was estimated by multiplying the rainfall hyetograph of the September 2011 flood by a conversion factor. The conversion factor for a 100-year return period was

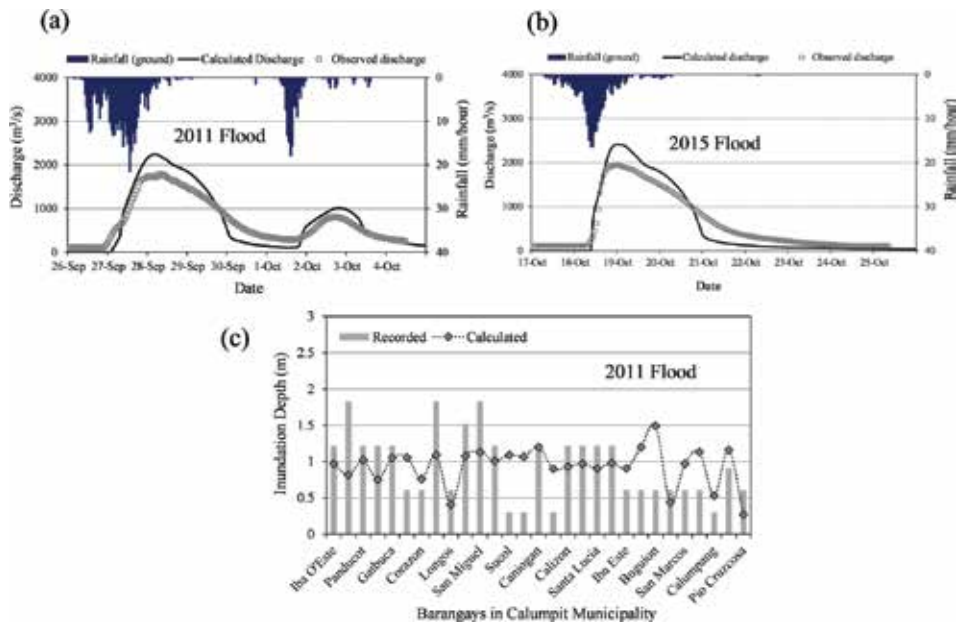


**Figure 8.** Comparison of calculated discharge with observed discharge at San Isidro station (a), (b) and comparison of calculated flood depth with recorded depth at each barangay (village) of Calumpit municipality (c).

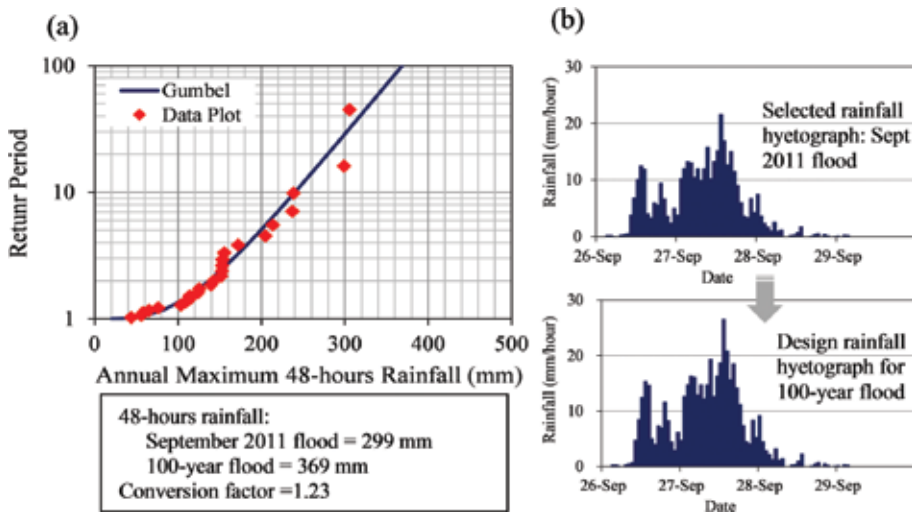


**Figure 9.** Flood frequency analysis and estimation of the design hyetograph for an event of a specific return period such as 100-year flood.

calculated as the ratio of the corresponding rainfall of the return period and the 48-hour maximum annual rainfall of 2011 based on a frequency curve. The return period of the September 2011 flood event was about 28 years. The flood characteristics for a 100-year flood were simulated by using the RRI model and the calculated design hyetograph.

**Figure 10(a)** shows the paddy fields in the Pampanga River basin, extracted using a land-cover map prepared by NWRB and JICA [12]. The rice-crop areas in the basin are about 397,247 ha. The paddy fields account for about 38% of the basin area in the Pampanga River basin. **Figure 10(b)** shows the cropping calendar for the

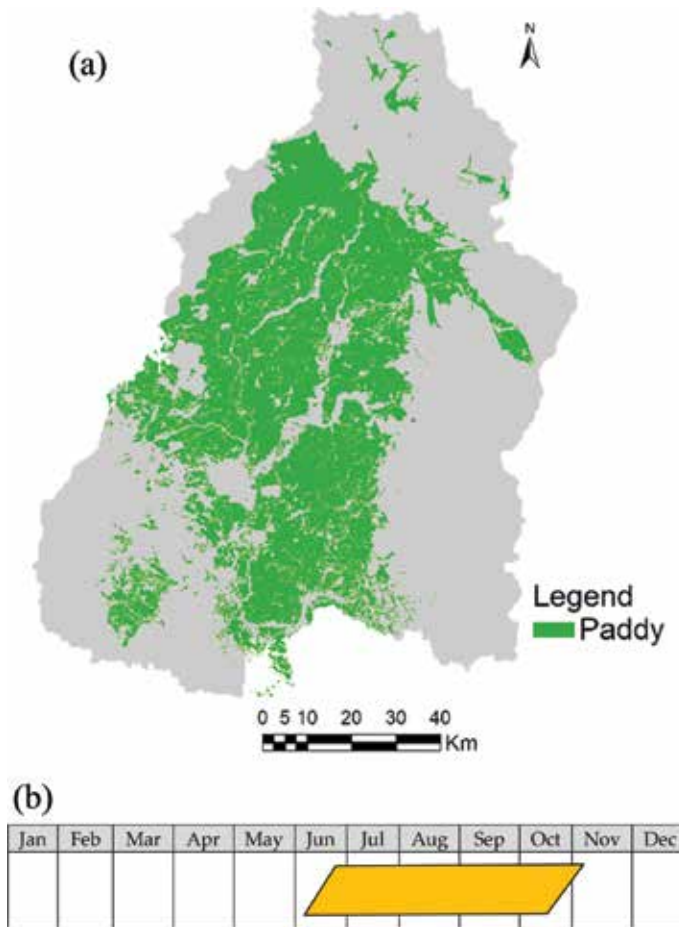


**Figure 10.**  
 Paddy field and cropping calendar for wet-season rice crop in the Pampanga River basin.

wet-season rice cultivation in the Pampanga River basin. The cropping calendar is based on the cropping calendar prepared by the National Irrigation Administration-Upper Pampanga River Integrated Irrigation System. The wet-season rice cultivation period in the Pampanga River basin is from June to October, and at least one flood event occurs every year during this period due to heavy rainfall or typhoons.

Flood damage was assessed for the 2011 flood event and 100-year flood cases. Based on the duration of the growing stage of rice crop and the cropping calendar (**Figure 5** and **Figure 10(b)**), the growth stage of rice crop during the flood event in 2011 was the maturity stage. The flood damage curves for the maturity stage presented in **Figure 6** were thus employed to estimate rice-crop damage. The rice-crop damage for a 100-year flood was estimated based on the current conditions, assuming that the rice plants were at the maturity stage, similar to the stage of rice crop during the past flood case. The flood damage to rice crop was estimated as volume of production losses using the calculation method presented in **Table 3**. **Figure 11** shows the calculated flood hazard areas and agricultural damage during the flood event from 26 September to 4 October 2011 caused by Typhoons Pedring and Quiel. The estimated flood inundation areas with a flood inundation depth greater than 0.5 m were 101,736 ha. The estimates of damaged rice-field area and rice-crop damage were 45,056 ha and 1475.78 million peso, respectively. The values of the farm gate price equal to 17 peso/kg [14] and the rice yield equal to 4360 kg/ha

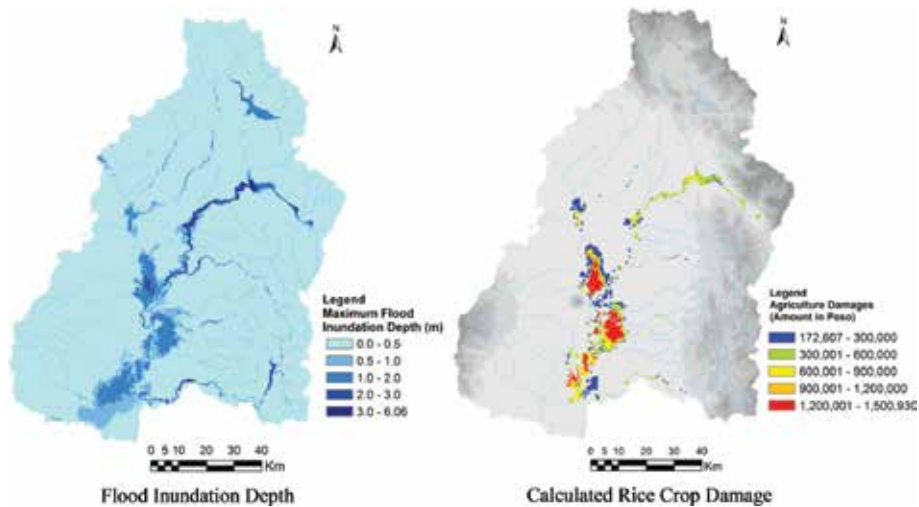


**Figure 11.** Calculated maximum flood inundation depth using the RRI model and estimated flood damage to rice crop by the flood event from 26 September to 4 October 2011.

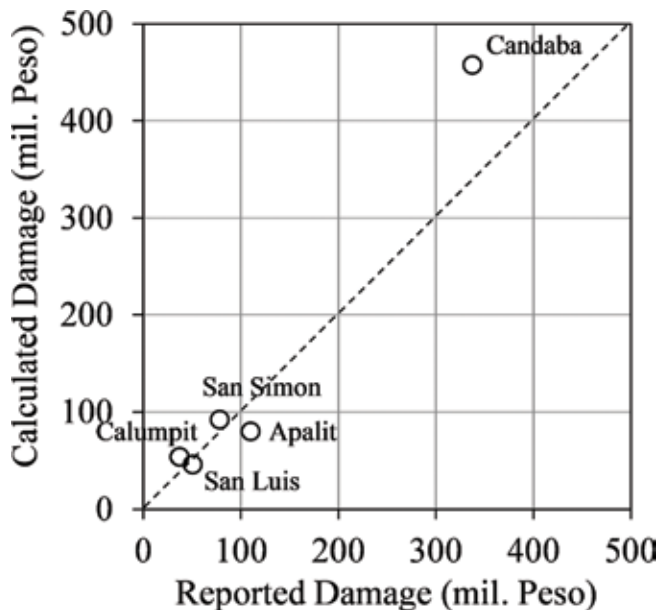


**Figure 12.** Comparison of calculated value of rice-crop damage with reported data for five municipalities during the flood from 26 September to 4 October 2011. Reported data source: [19, 20].

[19] were used in the calculation. About 11.3% of the total paddy-field area in the basin was damaged during this flood event. **Figure 12** compares the calculated rice-crop damage with the reported data for five municipalities in the basin. The calculated results reasonably agreed with the reported damage, although some difference was found in the case of Candaba Municipality. This discrepancy between the calculated and reported damage can be attributed to a variety of reasons, for example, accuracy of topographical and land-cover data.

**Figure 13** shows the calculated maximum flood inundation depth and flood damage to rice crop for a 100-year flood. The damaged paddy fields and value of rice-crop damage in the case of a 100-year flood were 67,655 ha and 2248.3 million



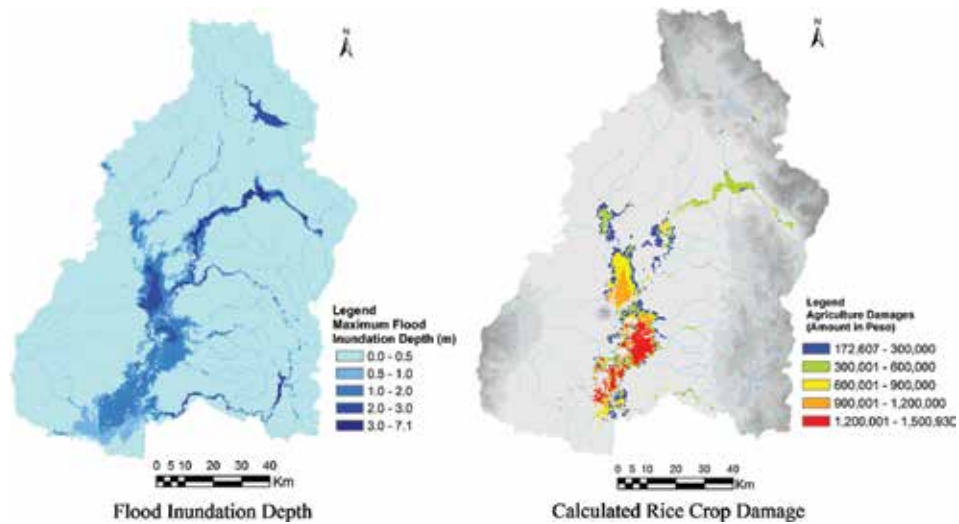


**Figure 13.**  
 Calculated flood inundation depth and rice-crop damage for a 100-year flood case.

pesos, respectively. In this case, the rainfall pattern and period of Typhoon Pedring were exclusively considered for designing a rainfall hyetograph for a 100-year flood. If the rainfall pattern and period of Typhoons Pedring and Quiel are considered, the damage might be more severe. The estimated value of rice crop in the case of a 100-year flood is about 1.52 times as high as that in the 2011 flood case. Identifying flood risk areas based on flood damage assessment provides essential information for designing future development activities. The results of flood hazard and damage assessment can be useful for implementing mitigation actions as well as for formulating policies for flood risk reduction including land-use management. To evaluate the risk of a flood with a specific return period, target scales for risk assessment should be determined. Basically, such target scales are decided based on the socioeconomic conditions of target areas and consensus among stakeholders such as national and local governments.

#### 4.2 Lower Indus River basin of Pakistan

**Figure 14** shows the location of the Lower Indus River basin in Pakistan. The area of the study basin is about 700,375 km<sup>2</sup>. The global land-cover data of GLCNMO were used to extract paddy fields, and **Figure 15(a)** shows the paddy

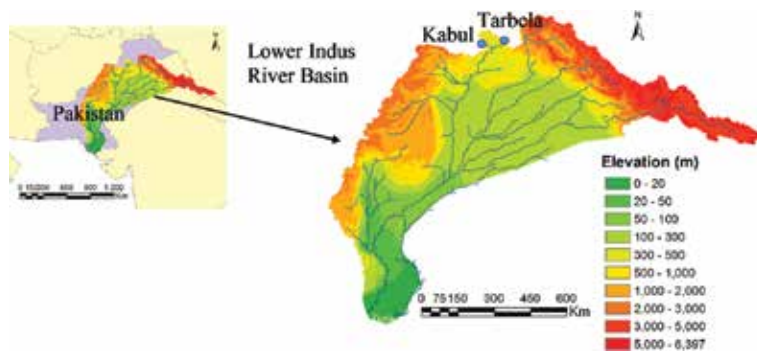


**Figure 14.**  
 Study area of the lower Indus River basin in Pakistan.

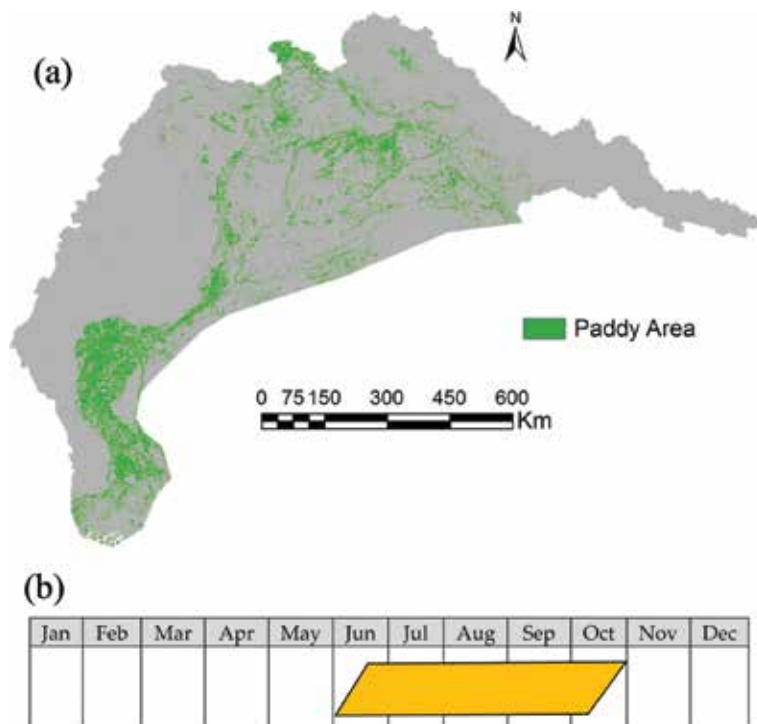


**Figure 15.**  
Paddy field in the study area and cropping calendar for wet-season rice crop.

fields in the Lower Indus study area. The paddy fields in the area are about 8.62 million ha (12.3% of the study basin area). **Figure 15(b)** shows the wet-season rice cultivation calendar in the study area, which was prepared based on FAO [21]. The wet-season rice cultivation period in the basin is from June to October.

The flood hazard was analyzed using the RRI Model for the August 2010 flood. DEM, flow accumulation, and flow direction data downloaded from the HydroSHEDS were used for the analysis. Since the study basin area is quite large, flood hazard simulation was conducted using a 60 arc-second grid size (approximately 1.8 km). In the RRI Model simulation, the observed river discharge boundary conditions at Tarbela and Kabul were defined, and recorded rainfall was also considered. The details of calibration and validation of the RRI Model can be found in Sayama et al. [10].

**Figure 16** shows the calculated maximum flood inundation depth and estimated flood damage to rice crop during the August 2010 flood event. The values of the farm gate price equal to 17.5 Rs/kg [22] and the rice yield equal to 2641 kg/ha, obtained from the Directorate of Agriculture Extension Sindh, Hyderabad, were used in the calculation. The damage curve for the maturity stage was used according to the cropping calendar and the duration of the growth stage. The calculated flood inundation areas with a flood inundation depth greater than 0.5 m and the damaged rice-field areas were found to be 1,611,252 ha and 662,580 ha, respectively. About 7.6% of the paddy-field area was damaged during the August 2010 flood. The total estimated flood damage to rice crop in the basin was found to be 19.72 billion Rs (Pakistani Rupees), while the reported damage was 21.17 billion Rs. The calculated damage values were also compared with the reported data for four provinces (**Figure 17**). The comparison results show that the calculated damage values reasonably agreed with the reported data. The results show that rice crops were severely damaged by flooding in Sindh and Punjab provinces.

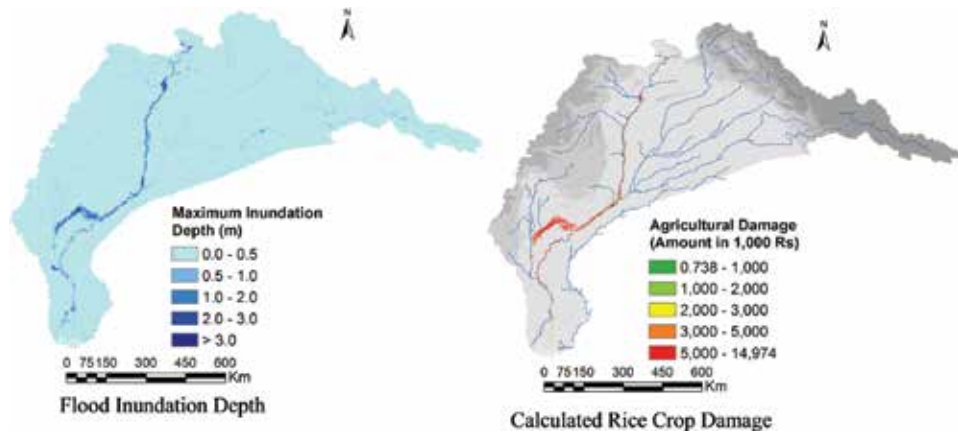


**Figure 16.** Calculated maximum flood inundation depth and rice-crop damage during the August 2010 flood in the lower Indus River basin.

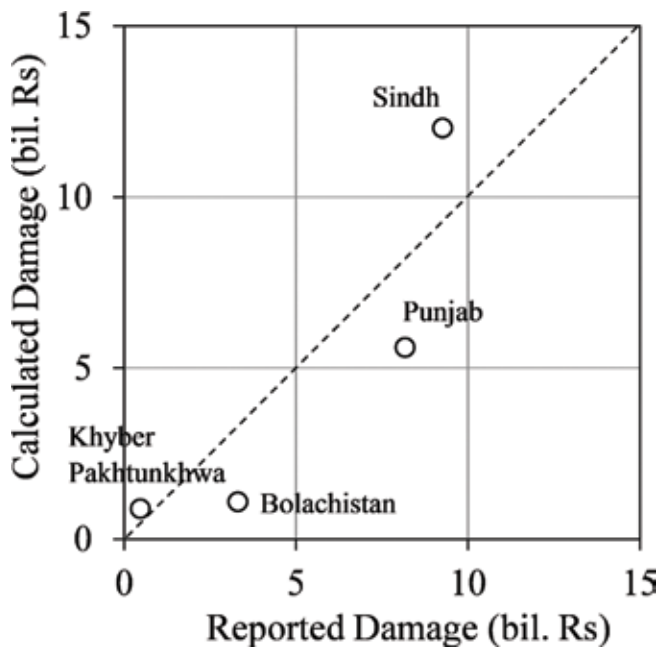


**Figure 17.** Comparison of calculated value of rice-crop damage with reported data for four provinces during the August 2010 flood. Reported data source: [22].

## 5. Conclusions

The method for assessing flood damage to rice crop with case studies in the Asian river basins was discussed. The results of flood damage assessment in the Pampanga River basin of the Philippines and the Lower Indus River basin of Pakistan were also presented in this paper. The calculated values of rice-crop damage were compared with reported data. The comparison results show that the values of calculated damage reasonably agreed with the reported damage values. The rice-crop damage estimation method presented in this paper can be easily applied to estimate damage for future flood events and can also be applied to other river basins

for flood risk assessment. The method was also introduced to the related organizations in several developing countries of Asia such as the Philippines, Indonesia, Cambodia, Thailand, and Myanmar. The results of flood damage provide a basis to identify areas at risk, and these results can be useful for planners, developers, policy makers, and decision-makers to establish policies required for flood damage reduction. The results may also be useful for them to implement flood mitigation actions including agricultural land-use regulations while taking into account the risk areas of rice-crop damage and adaptation measures.

The accuracy of flood disaster risk assessment can be further improved by considering the following points:

- The accuracy of flood hazard assessment and damage assessment highly depends on the quality of topographical data. For the case studies in this chapter, agricultural damage was assessed using remotely sensed topographical data and global land-cover data. Damage assessment can be further improved by adjusting remotely sensed topographical data with ground observed elevation data for certain points and also by using locally available land-cover data to reflect actual local conditions.
- Generally, flood damage curves are prepared based on actual flood damage and inundated depth. Data and information on actual flood events and damage with their relationships are very important for developing damage functions, as well as for validating calculated results. It is thus important to collect damage data and hazard information during or after a flood disaster.
- Risk indicators such as flood damage curves can differ from place to place according to the characteristics of exposed elements such as agricultural products and residential houses, even though some similarities may be found between some places. It is recommended that each country should develop damage curves to reflect the actual characteristics of their rice-crop cultivation.
- This chapter focused on assessment of flood damage to rice crops. However, for flood risk management in the river basins, it is also necessary to consider flood damage to other agricultural crops and also flood damage to buildings, residential properties, and other types of infrastructure.

## **Acknowledgements**

The authors would like to thank the National Mapping and Resource Information Authority of the Philippines for providing IfSAR data freely for the Pampanga River basin and also thank all related counterpart institutes in each country for their support.

## **Conflict of interest**

The authors declare no conflict of interest.

## Author details

Badri Bhakta Shrestha<sup>1,2\*</sup>, Hisaya Sawano<sup>1,2</sup>, Miho Ohara<sup>1,2</sup>, Yusuke Yamazaki<sup>2</sup> and Yoshio Tokunaga<sup>1,2</sup>

1 International Centre for Water Hazard and Risk Management (ICHARM) under the auspices of UNESCO, Tsukuba, Japan

2 Public Works Research Institute (PWRI), Tsukuba, Japan

\*Address all correspondence to: [shrestha@pwri.go.jp](mailto:shrestha@pwri.go.jp)

## IntechOpen

---

© 2018 The Author(s). Licensee IntechOpen. This chapter is distributed under the terms of the Creative Commons Attribution License (<http://creativecommons.org/licenses/by/3.0>), which permits unrestricted use, distribution, and reproduction in any medium, provided the original work is properly cited. 

## References

- [1] Shrestha BB, Okazumi T, Miyamoto M, Nabesaka S, Tanaka S, Sugiura A. Fundamental analysis for flood risk management in the selected river basins of Southeast Asia. *Journal of Disaster Research*. 2014;**9**(5):858-869. DOI: 10.20965/jdr.2014.p0858
- [2] Meyer V, Haase D, Scheuer S. GIS-based multicriteria analysis as decision support in flood risk management. *UFZ-Diskussionspapiere*. UFZ: Leipzig; 2007. Available from: <https://www.econstor.eu/bitstream/10419/45237/1/548359628.pdf> [Accessed: 26-06-2018]
- [3] Shrestha BB, Sawano H, Ohara M, Nagumo N. Improvement in flood disaster damage assessment using highly accurate IfSAR DEM. *Journal of Disaster Research*. 2016;**11**(6):1137-1149. DOI: 10.20965/jdr.2016.p1137
- [4] Okada T, McAneney KJ, Chen K. Estimating insured residential losses from large flood scenarios on the Tone River, Japan—A data integration approach. *Natural Hazards and Earth System Sciences*. 2011;**11**:3373-3382. DOI: 10.5194/nhess-11-3373-2011
- [5] Merz B, Kreibich H, Schwarze R, Thieken A. Review article “Assessment of economic flood damage”. *Natural Hazards and Earth System Sciences*. 2010;**10**:1697-1724. DOI: 10.5194/nhess-10-1697-2010
- [6] Brémond P, Grelot F, Agenais A-L. Review article: Economic evaluation of flood damage to agriculture—Review and analysis of existing methods. *Natural Hazards and Earth System Sciences*. 2013;**13**:2493-2512. DOI: 10.5194/nhess-13-2493-2013
- [7] Messner F, Meyer V. Flood damage, vulnerability and risk perception, challenges for flood damage research. In: Schanze J, Zeman E, Marsalek J, editors. *Flood Risk Management: Hazards, Vulnerability and Mitigation Measures*. Vol. 67. Dordrecht: NATO Science Series, Springer; 2006. pp. 149-167
- [8] Messner F, Penning-Rowsell E, Green C, Meyer V, Tunstall S, van der Veen A. *Evaluating flood damages: Guidance and recommendations on principles and methods*. 1st ed. HR Wallingford, UK: FLOOD site Consortium; 2007. p. 178
- [9] Penning-Rowsell E, Johnson C, Tunstall S, Tapsell S, Morris J, Chatterton J, et al. *The benefits of flood and coastal risk management: A handbook of assessment techniques*. 1st ed. London, UK: Middlesex University Press; 2005. p. 81
- [10] Sayama T, Ozawa G, Kawakami T, Nabesaka S, Fukami K. Rainfall-runoff-inundation analysis of Pakistan flood 2010 at the Kabul River basin. *Hydrological Sciences Journal*. 2012; **57**(2):298-312
- [11] Sayama T. *Rainfall-Runoff-Inundation (RRI) Model Technical Manual*. Technical Note of PWRI 4277. Tsukuba, Japan: Public Works Research Institute; 2014
- [12] National Water Resources Board (NWRB), Japan International Cooperation Agency (JICA). *The study on integrated water resources management for poverty alleviation and economic development in the Pampanga river basin*. IWRM Report, NWRB and JICA; 2011. Available from: [http://www.nwr.gov.ph/images/Publications/IWRM\\_Pampanga\\_River\\_Basin.pdf](http://www.nwr.gov.ph/images/Publications/IWRM_Pampanga_River_Basin.pdf) [Accessed: 25-02-2018]
- [13] Tateishi R, Bayaer U, Al-Bilbisi H, Aboel Ghar M, Tsend-Ayush J, Kobayashi T, et al. *Production of global*

land cover data—GLCNMO.  
International Journal of Digital Earth.  
2011;4:22-49

[14] Bureau of Agricultural Statistics (BAS). Manual on Damage Assessment and Reporting System. Philippines: Bureau of Agricultural Statistics, Department of Agriculture; 2013

[15] International Rice Research Institute (IRRI). Growth stages of the rice plant [Internet]. 2007. Available from: [http://www.knowledgebank.irri.org/ericeproduction/0.2.\\_Growth\\_stages\\_of\\_the\\_rice\\_plant.htm](http://www.knowledgebank.irri.org/ericeproduction/0.2._Growth_stages_of_the_rice_plant.htm) [Accessed: 03-07-2018]

[16] Shrestha BB, Okazumi T, Miyamoto M, Sawano H. Flood damage assessment in the Pampanga River basin of the Philippines. *Journal of Flood Risk Management*. 2016;9(4):355-369. DOI: 10.1111/jfr3.12174

[17] Chow VT, Maidment DR, Mays LW. *Handbook of Applied Hydrology*. New York: McGraw-Hill; 1988

[18] Xu Y, Booij MJ. Appropriate models in decision support systems for river basin management. In: *Proceedings of Conference on Water Observation and Information System for Decision Support*; 25-29 May 2004; Ohrid, Republic of Macedonia. 2004

[19] Bulacan Provincial Agricultural Office (BPAO). *Final Validation Report for Cereals*. Bulacan, the Philippines: Bulacan Provincial Agricultural Office; 2011

[20] Pampanga Provincial Agricultural Office (PPAO). *Damage Report of Typhoon Pedring*. Pampanga, the Philippines: Pampanga Provincial Agricultural Office; 2011

[21] Food and Agriculture Organization (FAO). *Global Information and Early Warning System—Country Briefs*

[Internet]. 2018. Available from: <http://www.fao.org/gIEWS/countrybrief/> [Accessed: 01-07-2018]

[22] Ahmad S, Ahmad B, Ali I, Ahmad I, Mustafa N, Ahmad B, et al. *Assessment of 2010 Flood Impacts*. Natural Resources Division, Pakistan Agricultural Research Council, Islamabad, Pakistan; 2010



*Edited by John Abbot and Andrew Hammond*

This book provides a series of topics on flood risk management from around the world. The first section includes models for improved approaches to flood risk management, the importance of groundwater management in the context of floods (focussing on Taiwan), contingency plan for local communities using flood simulation, deciding on response strategies against the identified flood risk before a flood occurs (illustrated for the Philippines) and models for estimating maximum flood heights (illustrated for Mozambique). The second section examines flood risk management relating to the urban environment, with examples from a coastal city in Saudi Arabia and a housing development in Mexico. The third section relates to flood risk management in the context of agriculture, particularly relating to damage to Asian rice crops.

Published in London, UK

© 2019 IntechOpen  
© GOLFX / iStock

**IntechOpen**

ISBN 978-1-83962-104-8



9 781839 621048

